Regulation of natural killer cell activity and inflammatory responses by mesenchymal stem cell secretome

Eunhee Ko

The Graduate School
Yonsei University
Department of Medical Science

Regulation of natural killer cell activity and inflammatory responses by mesenchymal stem cell secretome

A Dissertation Submitted to
the Department of Medical Science
and the Graduate School of Yonsei University
in partial fulfillment of
the requirements for the degree of
Doctor of Philosophy in Medical Science

Eunhee Ko

June 2024

This certifies that the Dissertation of
Eunhee Ko is approved.

Thesis Supervisor Yong-Beom Park

Thesis Committee Member Je-Wook Yu

Thesis Committee Member Young-Min Hyun

Thesis Committee Member Ho-Keun Kwon

Thesis Committee Member Hun Sik Kim

The Graduate School
Yonsei University
June 2024

ACKNOWLEDGEMENTS

박사과정 입학 전 1년 6개월의 연구원 기간과 5년의 학위 기간 동안 주도적으로 저만의 연구를 진행할 수 있도록 연구 환경을 조성해 주시고 저의 의견을 존중해 주시며 끝까지 믿어 주셨던 박용범 교수님께 먼저 감사의 마음을 전합니다. 특히 만 4년이 지날 무렵 몸과 마음이 탈진해서 일상이 불가한 지경에 이르렀을 때, 충분히 쉬고 회복될 수 있도록 한 달의 휴식을 기꺼이 허락해주신 덕분에 병원 치료와 심리 상담을 지속하며 일상을 되찾았고, 결국 오늘에 이를 수 있었습니다. 저의 안위를 걱정해주시고 잠시 멈춤의 시간을 허락해 주셨던 교수님께 다시 한 번 감사드립니다.

바쁘신 일정에도 제 연구를 점검해주시고 객관적인 과학적 평가와 아낌없는 조언으로 연구를 보완하여 단단해질 수 있도록 여러 차례 심사해 주셨던 유제욱 교수님, 현영민 교수님, 권호근 교수님, 아산병원 김헌식 교수님께도 깊이 감사드립니다.

마주칠 때마다 안부를 물으시며 반겨 주시고, 저널 클럽과 인뎁스 시간에서 임상적-기초적 학문 토론을 통해 많이 배우게 해주셨던 류마티스내과 교수님들께도 감사드립니다. 늘 유쾌한 말씀으로 미소 짓게 해주시고, 흥미롭고 귀한 임상 연구에 참여할 수 있는 기회를 주셨던 이상원 교수님, 질문 드릴 때마다 아낌없는 조언과 갖고 계신 지식들을 쏟아내 주셔서 제게 학문적인 흥미와 연구 의지를 북돋워 주셨던 송정식 교수님께 감사드립니다. 본 연구의 시작 초기, 맨땅에 기초석을 하나씩 세워가야 했던 중에 함께 고민해주시고, 실험적인 아이디어, 과학적인 조언과 더불어 저를 격려해 주셨던 정승민 교수님께도 감사드립니다.

학위에 전념할 수 있도록 재정적으로 후원해 주셨던 Brain Korea 21 (BK21) 사업 한국연구재단과 JW이종호재단에도 깊이 감사드리며, 앞으로 사회에 나가 기초과학 발전에 조금이나마 보탬이 될 수 있도록 늘 고민하며 실천으로 보답하는 과학인이 되겠습니다.

오랜 시간 동고동락하고 서로의 손과 발이 되어주며 같은 시간을 함께 견뎌왔던 태준이와 수정이, 두 사람의 존재 덕분에 무사히 박사과정 연구를

마칠 수 있어 정말 고맙고 고맙습니다. 제 연구 인생 스토리의 일부이며 연구 기반이자 자산이 되어준 제주대 생명공학부와 수의학과, 부산의대 해부학교실, 충남대 나노스코피 실험실에서 비롯된 저의 모든 인연들에게도 진심으로 감사드립니다.

언제나 딸이 좋아하고 딸이 하고자 하는 일을 하면서 건강하고, 행복하길 바라시는 부모님. 저의 오랜 학위 생활을 묵묵히 지켜봐 주시고 아낌없는 지원과 한결 같은 버팀목이 되어 주셔서 마음 깊이 존경과 감사를 드립니다. 사랑하는 가족들과 양가 친척분들, 저의 오랜 제주도 친구들, 충남대교회와 목동 지구촌교회 청년2부 공동체의 모든 이들의 응원과 기도 속에서 긴 여정의 마라톤을 완주하게 되었고, 저만큼 기뻐해 주시고 진심으로 축하해 주셔서 감사드립니다.

마지막으로, 오늘에 이르기까지 모든 순간을 함께 해주시며 저의 모든 필요를 채워주신, 독립적인 한 명의 연구자로 성장하게 해주신 나의 유일한 자랑, 아버지 하나님께 이 학위논문을 올려드립니다.

“만군의 여호와께서 말씀하시되
이는 힘으로 되지 아니하며 능력으로 되지 아니하고
오직 나의 영으로 되느니라”
(스가랴 4:6)

하나님이 하셨습니다!

2024년 8월
고은희

TABLE OF CONTENTS

LIST OF FIGURES

Introduction

3.1. Immunomodulatory effects of the ADSC secrtome on human NK cells

3.2. Immunomodulatory effects of the ADSC secretome on mouse NK cells and lupus murine model

LIST OF TABLES

ABSTRACT

Regulation of natural killer cell activity and inflammatory responses by mesenchymal stem cell secretome

Mesenchymal stem cells (MSCs) exhibit immunomodulatory properties by secreting a diverse range of soluble factors collectively known as the secretome. This secretome has displayed therapeutic potential not only in autoimmune diseases but also in various other medical conditions. Despite this, the specific key factors within the MSC secretome and their precise mechanisms of action on immune cells remain incompletely understood. While most *in vitro* experiments use various types of immune cells, studies specifically focusing on natural killer (NK) cells are limited and have yielded inconsistent results. NK cells play a crucial role in directly killing target cells, such as cancer or virus-infected cells, and supporting other immune cells. However, abnormalities in NK cell number and function are observed in autoimmune environments, and the exact cause or its implication in disease progression remain unclear.

This study has a dual purpose. First, to elucidate the impact and mechanisms of action of the adipose tissue-derived stem cell (ADSC) secretome on NK cell activity. Second, to analyze the characteristics of NK cells in lupus nephritis (LN), a common complication of systemic lupus erythematosus (SLE), an autoimmune disease, and investigate the *in vivo* changes and inflammatory regulation mechanisms due to ADSC secretome administration.

In Chapter 1, based on previously published data in Stem Cell Research & Therapy (November 2023), we conducted *in vitro* experiments utilizing human-derived NK cells and observed that the ADSC secretome selectively inhibited effector functions of NK cells induced by IL-2 while maintaining normal proliferation. This effect was associated with a decrease in the expression of

NK cell surface activating receptors (NKG2D, NKp30, NKp46) and IL-2 receptors (CD25, CD132), along with an increase in the expression of the inhibitory receptor CD96. Intracellularly, the ADSC secretome upregulated the negative regulators CIS and DUSP4, thereby interfering with the IL-2 signaling pathway in NK cells.

In Chapter 2, through *ex vivo* experiments utilizing mouse splenic NK cells, we observed that their activity and receptor expressions closely resembled those of human NK cells. Furthermore, upon employing NZB/W F1 mice with lupus nephritis, we observed infiltration of their NK cells into the target organ, the kidney, albeit displaying an exhaustion phenotype with dysfunction. While NK cells may paly a protective role in the lupus environment by eliminating autoreactive immune cells, their function appears impared due to prolonged inflammation over time. Moreover, the administration of the ADSC secretome mitigated the inflammatory response and preserved renal structure and function. This occurred as the ADSC secretome reduced the abundance of inflammatory immune cells in both the spleen and kidneys, and upregulated the suppressed regulatory function of NK cells, partially restoring the NK cell phenotype towards a normal state.

In conclusion, the ADSC secretome selectively modulates NK cell activity by suppressing effector functions while maintaining cell proliferation when NK cells are transiently stimulated. Additionally, it induces the recovery of suppressed NK cell function by regulating the expression of surface receptors to a normal phenotype in chronic inflammation. Therefore, the MSC secretome holds the potential as an immune modulator, targeting inflammatory and autoimmune diseases mediated by NK cells.

Key words: mesenchymal stem cell, secretome, natural killer cell, immunomodulation, systemic lupus erythematosus, lupus nephritis, inflammatory response

1. Introduction

Mesenchymal stem cells (MSCs) exhibit versatile biological properties contingent upon their cellular microenvironment, wherein they contribute to tissue regeneration and immune regulation.[1] Numerous researchers have directed their efforts toward leveraging the therapeutic capabilities of MSCs for the treatment of degenerative and inflammatory disorders. It is presently acknowledged that the immunomodulatory ability of MSCs is attributed to their secreted factors, collectively termed the secretome, which operates in a paracrine manner rather than relying on the cells themselves.[2-4] The current focus has shifted towards secretome-based therapy for clinical applications, considering it as a potential alternative to cell-based therapy.[5-7]

The MSC secretome comprises diverse molecules, including cytokines, chemokines, nucleic acids, growth factors, proteases, microvesicles, exosomes, and immune-modulatory factors. The composition of the MSC secretome is manipulated to enhance therapeutic effects through strategies such as priming with biological stimuli and genetic modification via transfection or transduction.[4,6] The MSC secretome is recognized for its therapeutic benefits, encompassing immunomodulatory, anti-inflammatory, anti-apoptotic, and proangiogenic properties (Figure 1).[8,9]

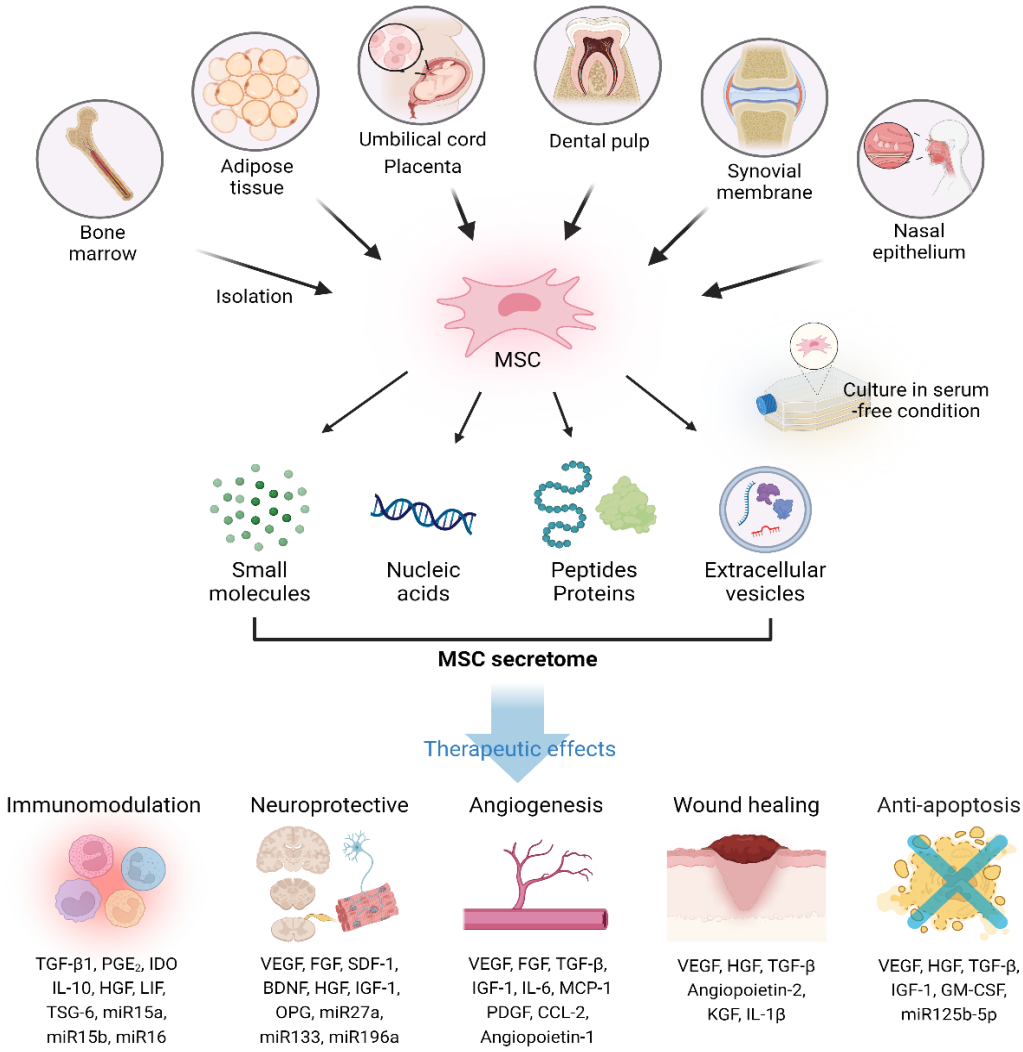

Figure 1. Sources of mesenchymal stem cells (MSCs), contents of MSC secretome, and its multiple therapeutic effects. This illustration was generated using the BioRender.com website.

Previous studies have documented that the MSC secretome encompasses a range of bioactive factors capable of regulating the proliferation, differentiation, and effector functions of immune cells, including NK cells, thereby exerting therapeutic effects in inflammatory and autoimmune diseases.[10,11]

For this reason, there is a growing body of evidence unveiling the precise composition of therapeutic potential within the MSC secretome through common techniques, including proteomic analysis, for clinical applicability.[12-21] However, many studies have not fully elucidated the specific key factors within the MSC secretome that mediate outcomes in immune cells or tissues, highlighting the challenge of accurately determining which factors are responsible for immunoregulation.[4] Therefore, studies that precisely characterize MSC-secreted factors and identify the major factors responsible for immunomodulation in the secretome, along with understanding their mechanisms of action, are essential for the development of advanced therapies using stem cells.[22] To reach this goal, most *in vitro* experiments utilize T cells, B cells, and macrophages, but only a few include natural killer (NK) cells.[23] Even among the limited studies on the effect of MSC-derived soluble factors on NK cells,[24-28] discrepancies have been observed. Hence, it is necessary to elucidate how the MSC secretome affects NK cells and understand the precise molecular mechanisms underlying these effects.

Natural killer (NK) cells, being large granular lymphocytes, trigger apoptosis in target cells by releasing cytotoxic granules like perforin and granzyme B through exocytosis, a process that doesn't require prior sensitization.[29] Additionally, they promptly release various cytokines and chemokines such as IFN-γ, GM-CSF, IL-10, TNF-α, and CCL3-5, employing diverse mechanisms to either induce or amplify the inflammatory response.[30,31] The activation of NK cells is primarily governed by the precise interaction and equilibrium between activating and inhibitory surface receptors. These receptors transmit signals through their immunoreceptor tyrosine-based activation motifs (ITAMs) or inhibition motifs (ITIMs) in their cytoplasmic tails.[32,33] Furthermore, signals from cytokines like IL-2, IL-12, IL-15, and IL-18 play a crucial role in NK cell activation and integration.[34,35] Activating receptors recognize ligands derived from pathogens or induced by

stress, leading to cytokine secretion and cytotoxicity for target cell elimination. Conversely, inhibitory receptors identify the major histocompatibility complex (MHC) class I present on healthy host cells, providing protection against NK cell-mediated killing (Figure 2).[36,37]

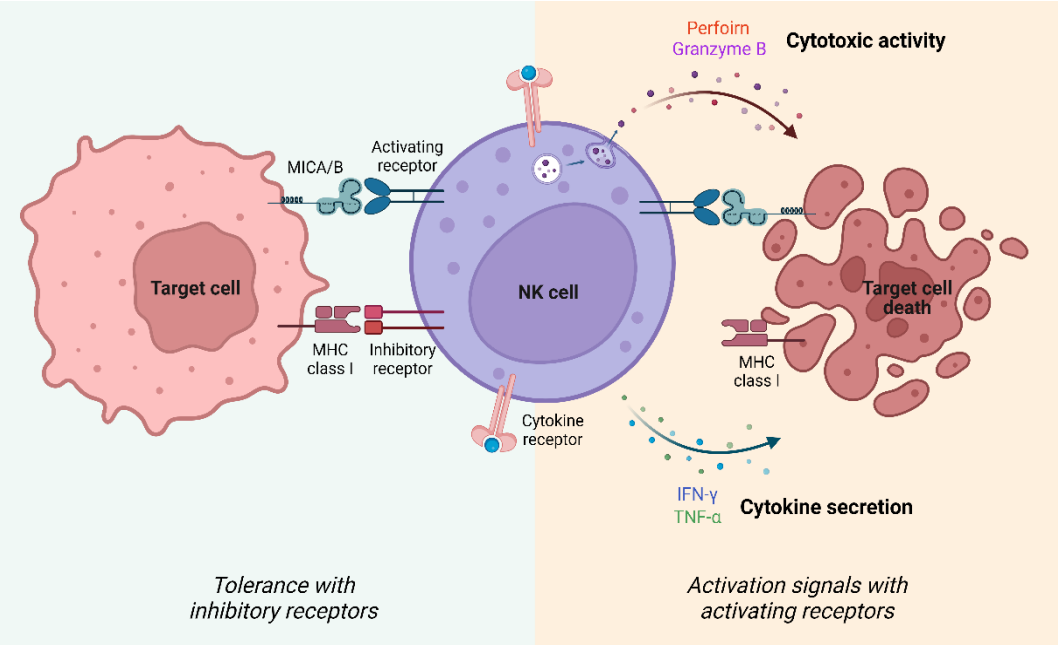

Figure 2. Differences in natural killer (NK) cell effector function and regulation of their activity by recognition of target cells. This illustration was generated using the BioRender.com website.

When NK inhibitory receptors with ITIMs bind to their ligands, there is a recruitment of protein tyrosine phosphatases (PTPs) such as Src homology 2 (SH2) domain-containing protein tyrosine phosphatases (SHP-1 and SHP-2) and SH2 domain-containing inositol phosphatases (SHIP-1 and SHIP-2). These PTPs dephosphorylate signaling proteins associated with activation signals, leading to the suppression of NK cell responses.[33,38] Furthermore, these PTPs also regulate the cytokine-mediated Janus kinase (JAK)-signal transducer and activator of transcription (STAT) pathway, along with suppressor of cytokine signaling (SOCS) proteins, forming a negative-feedback loop induced by cytokines to block further signal transduction (Figure 3).[39,40]

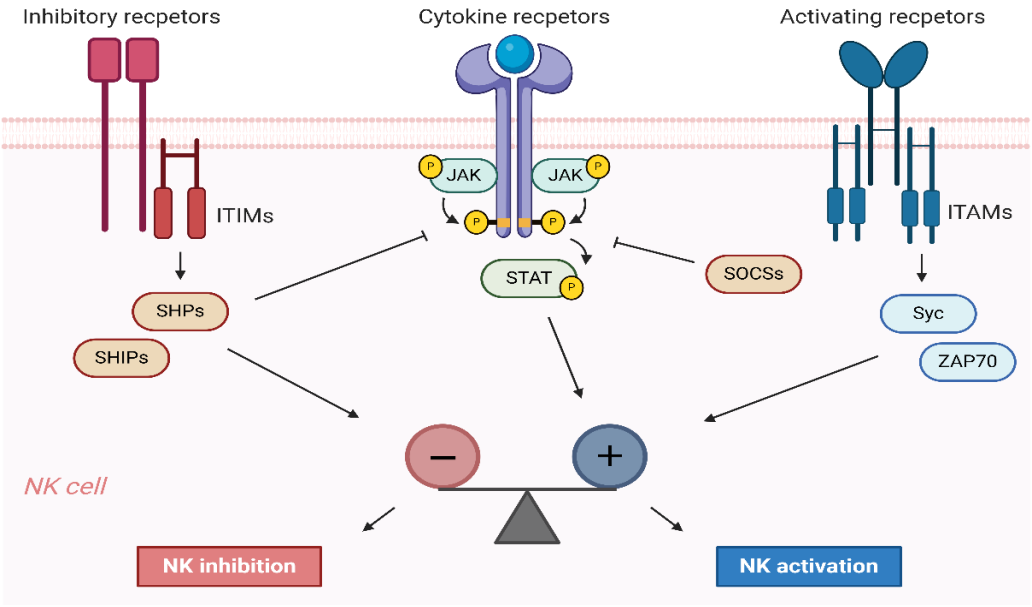

Figure 3. Regulation of natural killer (NK) cell functions by the balance of activating and inhibitory signals. This illustration was generated using the BioRender.com website.

This results in the degradation of target proteins (tyrosine-phosphorylated JAKs or STATs) via ubiquitination.[41] Impaired NK cell activity may enhance susceptibility to infection and cancer, while excessive NK cell activity can lead to severe tissue damage.[42,43] Although the adjustment of NK cell activity is crucial for controlling various pathological conditions, the fundamental endogenous mechanisms for modulating the functional outcome of NK cell activity still need to be investigated.

Systemic lupus erythematosus (SLE) is a chronic autoimmune disorder capable of impacting multiple tissues and organs.[44] Lupus nephritis (LN), kidney involvement and a prevalent complication of SLE, affects approximately 30–60% of individuals with SLE, contributing significantly to morbidity and mortality.[44,45] The pathogenesis of LN involves immune complex (IC) deposition that occurs when there are elevated levels of autoantibodies in the circulation, complement activation within the kidneys, leukocyte infiltration, and heightened expression of inflammatory cytokines (Figure 4).[46]

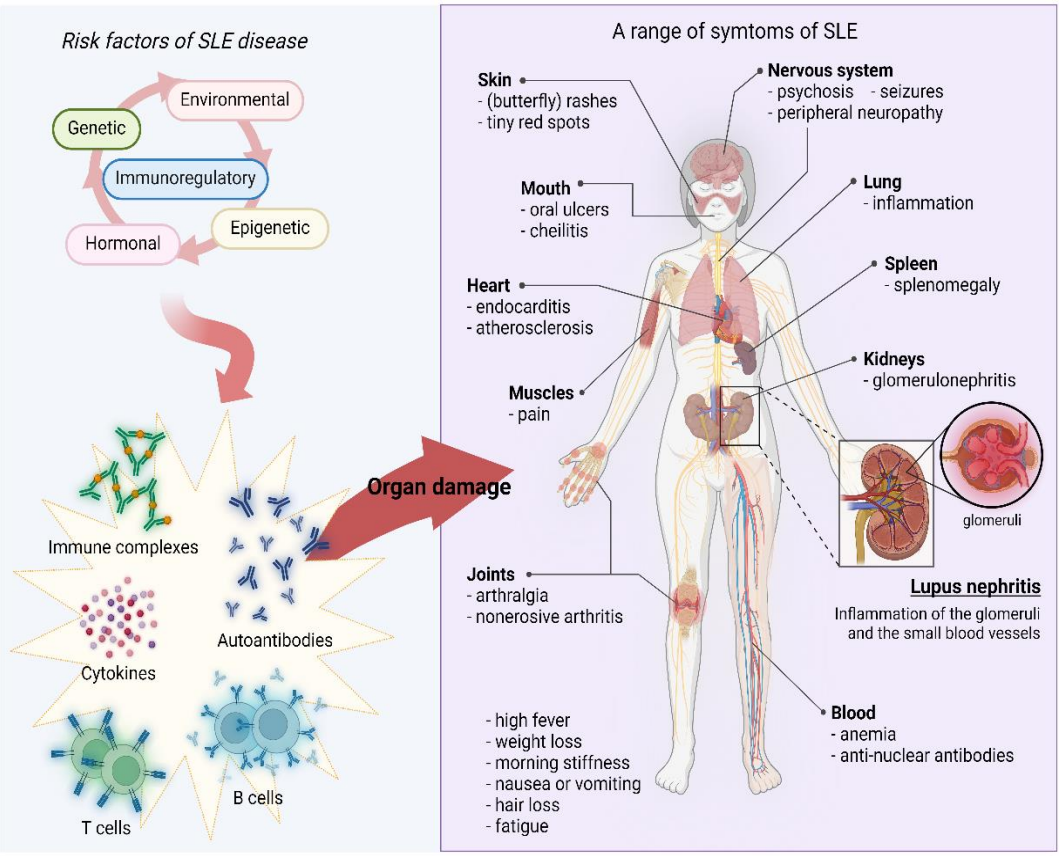

Figure 4. Overview of the pathophysiology and common manifestations of systemic lupus erythematosus (SLE). This illustration was generated using the BioRender.com website.

Current treatment options for LN are inadequate, given the severe adverse effects associated with the use of existing immunosuppressive cytotoxic therapies.[47,48] With only one new drug approved for the treatment of SLE in the last five decades, there is an urgent need to unravel the immune mechanisms underlying LN.[48]

Gathering evidence suggests the involvement of NK cells in the pathogenesis of SLE. Numerous studies have demonstrated reduced numbers and proportions of NK cells in the peripheral blood of SLE patients, alongside compromised cytotoxic functions, impaired differentiation, altered

phenotypes, and modified cytokine production in NK cells.[49-57] Studies using a lupus murine model have unveiled the involvement of NK cells in the pathogenesis of lupus.[58,59] Although it seems evident that NK cells play a contributory role, the causal or consequential nature of these abnormalities in the SLE pathological process, including specifically in the target organs of this disease, remains unknown. Although the MSC secretome demonstrates potent anti-inflammatory and immunomodulatory effects in some inflammatory models,[60-62] its utilization in SLE treatment has yet to be realized. Moreover, despite the significance of NK cells in SLE, this mechanism has not been characterized in lupus NK cells, nor has it been considered as a therapeutic target in lupus.

In this study, we present the outcomes of an investigation with two primary objectives. Firstly, to examine the effects of the adipose tissue-derived stem cell (ADSC) secretome on NK cells and elucidate its mechanisms, we employed a human NK cell line (NK-92) and human blood NK cells from healthy individuals in Chapter 1. We observed that the ADSC secretome selectively inhibited effector functions of NK cells stimulated with IL-2 while maintaining normal proliferation. This effect was associated with a reduction in the expression of NK cell surface activating receptors (NKG2D, NKp30, NKp46) and IL-2 receptors (CD25, CD132), coupled with an increase in the expression of the inhibitory receptor CD96. Intracellularly, the ADSC secretome upregulated the negative regulators CIS and DUSP4, thereby interfering with the IL-2 signaling pathway in NK cells. The data presented in Chapter 1 have been previously published in Stem Cell Research & Therapy in November 2023.[63]

Secondly, to assess the characteristics of NK cells in the LN environment and investigate the impact of the ADSC secretome, we utilized mouse splenic NK cells and employed lupus-prone NZB/W F1 mice in Chapter 2. We observed that the activity and receptor expressions of mouse NK cells closely resembled those observed in human NK cells. Furthermore, NK cells in LN mice infiltrated the target organ, the kidney, and exhibited an exhaustion phenotype due to prolonged

inflammation. Nevertheless, the administration of the ADSC secretome alleviated the inflammatory response, preserved renal structure and function, suppressed NK cell infiltration into the kidneys, and partially directed the NK cell phenotype towards a normal state. The results of this study provide a detailed perspective on how the ADSC secretome regulates NK cell activity in the context of IL-2 stimulation and chronic inflammation, suggesting its potential as a therapeutic tool for treating NK-mediated inflammatory diseases.

2. Materials and methods

2.1. Cell lines and culture conditions

The cell lines used in this study were generously provided by Professor Jongsun Kim from Yonsei University College of Medicine. NK-92 cells, a human NK cell line, were cultured following the guidelines outlined in the ATCC's product sheet (CRL-2407; ATCC, Manassas, VA, USA). The complete growth medium for NK-92 cells consisted of α minimum essential medium (α-MEM; Gibco, Grand Island, NY, USA) supplemented with 0.2 mM inositol (Sigma-Aldrich, St. Louis, MO, USA), 0.1 mM 2-mercaptoethanol (Gibco), 0.02 mM folic acid (Sigma-Aldrich), 1% penicillin/streptomycin (Gibco), 12.5% heat-inactivated fetal bovine serum (FBS; Corning Inc., Corning, NY, USA), 12.5% heat-inactivated horse serum (Gibco), and recombinant human (rh) IL-2 (5 ng/ml; NKMAX Co Ltd., Seongnam, Republic of Korea), essential for cell survival and activation.

K562, a human myelogenous leukemia cell line, and YAC-1, a mouse lymphoma cell line, were cultured in RPMI-1640 medium (Corning Inc.) supplemented with 10% FBS (Corning Inc.), 1% nonessential amino acids (Gibco), 2% HEPES (Corning Inc.), 1% sodium pyruvate (Corning Inc.), 55 μM 2-mercaptoethanol (Gibco), 0.2% gentamycin (Gibco), and 1% penicillin/streptomycin (Gibco). The cells were maintained in a cell incubator at 37 ℃ with 5% CO_2.

2.2. Human primary cells and culture conditions

MSCs derived from adipose tissue were chosen for their ease of accessibility compared to other tissues like bone marrow, umbilical cord, and placenta. Additionally, they offer the advantage of being suitable for autologous transplantation. Human ADSCs from PromoCell

(Heidelberg, Germany) were expanded in low-glucose Dulbecco's modified Eagle's medium (DMEM; Corning Inc.) supplemented with 10% FBS (Corning Inc.), 1% nonessential amino acids (Gibco), and 1% penicillin/streptomycin (Gibco) for five to six passages. To obtain the ADSC secretome, the culture medium was replaced with low-glucose DMEM without phenol red (Gibco), supplemented with 2 mM L-glutamine (Sigma-Aldrich) and 1% penicillin/streptomycin (Gibco) under serum-free conditions.

Human primary NK cells were isolated from peripheral blood mononuclear cells (PBMCs) of a healthy donor using a human NK Cell Isolation Kit (Miltenyi Biotec, Westphalia, Germany) through negative selection according to the manufacturer's instructions. All procedures were approved by the Institutional Review Board of Severance Hospital at Yonsei University (IRB no. 4-2020-1062; Date of approval: Nov 9, 2020), and informed consent was obtained from healthy donors after thoroughly explaining the nature and potential consequences of the study. Following isolation, purified NK cells (purity > 90%) were immediately cultured in α-MEM-based complete growth medium with 10 ng/mL rhIL-2 for their survival and activation. The cells were maintained in a cell incubator at 37 ℃ with 5% CO_2.

2.3. Generation of human ADSC secretome

Human ADSCs at passage 5 or 6 (P5 or P6) were distributed across a total of 100 10-cm culture dishes (Corning Inc.) at a density of 2×10^5 cells/plate. The cells were then incubated with growth medium in a cell incubator at 37 ℃ and 5% CO_2, allowing expansion to over 90% confluence. After incubation, ADSCs were washed twice with Dulbecco's phosphate-buffered saline (DPBS) to remove serum and phenol red. The medium was replaced with FBS-free medium to induce secretome generation, and the cells were incubated for 48 hours. Subsequently, 1 L of conditioned medium, devoid of serum and phenol red derived from ADSCs, was collected and

centrifuged at 1,800–2,000 rpm for 10 minutes to eliminate cell debris or dead cells. The medium was then concentrated by ultrafiltration using a tangential flow filtration (TFF) capsule (Pall Corporation, New York, NY, USA) containing a 3-kDa molecular weight cut-off (MWCO) membrane, following the manufacturer's instructions. After completing the enrichment, the ADSC secretome was analyzed using a bicinchoninic acid (BCA) protein assay (Thermo Fisher Scientific, Waltham, MA, USA) to estimate protein concentration and immediately stored at −80 ℃. The efficacy of all secretomes used in this study was verified by screening the secretion level of IFN-γ by NK-92 cells.

2.4. Cell cultures

For NK-92 cell maintenance, cells were dispensed in complete medium in T-25 culture flasks (Thermo Fisher Scientific) at a density of 7×10^4 cells/mL with 5 or 10 ng/mL of rhIL-2 (NKMAX Co Ltd.) at a final volume of 5–15 mL. The culture medium was replaced every 2–3 days based on cell density. Strict adherence to the subculturing procedure was maintained, as NK-92 cells are highly sensitive to overgrowth and IL-2 depletion. For ADSC secretome studies, NK-92 cells were seeded into 6-well culture plates (Corning Inc.) at 1×10^5 cells/mL and a final volume of 2 mL, and stimulated using rhIL-2 (5 ng/mL; NKMAX Co Ltd.). In the case of human primary cells, after isolation from the blood of a healthy donor, NK cells were plated at a density of 1×10^6 cells/mL in growth medium and distributed into 24-well culture plates (Corning Inc.) with or without 10 ng/mL of rhIL-2 (NKMAX Co Ltd.). In the case of mouse priary cells, after isolation from the spleen of mice, NK cells were palted at a density of 8×10^5 or 1×10^6 cells/mL in growth medium and distributed into 48-well culture plates (Corning Inc.) with 100 ng/mL of recombinant mouse (rm) IL-2 (NKMAX Co Ltd.).

2.5. Cell counting kit (CCK)-8 assay

To assess cell viability, a CCK-8 assay kit (Sigma-Aldrich) was employed following the manufacturer's guidelines. Briefly, 1×10^4 NK-92 cells were seeded in triplicate in a 96-well flat-bottom plate (SPL Life Sciences, Pocheon, Republic of Korea), each well containing 100 μL of medium. The cells were then incubated with or without the ADSC secretome for 48 hours. Subsequently, 10 μL of CCK-8 reagent was added to each well, and the plate was incubated for 4 hours at 37 ℃. Finally, the absorbance was measured at 450 nm using a microplate reader (Molecular Devices, San Jose, CA, USA).

2.6. Cell proliferation assay

Cell proliferation was evaluated using carboxyfluorescein diacetate succinimidyl- ester (CFSE; eBioscience, San Diego, CA, USA) following the manufacturer's protocol. NK-92 cells were labeled with 1 μM CFSE and cultured at 1×10^5 cells/mL in a 24-well plate (Corning Inc.) for 48 or 96 hours with various concentrations of the ADSC secretome. The cells were analyzed using a BD FACSVerse instrument (BD Biosciences, Franklin Lakes, NJ, USA), and data were processed using FlowJo v10 software (FlowJo LLC, Ashland, OR, USA).

2.7. Enzyme-Linked Immunosorbent Assay (ELISA)

The concentrations of IFN-γ, IL-10, GM-CSF, perforin, and granzyme B in the culture supernatants were quantified using ELISA kits (BD Biosciences; R&D Systems, Minneapolis, MN, USA; Mabtech AB, Nacka Strand, Sweden) as per the manufacturer's instructions. Absorbance was measured at 450 and 570 nm using an ELISA microplate reader (Molecular Devices).

2.8. Cytotoxicity assay

The cytolytic activity of NK cells against target cells was assessed using a Calcein-AM Release Assay (Invitrogen, Carlsbad, CA, USA). K562 or YAC-1 target cells were stained with 1 μM calcein-AM for 10 minutes at 37 ℃, washed with PBS, and resuspended in RPMI complete medium. Subsequently, 1×10^4 target cells in 100 μL medium were plated in quadruplicate into a round-bottom 96-well plate (Thermo Fisher Scientific) and incubated for 3–4 hours with 100 μL of NK cells at varying concentrations to achieve effector-to-target (E:T) ratios. The co-culture supernatant, containing calcein-AM released from lysed target cells, was measured using a Varioskan Flash fluorometer (ex/em = 494/517 nm; Thermo Fisher Scientific). The percentage of specific lysis induced by NK cells was calculated using the following formula: The percentage of specific lysis caused by NK cells was calculated according to the following formula:

$$\%\ \textbf{specific lysis} = \frac{experimental\ \ release_{Avg} - spontaneous\ \ release_{Avg}}{maximal\ \ release_{Avg} - spontaneous\ \ release_{Avg}} \times 100$$

where maximal release was achieved with the addition of Triton X-100 (final concentration of 2%; Sigma-Aldrich).

2.9. CD107a degranulation assay

NK cell degranulation was quantified using PE-conjugated CD107a detection. NK cells pre-treated with or without the ADSC secretome for 48 hours were plated into a round-bottom 96-well plate (Thermo Fisher Scientific) with 2×10^4 K562 target cells in a final volume of 200 μL. After incubation with PE-anti-CD107a antibody (BD Biosciences) at a final dilution of 1:20 for 1 hour at 37 ℃, GolgiPlug (1,000× dilution; BD Biosciences) containing brefeldin A, inhibiting intracellular protein transport, was added and incubated for 2–3 hours. Subsequently, cells were stained with a PE-Cy7-conjugated CD56 monoclonal antibody for 30 minutes at 4 ℃. CD107a

expression in NK cells was analyzed using a BD LSRFortessa X-20 instrument (BD Biosciences), and data were processed using FlowJo v10 software (FlowJo LLC).

2.10. Flow cytometry and antibodies

For surface antigens, cells were incubated with the appropriate monoclonal antibodies (mAbs) diluted 1:100 or 1:200 for 30 minutes at 4 ℃ and washed with PBS supplemented with 5% FBS. For intracellular antigens, cell suspensions were preincubated with phorbol 12-myristate 13-acetate (PMA; 50 ng/mL; Sigma-Aldrich), ionomycin (750 ng/mL; Sigma-Aldrich), and GolgiPlug (1 μg/mL; BD Biosciences) for 4 hours. Subsequently, cells were surface-stained for the indicated markers after harvesting from *in vitro* cultures. After fixing with intracellular (IC) fixation buffer (eBioscience) for 20 minutes at 18 ℃ to 25 ℃ and permeabilizing with permeabilization buffer (eBioscience), intracellular cytokine staining was performed using the appropriate monoclonal antibodies diluted 1:100 or 1:200 for 45 minutes at 18 ℃ to 25 ℃. For intranuclear antigen FOXP3, cells were fixed and permeabilized using the FOXP3/Transcription Factor Staining Buffer Set (eBioscience), following the manufacturer's instructions. Data were acquired using a BD LSRFortessa X-20 instrument (BD Biosciences) and analyzed with FlowJo v10 software (FlowJo LLC). Fluorophore-conjugated mAbs against humans used are as follows. BV421-CD56 (HCD56), FITC-CD56 (HCD56), FITC-CD3 (HIT3a), PE-CD56 (HCD56), PE-NKp46 (9E2), PE-CD96 (NK92.39), PE-TIGIT (A15153G), PE-CD94 (DX22), PE-TIM-3 (F38-2E2), PE-IL-10 (JES3-19F1), PE-granzyme B (QA16A02), BV711-CD56 (HCD56), BV711-NKp30 (P30-15), BV711-IFN-γ (4S.B3), BV711-perforin (dG9), PE-Cy7-CD16 (3G8), and PE-Cy7-CD25 (BC96) were obtained from BioLegend. PE-CD107a (H4A3), PE-CD122 (Mik-β2), BV711-NKG2D (1D11), BV711-CD132 (AG184), and PE-Cy7-CD56 (B159) were purchased from BD Biosciences. All fluorophore-conjugated mAbs were diluted at 1:100 or 1:200.

Neutralizing antibodies, anti-ANXA1, anti-DKK3, anti-LGALS3BP, anti-PROS1, and anti-PEDF were purchased from Abcam (Cambridge, UK).

Fluorophore-conjugated mAbs against mice used are as follows. BV421-NK1.1 (PK136), BV421-NKp46 (29A1.4), BV421-granzyme B (QA18A28), BV421-Ly6G (1A8), BV421-IL-17A (TC11-18H10.1), BV421-CD44 (IM7), BV421-IgM (RMM-1), BV421-CD8 (53-6.7), FITC-NK1.1 (PK136), FITC-CD3 (145-2C11), FITC-CD45 (30-F11), FITC-B220 (RA3-6B2), FITC-CD11b (M1/70), PE-NK1.1 (PK136), PE-DNAM1 (10E5), PE-perforin (S16009A), PE-CD96 (3.3), PE-FOXP3 (MF-14), PE-CD45 (30-F11), PE-F4/80 (BM8), PE-CD62L (MEL-14), PE-IgD (11-26c.2a), BV650-NK1.1 (PK136), BV650-CD45 (30-F11), BV650-CD25 (PC61), BV650-CD4 (RM4-5), BV711-NK1.1 (PK136), BV711-CD45 (30-F11), BV711-CXCR5 (L138D7), BV711-CD8 (53-6.7), PE-Cy7-NK1.1 (PK136), PE-Cy7-CD45 (30-F11), PE-Cy7-CD19 (6D5), and PE-Cy7-TCRβ (H57-597) were obtained from BioLegend. BV421-CD94 (18d3), BV421-CD45 (30-F11), BV421-CD25 (PC61), BV421-CD138 (281-2), BV421-CD132 (TUGm2), FITC-CD8 (53-6.7), PE-CD4 (GK1.5), PE-T- and B-cell activation Ag (GL7), BV650-CD244 (2B4), BV650-Ly49C/I (5E6), BV650-IL-10 (JES5-16E3), BV650-TCRβ (H57-597), BV711-NKG2D (CX5), BV711-Ly49A (A1), and BV711-IFN-γ (XMG1.2), BV711-TCRβ (H57-597), BV711-CD122 (TM-b1), BV711-IgG1 (A85-1), BV711-CD1d (1B1), and PE-Cy7-CD86 (GL1) were purchased from BD Biosciences. PE-Cy7-CD4 (GK1.5) was purchased from Cytek Biosciences (Fremont, CA, USA). PE-IL-21 (149204) was purchased from R&D systems. PE-Ly49G (AT-8) was purchased from Miltenyi Biotec. Flow cytometry analyses were performed after Fc receptor blocking with anti-CD16/32 (2.4G2; Biolegend).

2.11. Western blotting and antibodies

To investigate the downstream signaling cascade of IL-2, responsible for the survival and activation of NK cells, phosphorylated and total proteins were analyzed. NK cells were collected and washed twice with PBS to remove residual medium. Subsequently, they were lysed in RIPA buffer (Biosesang, Seongnam, Republic of Korea) containing a complete mini protease inhibitor cocktail (Roche Diagnostics, Pleasanton, CA, USA) and PhosSTOP phosphatase inhibitor cocktail (Roche Ciagnostics). The homogenization was carried out on ice, and the cell lysates were then centrifuged at 12,000 rpm for 15 minutes at 4 ℃ to remove cell debris. Protein concentrations were determined using a BCA protein assay (Thermo Fisher Scientific).

Next, equal amounts of cellular proteins were separated through sodium dodecyl- sulfate (SDS)-polyacrylamide gel electrophoresis (PAGE) and transferred onto methanol-activated polyvinylidene difluoride (PVDF) membranes (Merck Millipore, Darmstadt, Germany). Following blocking with a blocking solution (TransLab, Elgin, IL, USA), membranes were probed with primary antibodies for 2 hours at 18 ℃ to 25 ℃. Subsequently, the membranes underwent six washes for 30 minutes in Tris-buffered saline with Tween 20 (TBS-T), followed by incubation with species-appropriate horseradish peroxidase (HRP)-conjugated secondary antibodies for 1 hour at 18 ℃ to 25 ℃. After an additional eight washes lasting 40 minutes, proteins were visualized using a West-Q Pico ECL solution (GenDEPOT, Katy, TX, USA) or an EZ-Western Lumi Femto kit (DoGenBio, Seoul, Republic of Korea) and detected with an Amersham ImageQuant 800 biomolecular imager (Cytiva, Marlborough, MA, USA). The signal intensities of immunoblot bands were quantified using ImageJ software (NIH, Bethesda, MD, USA) and Multi Gauge V3.0 software (Fujifilm, Tokyo, Japan). Primary and secondary antibodies were used for western blotting. JAK1 (D1T6W; 1:1000 dilution), p-JAK1(cat. no. 3331; 1:1000), JAK3 (5H2; 1:1000), p-JAK3 (D44E3; 1:1000), p-STAT5 (C11C5; 1:1000), AKT (cat.

no. 9272; 1:1000), p-AKT (D9E; 1:1000), ERK1/2 (137F5; 1:1000), p-ERK1/2 (D13.14.4E; 1:2000), CIS (D4D9; 1:500), DUSP4 (D9A5; 1:500), SHP1 (C14H6; 1:1000), p-SHP1 (D11G5; 1:1000), SHP2 (D50F2; 1:1000), p-SHP2 (cat. no. 3703; 1:1000), SHIP1 (D1163; 1:500), p-SHIP1 (cat. no. 3941; 1:500), HRP-linked mouse IgG (cat. no. 7076; 1:2000), and HRP-linked rabbit IgG (cat. no. 7074; 1:2000) were purchased from Cell Signaling Technology (Danvers, MA, USA). DTX1 (cat. no. HPA055275; 1:500) was purchased from Atlas Antibodies (Bromma, Sweden), STAT5 (cat. no. 610191; 1:200) was purchased from BD Biosciences, and β-Actin (C4; 1:1000) was purchased from Santa Cruz Biotechnology (Dallas, TX, USA).

2.12. Quantitative real-time PCR (qRT-PCR)

To analyze gene expression, total RNA was isolated using the RNeasy Micro kit (QIAGEN, Hilden, Germany) and converted to complementary DNA (cDNA) utilizing the RT PreMix cDNA synthesis kit (iNtRON-Biotechnology, Seongnam, Republic of Korea) following the manufacturer's protocols. Quantitative real-time polymerase chain reaction (qPCR) was conducted using a StepOne Plus or Viia7 system (Applied Biosystems) with qPCRBIO SyGreen Mix (PCR Biosystems, London, UK), as per the manufacturer's instructions. Melting curve analysis was immediately performed after amplification to confirm primer specificity. Relative RNA expression levels were normalized to *GAPDH* messenger RNA (mRNA), a housekeeping gene, utilizing the $2^{-\triangle\triangle Ct}$ calculation method. The human primer sequences used for the qRT-PCR analysis were as follows:

CISH, 5′-GAACACACCAGCCACTGTCC-3′ (forward) and
5′-GCCAGCAAAGGACGAGGTC-3′ (reverse);

SOCS1, 5′-GTAGCACACAACCAGGTGGC-3′ (forward) and
5′-GGAGGAGGAAGAGGAGGAAGG-3′ (reverse);

SOCS2, 5′-TGCAAGGATAAGCGGACAGG-3′ (forward) and
5′-CTGCAGAGATGGTGCTGACG-3′ (reverse);

SOCS3, 5′-TTTCGCTTCGGGACTAGCTC-3′ (forward) and
5′-TTGCTGTGGGTGACCATGG-3′ (reverse);

DTX1, 5′-CCTGTGAATGGTCTGGGCTTC-3′ (forward) and
5′-CAGCGGCTGTGCTCATTCA-3′ (reverse);

DUSP4, 5′-CTGGACTGCAGACCGTTCCT-3′ (forward) and
5′-GCCGCACGATGGTGTTACAG-3′ (reverse);

PTPN14, 5′-GCAAGAAAGGACGGTGTGGC-3′ (forward) and
5′-ACGGACCGACTGGATCT-CCT-3′ (reverse);

PTPRF, 5′-GCGCTTCGAGGTCATTGAGT-3′ (forward) and
5′-ATGGCTTCATCTCGCTGCAC-3′ (reverse);

GAPDH, 5′-CAGCGACACCCACTCCTCCACCTT-3′ (forward) and
5′-CATGAGGTCCACCACCCTGTTGCT-3′ (reverse).

2.13. Proteomic analysis

Proteomic analysis was conducted by the Proteomics Platform at ProteomTech Inc. (Seoul, Republic of Korea) using secretome sets obtained from three independent donors. The Braford protein assay was employed for the quantification of secretome sets. Additionally, 2-dimensional gel electrophoresis (2-DE) was performed to separate proteins, with visualization achieved using

the Coomassie Brilliant Blue G-250 staining method. Image Master 2D Platinum Software (Cytiva) was utilized for computer analysis of the 2-DE images, determining the expression level of each spot by dividing the volume of each spot by the total volume of all spots in the gel.

Following image analysis, spots were subjected to in-gel trypsin digestion and analyzed through liquid chromatography with tandem mass spectrometry (LC-MS/MS) using a nanoACQUITY UPLC and LTQ Orbitrap XL mass spectrometer (Thermo Fisher Scientific). Individual MS/MS spectra were processed with SEQUEST software (Thermo Fisher Scientific) and searched in the NCBI database via the MASCOT search program (Matrix Sciences, Chicago, IL, USA). Search parameters for data analysis were set as follows: carbamidomethyl (C) as a fixed modification, deamidated (NQ), and oxidation (M) as variable modifications, with 10 ppm as the tolerance of peptide mass, 0.8 Da as MS/MS ion mass tolerance, and 2 as the allowance of missed cleavage. For bioinformatics analysis, Gene Ontology (GO) terms were assessed using the Database for Annotation, Visualization, and Integrated Discovery (DAVID) tools. Peptides were selected based on the significance threshold in the identity score, with a *P*-value of $\leq$ 0.05.

2.14. mRNA sequencing and analysis

To investigate gene expression patterns in human primary NK cells influenced by the ADSC secretome, RNA was isolated from NK cells obtained from six healthy donors. The RNeasy Micro kit (QIAGEN) was used for RNA isolation, following the manufacturer's protocols. The integrity of the extracted RNA was assessed using a 2100 Bioanalyzer instrument (Agilent Technologies), which provided an RNA Integrity Number (RIN) value.

RNA libraries were prepared employing the TruSeq stranded mRNA library kit (Illumina), incorporating polyA selection of mRNA according to the manufacturer's guidelines. The purified RNA underwent random fragmentation for short-read sequencing, and cDNA was synthesized.

Adaptors were added to both ends of the synthesized cDNA fragments, followed by PCR amplification to generate a sufficient amount for sequencing. Sequencing was carried out using a NovaSeq 6000 platform (Illumina). Raw RNA-seq reads underwent quality control (QC) using FastQC v0.11.7 (Babraham Institute) and were subsequently trimmed with Trimmomatic v0.38 to minimize alignment errors. HISAT2 v2.1.0 was employed to map RNA-seq reads to a human genome population, and StringTie v2.1.3b facilitated transcript assembly to obtain expression profile values. Differential gene expression analysis between control and treatment groups was conducted by normalizing gene-level read counts using the DESeq2 package. A total of 352 genes meeting the criteria of $|fc| \geq$ 2-fold pairwise change and nbinomWaldTest raw *P*-value < 0.05 were selected.

The selected genes underwent hierarchical clustering for visualization on a heatmap and dendrogram image. Volcano plots, created using the composite metric ($\log_2 fc \times -\log_{10}$ adjusted *P*-value), and dot plots for Gene Ontology (GO) enrichment were generated to provide a comprehensive understanding of differentially expressed genes (DEGs) between the two groups.

2.15. Animals

Nine-week-old male C57BL/6 mice were purchased from OrientBio (Sungnam, Republic of Korea) and allowed to acclimatize for at least 1 week under specific pathogen-free (SPF) conditions prior to sacrifice for obtaining NK cells. Twenty-week-old female NZB/W F1 mice, used as a lupus nephritis model, were purchased from SLC Inc. (Shizuoka, Japan), acclimated for 1 week prior to the start of the study, and maintained under SPF conditions. The NZB/W F1 mouse, a hybrid breed resulting from the crossbreeding of New Zealand black (NZB) and New Zealand white (NZW) mice, is well-established model for lupus research. These female mice spontaneously develop lupus-like symptoms, including splenomegaly, lymphadenopathy,

circulating anti-dsDNA autoantibodies, and glomerulonephritis.[64] Lupus symptoms manifest in these mice after reaching 20 weeks of age, progressing to glomerulonephritis, which ultimately leads to end-stage renal disease between 40 to 48 weeks old.[65,66] Failure to intervene can result in fatal outcomes. All animal experiments were reviewed and approved by the Institutional Animal Care and Use Committee (IACUC) of Yonsei University Health System (approval no.: 2020-0291; Date of approval: Mar 24, 2021 and approval no.:2023-0059; Date of approval: Mar 28, 2023). Every effort was made to reduce animal discomfort and minimize the number of animals utilized.

2.16. SLE study design

At 21 weeks of age, NZB/W F1 mice were divided evenly based on body weight and proteinuria score into two groups, each consisting of 9–10 mice and then tail cutting was performed for blood collection. Administration commenced at 22 weeks of age with intrapaeritoneal (i.p.) injections of ADSC secretome (200 μg/mouse; n = 9) or PBS (equal volume as ADSC secretome; n = 10), serving as a vehicle control, administered twice weekly for 19 weeks. Additionally, 21-week-old young female NZB/W F1 mice were employed as healthy controls (n = 4) at the end of the study. Disease progression was monitored weekly based on proteinuria, body weight, and behavior, while serum samples were collected every two weeks. Spot urine proteinuria was assessed using albumin reagent strips (URiSCAN; Yongdong Pharmaceutical Co., Seoul, Republic of Korea) and scored semi-quantitively according to manufacturer's instructions: grade 0 (negative), grade 1+ (30 mg/dl), grade 2+ (100 mg/dl), grade 3+ (300 mg/dl), or grade 4+ (≥1000 mg/dl). Half scores were given when the color fell between two whole values. Severe proteinuria was defined as having more than two consecutive URiSCAN readings of grade 3+ or higher. The experiment was terminated upon reaching 42 weeks of age, at which point all surviving animals were euthanized, and major tissues (whole blood, spleen, and kidneys) were harvested for further analysis.

2.17. Preparation of mouse primary cells

Mouse primary NK cells were isolated from splenocytes of C57BL/6 mice using a mouse NK Cell Isolation Kit (Miltenyi Biotec) via negative selection following the manufacturer's instructions. After isolation, purified NK cells (purity > 90%) were promptly cultured in α-MEM-based complete growth medium with 100 ng/mL rmIL-2 to support their survival and activation. The cells were maintained in a cell incubator at 37 ℃ with 5% CO_2.

Single-cell suspenstions were prepared from the blood, spleen, and kidneys of NZB/W F1 mice. Whole blood was obtained by cardiac puncture; half was collected in Microtainer tubes with K_2EDTA (BD Biosciences) for flow cytometry analysis of leukocytes, and the other half was collected in Microtainer Serum Separator Tubes (SST) (BD Biosciences) for serological analaysis. For leukocyte analysis of blood, collected blood was transferred into FACS tubes, briefly vortexed with RBC Lysis Buffer (Biolegend), and incubated for 20 minutes at 18 ℃ to 25 ℃. After RBC lysis, blood cells were washed with PBS until the redness disappeared.

Mouse spleen cells were obtained by puncturing both ends of the spleen with a 19G needle and gently scraping out the spleen's interior, leaving the splenic capsule behind. These cells were incubated in RBC Lysis Buffer to remove red blood cells (RBCs) and passed through a 70-μm cell strainer (SPL Life Sciences).

For leukocytes analysis of kidneys, kidneys were cut into several pieces, transferred into the gentleMACS C tube containing the enzyme mix of the Multi Tissue Dissociation Kit 2 (Miltenyi Biotec), and digested using the gentleMACS Dissociator with Heaters (Miltenyi Biotec) following manufacturer's instructions. Digested kidneys were passed through a 100-μm cell strainer (SPL Life Sciences), and RBCs were lysed with RBC Lysis Buffer.

2.18. Serological evaluation

To assess renal function, we measured blood urea nitrogen (BUN), serum creatinine (Cr), and serum albumin (Alb) levels in mouse serum samples. These samples were applied onto DRI-CHEM slides (BUN-P Ⅲ, CRE-P Ⅲ, ALB-P Ⅲ; Fujifilm) and analyzed using the DRI-CHEM NX500 automatic dry-chemistry analyzer (Fujifilm).

For cytokine analysis, we quantified TNF-α, IFN-γ, IL-4, IL-6, IL-10, IL-12p70, IL-17A, and MCP-1 levels in serum samples. This quantification was performed using a Milliplex Mouse Cytokine/Chemokine Magnetic Bead Panel assay (Merck Millipore) at a final dilution of 1:2, following the manufacturer's protocol. Additionally, we measured serum immunoglobulin levels, including IgM, IgG1, IgG2a, IgG2b, and IgG3, using a Milliplex Mouse Immunogolobulin Isotyping Magnetic Bead Panel assay (Merk Millipore) at a final dilution of 1:25,000. The analysis was conducted on the Luminex 200 system (Luminex, Austin, TX, USA).

2.19. Renal histology

For pathological analysis, kidneys were fixed in 10% phosphate-buffered formalin, embedded in paraffin, and stained with hematoxylin and eosin (H&E) and periodic acid-Schiff (PAS) by the histopathology service of the Department of Pathology, Yonsei Biomedical Research Institute, Yonsei University College of Medicine. Nephritis grading was conducted using a semi-quantitative 0−4 scale: 0 (no damage), 1 (mild damage, 1–19%), 2 (moderated damage, 20–50%), 3 (marked damage, 51–75%), or 4 (severe damage, >75% of the glomeruli affected).[67] Thirty glomeruli from each slide were examined, and abnormal glomeruli (e.g., with endocpillary proliferation, mesangial expansion, extracapillary proliferation, crescent formation, necrosis) were counted. The diameter of 15 randomly selected glomeruli from each slide was determined using ImageJ software (NIH).

For immunofluorescence staining, fresh kidneys were frozen in liquid nitrogen, embedded in optical cutting temperature (OCT) compound, and stored at −80 ℃ until subsequent experiments. Tissues were cryosectioned, air-dried, fixed in 4% paraformaldehyde, stained with FITC-conjugated anti-mouse C3 (cat. no. 55500; 1:400, MP Biomedicals, Irvine, CA, USA), Alexa-594-conjugated goat anti-mouse IgG (cat. no. A-21203; 1:500, Invitrogen), and mounted with VECTASHIELD HardSet media containing DAPI (Vector Laboratories, Burlingame, CA, USA) by the histopathology service of the Department of Pathology, Yonsei Biomedical Research Institute, Yonsei University College of Medicine. Stained sections were observed under an LSM 780 confocal laser scanning microscope (Carl Zeiss, Oberkochen, Germany), and image processing was conducted using the ZEN software system (Carl Zeiss). Mean fluorescence intensity (MFI) of C3 and IgG deposition in the glomeruli of the sections was quantitated by ImageJ software (NIH).

2.20. Statistical analysis

Experiments were independently conducted and repeated at least three times, consistently yielding similar results. Statistical analyses were performed using GraphPad Prism 5 or 8 software (GraphPad Software, San Diego, CA, USA). The data are presented as mean ± SEM (standard error of the mean). Two-tailed Student's *t*-tests were used to evaluate the statistical significance between treatment and control values for both paired and unpaired data. In some experiments, data were underwent one- or two-way analysis of variance (ANOVA) followed by Dunnett's or Holm-Sidak's multiple comparisons test to compare the control group against all treatment groups. Survival data were analyzed using the Log-rank (Mantel-Cox) test. Statistical significance levels were denoted as follows: not significant (ns), $*P < 0.05$, $**P < 0.01$, $***P < 0.001$, and $****P < 0.0001$.

3. Results

Chapter 1

3.1. Immunomodulatory effects of the ADSC secretome on human NK cells

3.1.1. Impact of the ADSC secretome on NK-92 cell viability and proliferation

In light of the contradictory effects of MSCs on NK cells, particularly their secretome's ability to impede NK cell proliferation and activation, our investigation centered on the influence of the ADSC secretome on the viability and proliferation of NK-92 cells, a human NK cell line. The ADSC secretome was introduced at varying concentrations, ranging from 25 μg/ml to 200 μg/ml, for durations spanning 48 to 96 hours. Notably, IL-2, acknowledged for its essential role in NK-92 cell survival and activation,[68] served as the stimulus for NK cell activation throughout all experiments. Evaluation of cell viability revealed no observable changes at concentrations below 200 μg/ml of the ADSC secretome when compared to the IL-2 alone control group (Fig. 4A). It is noteworthy that NK-92 cells exhibited minimal proliferation without IL-2 stimulation for 48 hours. Furthermore, the ADSC secretome demonstrated negligible impact on NK-92 cell proliferation, as indicated by CFSE dilution, relative to the IL-2 control (Fig. 4B). Subsequent examination of IFN-γ levels in the culture supernatant of NK-92 cells aided in identifying optimal inhibitory concentrations of the ADSC secretome. At all concentrations assessed at 48 hours, the ADSC secretome effectively suppressed IFN-γ secretion by NK-92 cells (Fig. 4C). Consequently, all experiments were conducted at non-toxic concentrations of the ADSC secretome, specifically those inhibiting cytokine secretion by NK-92 cells (25 and 150 μg/ml). These findings underscore that while the ADSC secretome inhibits IFN-γ secretion by NK-92 cells, it does not exert discernible effects on cell viability and proliferation.

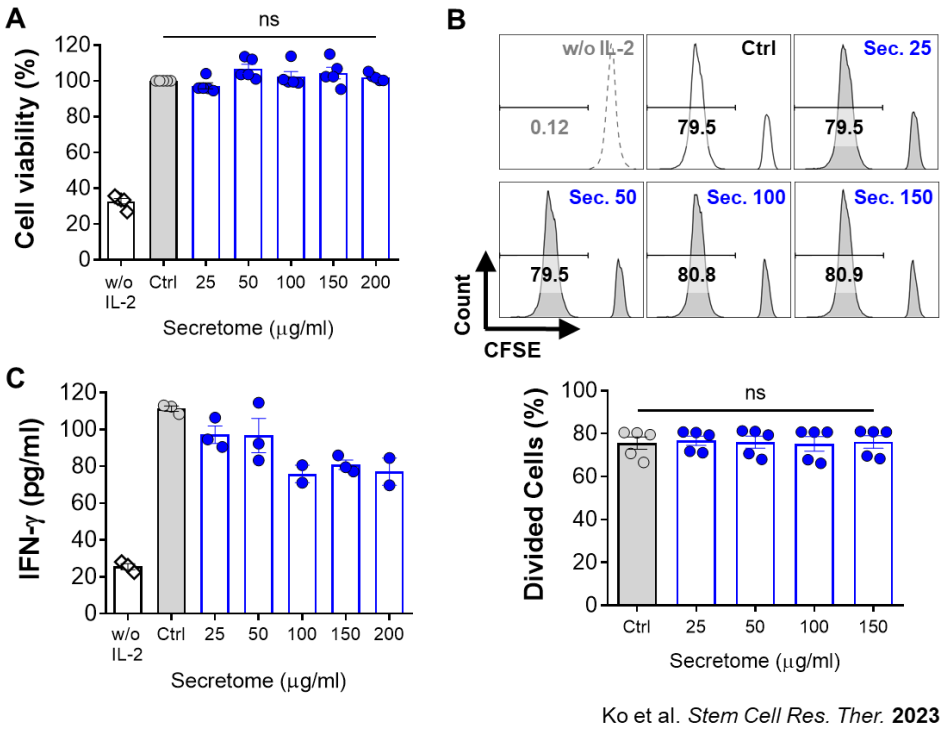

Ko et al. *Stem Cell Res. Ther.* **2023**

Figure 4. Viability, proliferation, and natural killer (NK) cell-inhibitory concentrations of the adipose tissue-derived stem cell (ADSC) secretome. (A) Cell viability of IL-2-activated NK-92 cells after 48-hour incubation with the ADSC secretome (blue circles) at various concentrations (horizontal axes) using the CCK-8 assay. (B) Cell proliferation of IL-2-activated NK-92 cells treated as described in A for 96 hours using the CFSE staining assay. Error bars represent mean ± SEM of five independent experiments. Statistical significance was determined using one-way ANOVA with Dunnett's multiple comparison test; not significant (ns). (C) The level of IFN-γ secretion by NK-92 cells treated with the ADSC secretome at various concentrations (blue circles; horizontal axis) after stimulation with 5 ng/ml of rhIL-2 for 48 hours. IFN-γ concentration in the culture supernatant of NK-92 cells was estimated by ELISA. Data represent two or three independent experiments, and error bars indicate mean ± SEM.

3.1.2. Modulation of IL-2–induced activation in NK-92 cells by the ADSC secretome

In recent years, the immunomodulatory potential of MSCs, particularly through their secretome, has been a subject of extensive research. However, conflicting findings persist, especially in the context of NK cells. This study aimed to explore the impact of the ADSC secretome on NK-92 cell activity. Initially, we assessed effector cytokine and cytolytic granule levels in the supernatant of IL-2–stimulated NK cells. Subsequently, we examined NK cell cytolytic function and degranulation, characterized by granule exocytosis. The ADSC secretome demonstrated a dose-dependent inhibition of IFN-γ, IL-10, and granzyme B (excluding perforin) in the supernatant of IL-2–stimulated NK-92 cells compared to the IL-2 alone control group (Fig. 5A). NK cell cytotoxicity against K562 target cells, a human erythromyeloid leukemia cell line, exhibited an inverse correlation with the concentration of the ADSC secretome in an effector-to-target (E:T) ratio-dependent manner (Fig. 5B, upper). Notably, IL-2–activated NK cells treated with 150 μg/ml ADSC secretome demonstrated a statistically significant reduction in their ability to kill target cells compared to IL-2 alone control NK cells (Fig. 5B, bottom). In the degranulation assay, surface expression and frequency of $CD107a^+$ NK cells, serving as functional markers, were markedly diminished in ADSC secretome-treated NK cells compared to IL-2 alone control NK cells. This was evident through both the lower frequency of $CD107a^+$ NK cells (Fig. 5C, upper and bottom) and reduced mean fluorescence intensity (MFI) (Fig. 5C, right) at all E:T ratios.

NK cell activity is intricately regulated by the interplay of signals from both activating and inhibitory receptors on their surface.[32,33,38,69] Activating receptors of NK cells exhibit specificity for ligands expressed on stressed, virally infected, or tumorigenic cells.[70] Conversely, inhibitory receptors recognize the presence of MHC Class I molecules, thereby integrating multilateral signals to prevent inadvertent NK-mediated damage to healthy cells.[70,71] Given the observed

suppression of NK cell activity by the ADSC secretome, we proceeded to investigate the expression profiles of activating and inhibitory receptors in NK cells. As the concentration of the ADSC secretome increased, the expression level and frequency of activating receptors, including NKG2D, NKp30, and NKp46, in NK-92 cells gradually decreased compared to the IL-2 alone control group (Fig. 6A). This downregulation of the natural cytotoxicity receptor (NCR) family, such as NKp30 and NKp46, and natural killer group 2D (NKG2D), contribute to decreased levels of cytokine secretion and diminished cytolytic function in NK cells.[71,72] Concurrently, the surface expression of inhibitory receptors, such as T-cell immunoglobulin and ITIM domain (TIGIT), CD94, and T-cell immunoglobulin mucin-3 (TIM-3), on NK-92 cells remained stable even in the presence of the ADSC secretome. Interestingly, among these receptors, only CD96 exhibited increased expression in a dose-dependent manner compared with the control group (Fig. 6B). Conversely, the proportion of inhibitory receptor-positive NK cells was minimally affected by the ADSC secretome, with consistently high rates across all groups (Fig. 6B, bottom).

NK cell activity is intricately regulated by the integration of signals from cytokines, notably IL-2.[37,73] IL-2 modulates immune responses by binding to three subunits of the IL-2 receptor (IL-2R): IL-2Rα (CD25), IL-2Rβ (CD122), and IL-2Rγ (CD132), each with varying affinities for IL-2.[74,75] To assess the impact of the ADSC secretome on IL-2R in NK-92 cells, we examined the expression levels of these three IL-2R subunits. The ADSC secretome resulted in decreased expression of CD25 and CD132, while the level of CD122 remained comparable to that observed with IL-2 alone in NK-92 cells (Fig. 6C).

In summary, these findings substantiate that the ADSC secretome restricts IL-2-mediated effector functions of NK cells, encompassing the secretion of effector cytokines and cytolytic granules, as well as impairing cytotoxicity and degranulation. Additionally, the mean expression

level and the proportion of activating receptor-positive (NKG2D, NKp30, and NKp46) NK cells exhibited a gradual reduction with increasing doses of the ADSC secretome. Among inhibitory receptors, only CD96 expression increased notably with a high dose of secretome. Furthermore, the ADSC secretome led to diminished expression levels of IL-2Rα and IL-2Rγ in NK cells.

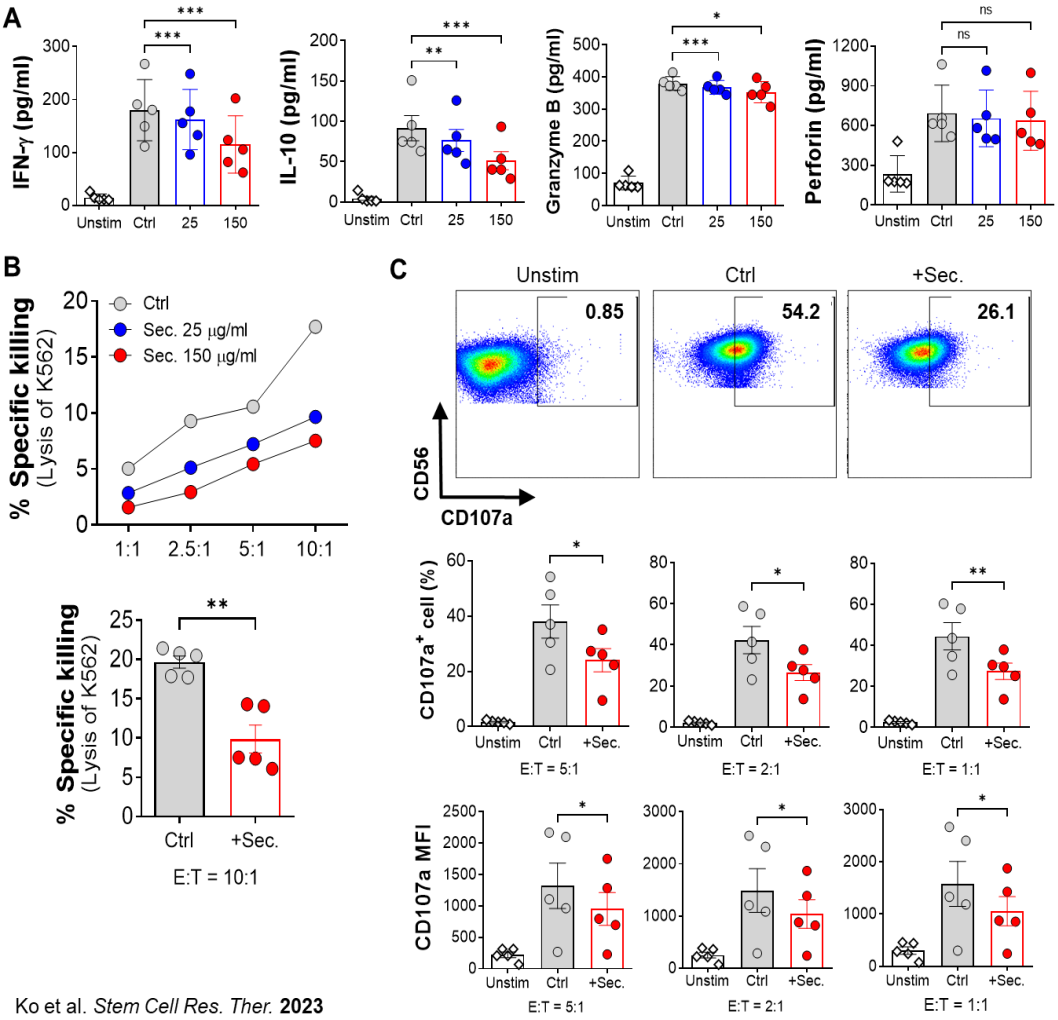

Ko et al. *Stem Cell Res. Ther.* **2023**

Figure 5. Effects of the adipose tissue-derived stem cell (ADSC) secretome on NK-92 cell function. NK-92 cells were cultured for 48 hours with 25 (*25*; blue circles) or 150 μg/ml ADSC secretome (*150*; red circles), or without (*Ctrl*; gray circles), in the presence of 5 ng/ml of rhIL-2. Unstimulated NK cells were also cultured for the negative control (*Unstim*; white diamonds). After treatment with the ADSC secretome (*+Sec.*; red circles) for 48 hours, NK cells were co-cultured with K562 target cells for 4 hours to examine their cytotoxic ability. (A) ELISA measurement of effector cytokines (IFN-γ and IL-10) and cytolytic granules (granzyme B and perforin) in the

supernatant. (B) Cytotoxicity of NK-92 cells against K562 target cells at the indicated NK:K562 (E:T, effector:target) ratios of 1:1, 2.5:1, 5:1, or 10:1 (upper). Cytotoxicity of NK-92 cells at a 10:1 ratio (bottom). (C) Assessment of degranulation marker ($CD56^+$ $CD107a^+$) in activated NK-92 cells using flow cytometry. Dot blot (at a 5:1 ratio, upper), frequency of $CD107a^+$ NK cells (at the indicated ratios, middle), and the expression level of CD107a on NK cells (at the indicated ratios, bottom). Error bars represent mean ± SEM of five to seven independent experiments. Statistical significance was determined using Student's paired two-tailed *t*-test; not significant (ns), $*P < 0.05$, $**P < 0.01$, $***P < 0.001$.

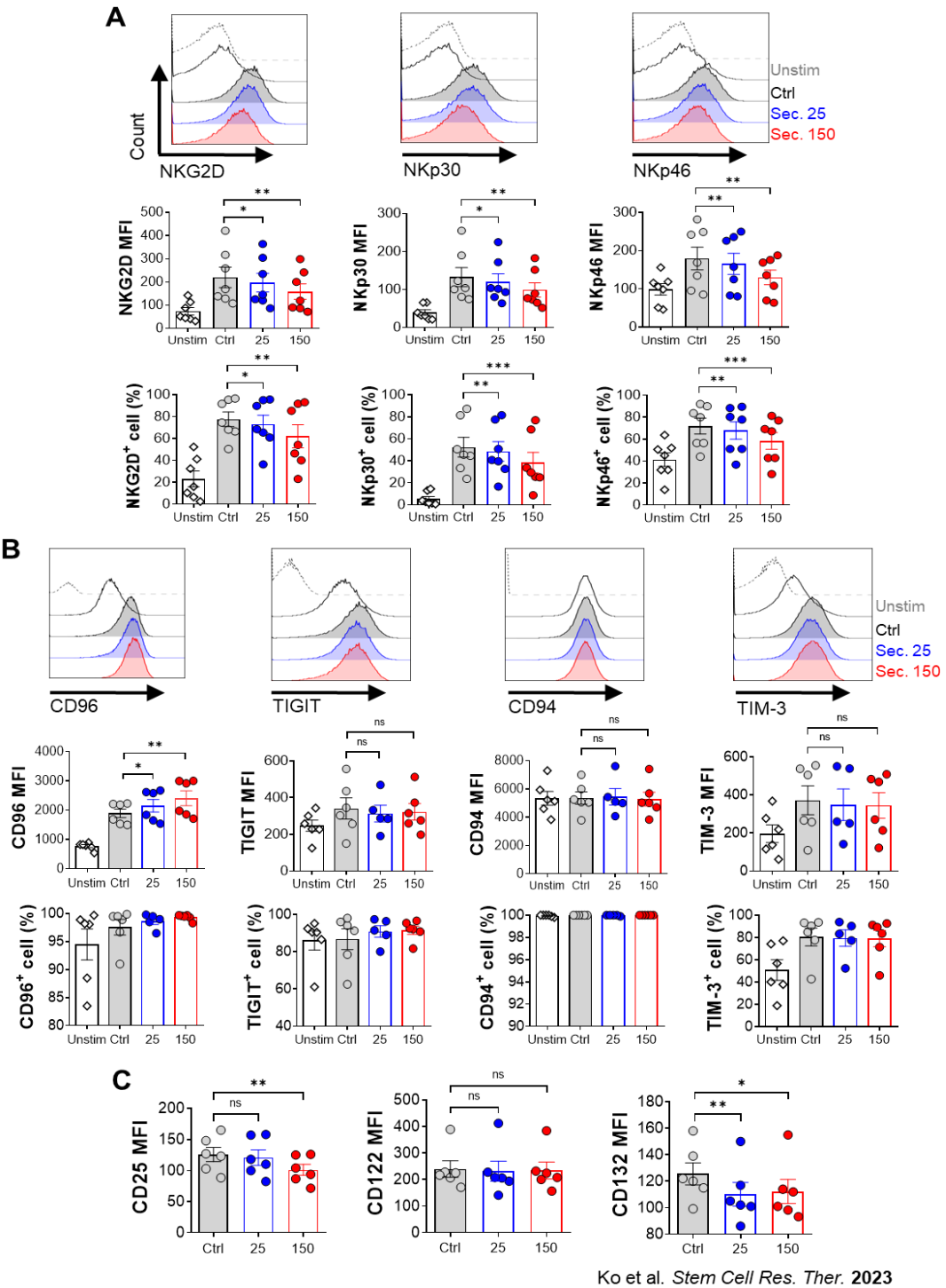

Ko et al. *Stem Cell Res. Ther.* **2023**

Figure 6. Effects of the adipose tissue-derived stem cell (ADSC) secretome on NK-92 cell receptor expression. NK-92 cells were cultured for 48 hours with 25 (*25*; blue circles) or 150 μg/ml ADSC secretome (*150*; red circles), or without (*Ctrl*; gray circles), in the presence of 5 ng/ml of rhIL-2. Unstimulated NK cells were also cultured for the negative control (*Unstim*; white diamonds). (A to C) Flow cytometry analysis of activating receptors (NKG2D, NKp30, and NKp46) (A; histogram, MFI, and frequencies), inhibitory receptors (CD96, TIGIT, CD94, and TIM-3) (B; histogram, MFI, and frequencies), and IL-2 receptors (CD25, CD122, and CD132) (C; MFI only). Error bars represent mean ± SEM of five to seven independent experiments. Statistical significance was determined using Student's paired two-tailed *t*-test; not significant (ns), $*P < 0.05$, $**P < 0.01$, $***P < 0.001$.

3.1.3. Modulation of IL-2 signaling pathways by the ADSC secretome: Focus on JAK-STAT and AKT pathways through CIS regulation

The cytokine IL-2 initiates three key signaling pathways crucial for maturation, homeostasis, and activation: the JAK/STAT, phosphoinositide 3-kinase (PI3K)/protein kinase B (AKT), and extracellular signal-regulated kinase (ERK) 1/2 pathways.[74,76] To elucidate the mechanisms underlying the suppression of IL-2–mediated NK cell activity by the ADSC secretome, we examined the changes in phosphorylated proteins such as pSTAT5, pAKT, and pERK, which are the primary downstream molecules of these signaling pathways triggered by IL-2. In IL-2–stimulated NK-92 cells treated with the ADSC secretome, a significant reduction in phosphorylation levels of STAT5 and AKT, but not ERK, was observed compared to the IL-2 alone control group (Fig. 7A). Subsequently, we investigated whether this reduction in downstream molecules is dependent on the inactivation of IL-2Rβ/γc-associated JAK1 and JAK3 tyrosine kinases. The addition of the ADSC secretome led to a significant reduction in IL-2–supported phosphorylation of JAK1 and JAK3 without altering total JAKs levels compared to IL-2 alone in NK-92 cells (Fig. 7B). This observation suggests that the ADSC secretome diminishes JAK1 and JAK3 phosphorylation, thereby disrupting JAK/STAT and PI3K/AKT pathways by targeting pSTAT5 and pAKT.

We sought to identify the molecular factors responsible for inhibiting IL-2–mediated JAK activity in the cytoplasm of NK cells. As previously documented, several negative regulators govern JAK-STAT signaling through distinct mechanisms, including protein tyrosine phosphatases (PTPs) and suppressors of cytokine signaling (SOCS) proteins.[39,40] PTPs also play a crucial role in inhibitory receptor-mediated suppression by dephosphorylating signaling proteins associated with activating receptors in NK cells.[33,38,77] On the other hand, the SOCS family is induced by various cytokines to negatively regulate cytokine signaling by inhibiting JAK/STAT

activation and promoting proteasomal degradation of signaling substrates.[39,40]

Initially, we explored which cellular phosphatases (SHP-1, SHP-2, and SHIP-1) are involved in JAK/STAT inhibition in NK-92 cells. Despite a notable decrease in the phosphorylation of JAK1 and STAT5 in NK-92 cells treated with the ADSC secretome, there was no discernible increase in the levels of these phosphatases, namely SHPs or SHIP (Fig. 7C). The substantial reduction in JAK1, JAK3, and STAT5 phosphorylation by the ADSC secretome in NK cells did not correlate with the levels of these phosphatases. However, among the SOCS proteins, protein CIS was upregulated during IL-2–mediated activation, and notably, this increase was more pronounced upon treatment with the ADSC secretome (Fig. 7D). These findings suggest that among the SOCS family, protein CIS may serve as a major regulator of NK cell activity through the ADSC secretome.

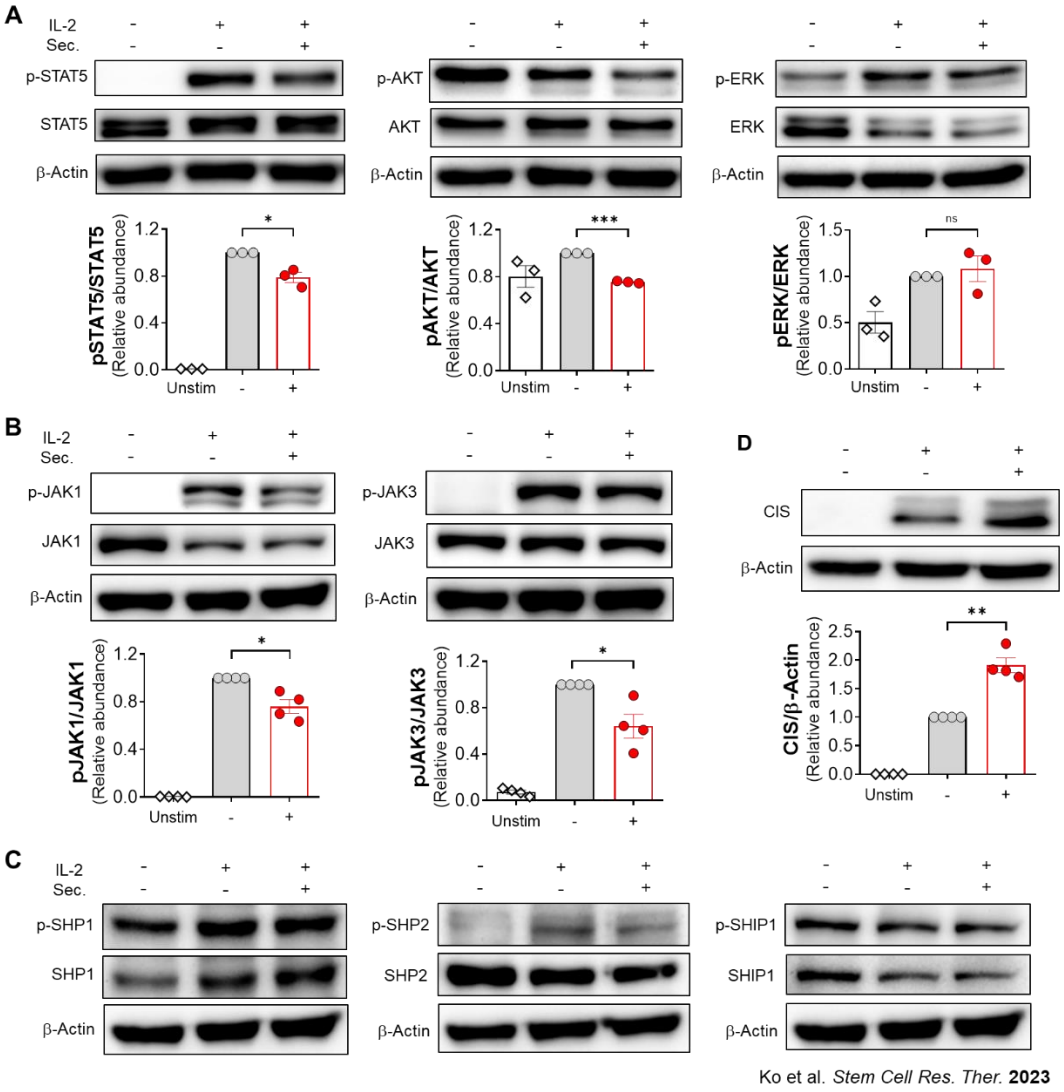

Figure 7. Suppression of JAK-STAT and AKT signaling pathways by the adipose tissue-derived stem cell (ADSC) secretome via upregulation of CIS regulator. NK-92 cells were cultured for 36 hours with 150 μg/ml ADSC secretome (+; red circles), or without (–; gray circles), in the presence of 5 ng/ml of rhIL-2. Unstimulated NK cells were also cultured for the negative control (*Unstim*; white diamonds). Immunoblot analysis revealed alterations in (A) STAT5, AKT, ERK, (B) JAK1, JAK3, (C) SHP1, SHP2, SHIP1, and (D) CIS expressions in NK-92 cells. In groups

A, B, and C, the prefix "p-" denotes a phosphorylated protein. Error bars indicate mean ± SEM of three to four independent experiments. Statistical significance was determined by Student's paired two-tailed *t*-test; not significant (ns), $*P < 0.05$, $**P < 0.01$, $***P < 0.001$.

3.1.4. The ADSC secretome suppresses effector function in human primary NK cells

To validate the observed suppression of effector function by the ADSC secretome in the NK-92 cell line, we collected whole blood samples from healthy donors and isolated NK cells from peripheral blood mononuclear cells (PBMCs). We investigated the production of effector cytokines and cytolytic granules by primary NK cells in the presence or absence of the ADSC secretome. Consistent with the findings in NK-92 cells, the ADSC secretome inhibited the secretion of effector molecules by human primary NK cells in a concentration-dependent manner, leading to decreased production of IFN-γ, GM-CSF, granzyme B, and perforin (Fig. 8A). Meanwhile, unstimulated NK cells lacking IL-2 secreted only trace amounts of cytokines. Furthermore, the cytotoxic activity of human primary NK cells was significantly diminished in the presence of the ADSC secretome compared to IL-2 alone control NK cells, aligning with the results obtained from the NK-92 cell line (Fig. 8B). Additionally, the degranulation assay demonstrated a substantial decrease in the frequency and MFI of membrane CD107a in primary NK cells cultured with the ADSC secretome compared to control NK cells when exposed to K562 cells (Fig. 8C). These findings underscore the inhibitory impact of the ADSC secretome on human primary NK cells.

Continuing with the analysis, we utilized flow cytometry to examine the expression patterns of NK cell activating and inhibitory receptors. Similar to NK-92 cells, human primary NK cells treated with the ADSC secretome exhibited a significant reduction in both expression levels and percentages of activating receptors, with the exception of the proportion of $NKp46^{+}$ cells (Fig. 9A). Concurrently, there was an elevated expression level and percentage of the inhibitory receptor CD96 compared to the control group (Fig. 9B). These findings affirm the consistency between human primary NK cells and NK-92 cells, highlighting the dose-dependent impact of

the ADSC secretome on diminishing the expression levels of NKG2D, NKp30, and NKp46, while elevating the expression level of CD96 in NK cells.

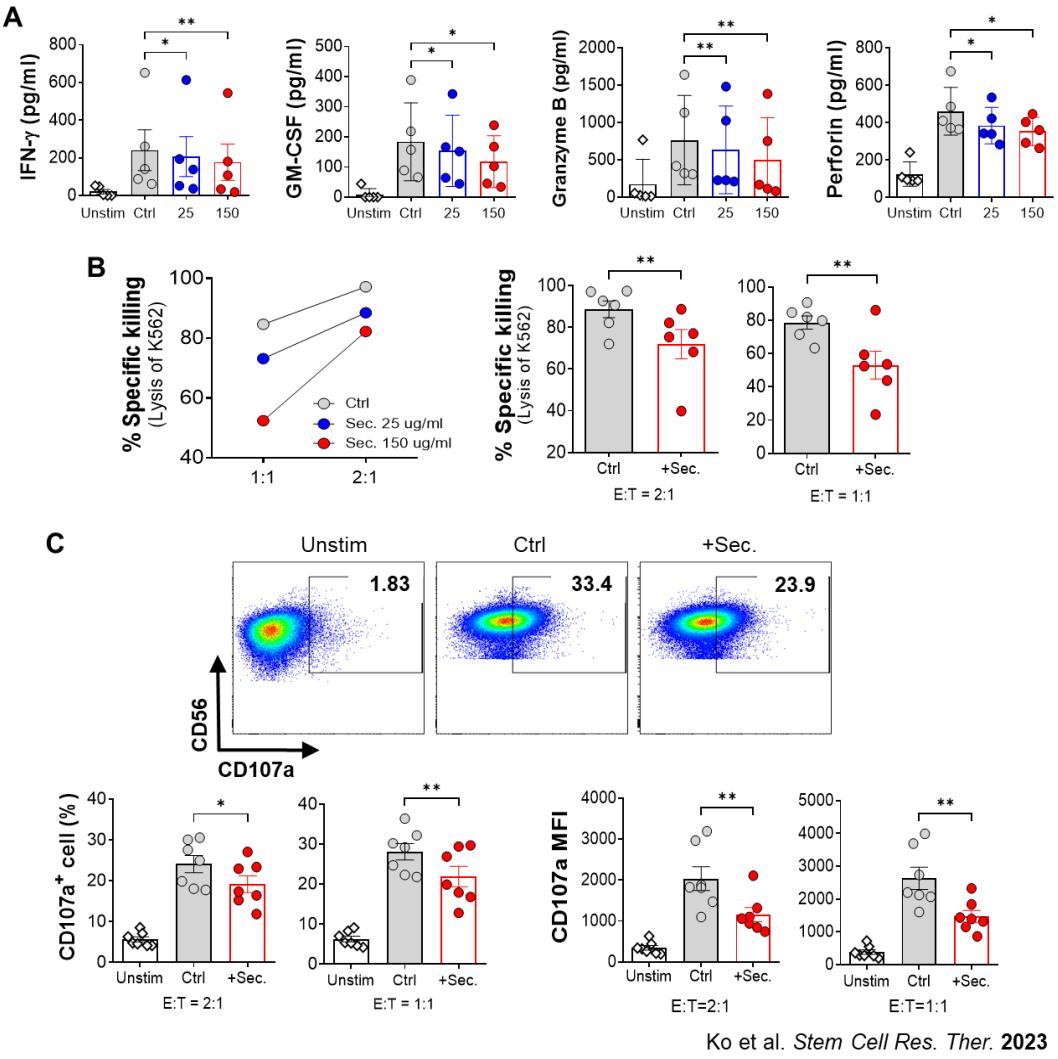

Ko et al. *Stem Cell Res. Ther.* **2023**

Figure 8. Alteration in effector function of human primary NK cells by the adipose tissue-derived stem cell (ADSC) secretome. Human primary NK cells, isolated from PBMCs of a healthy donor, were cultured for 48 hours with 25 (*25*; blue circles) or 150 μg/ml ADSC secretome (*150*; red circles), or without (*Ctrl*; gray circles), in the presence of 10 ng/ml of rhIL-2. Unstimulated NK cells were also cultured for the negative control (*Unstim*; white diamonds). (A) The production of effector cytokines (IFN-γ and GM-CSF) and cytolytic granules (granzyme B and perforin) in the

supernatant was measured by ELISA. (B) Cytotoxicity of primary NK cells against K562 target cells at the indicated NK:K562 (E:T, effector:target) ratios of 1:1 or 2:1 (left side). Stimulated primary NK cells were treated with 150 μg/ml ADSC secretome (+*Sec*.; red circles) for 48 hours, followed by co-culture with K562 target cells at the indicated ratios for 4 hours (right side). (C) Degranulation marker from activated primary NK cells was assessed using flow cytometry ($CD3^-$ $CD56^+$ $CD107a^+$) as shown in the dot blot (at a 1:1 ratio, upper), frequency of $CD107a^+$ NK cells (at the indicated ratios, bottom left side), and the expression level of CD107a on primary NK cells (at the indicated ratios, bottom right side). Error bars represent mean ± SEM of five to seven healthy donors. Statistical tests were determined by Student's paired two-tailed *t*-test; not significant (ns), $*P < 0.05$, $**P < 0.01$, $***P < 0.001$.

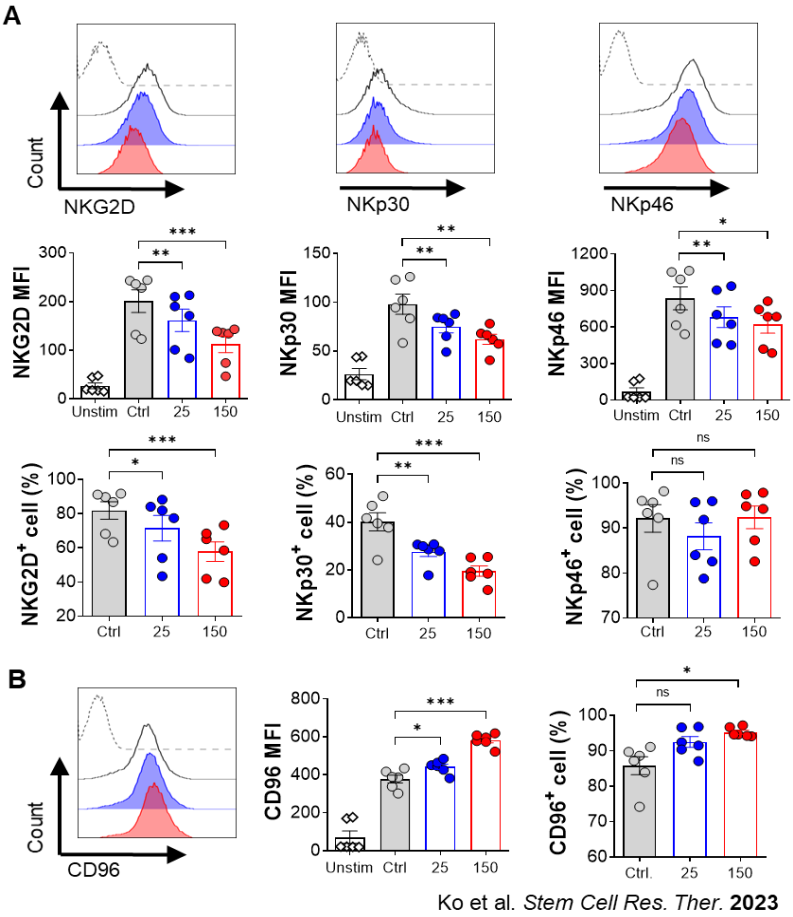

Ko et al. *Stem Cell Res. Ther.* **2023**

Figure 9. Alteration in receptor expression of human primary NK cells by the adipose tissue-derived stem cell (ADSC) secretome. Human primary NK cells, isolated from PBMCs of a healthy donor, were cultured for 48 hours with 25 (*25*; blue circles) or 150 μg/ml ADSC secretome (*150*; red circles), or without (*Ctrl*; gray circles), in the presence of 10 ng/ml of rhIL-2. Unstimulated NK cells were also cultured for the negative control (*Unstim*; white diamonds). Flow cytometry analysis of activating receptors, such as NKG2D, NKp30, and NKp46 (A; histogram, MFI, and frequencies), and inhibitory receptor CD96 (B; histogram, MFI, and frequencies). Error bars represent mean ± SEM of five to seven healthy donors. Statistical tests were determined by Student's paired two-tailed *t*-test; not significant (ns), **P* < 0.05, ***P* < 0.01, ****P* < 0.001.

3.1.5. Proteomic profiling reveals the putative factors for immune-modulation within the ADSC secretome

To decipher the protein composition released by ADSCs, the ADSC secretome's proteome underwent LC-MS/MS analysis, employing 2-DE gel electrophoresis and gel digestion. Three independent ADSC secretome samples from different donors were examined, and the sample from the donor exhibiting the most significant suppression effect was selected, revealing 71 protein spots (Fig. 10A). Through LC-MS/MS profiling and bioinformatics analysis, 83 proteins were identified in the ADSC secretome (Table 1). Gene ontology (GO) enrichment analysis was performed to understand the functional significance of these proteins based on biological process (BP), molecular function (MF), and cellular component (CC) (Fig. 10B). In terms of BP, 20.7% of the proteins were related to extracellular matrix organization, with 7.3% involved in the innate immune response. Other categories included negative regulation of endopeptidase activity (11%), proteolysis (8.5%), cellular response to amino acid stimulus (7.3%), and cellular protein metabolic process (6.1%). Concerning MF, 61% of the proteins were related to protein binding, with the next largest category being calcium ion binding (18.3%). In CC, 74.4% of the proteins were associated with extracellular exosomes, suggesting a pivotal role in the immunomodulatory effects of MSCs.

Despite consistent effects on both NK-92 cells and primary NK cells, the specific soluble protein components responsible for the immune suppressive effects needed clarification. A functional enrichment analysis identified 12 proteins with immunomodulatory potential within the ADSC secretome, particularly those more related to NK cells (Fig. 10C). These proteins play roles in structural composition, cell migration, adhesion, proliferation, development, and immune regulation.

To assess the impact of these proteins on NK cell activity, neutralizing antibodies against each

immunomodulatory candidate were employed. Notably, five antibodies out of 12 restored NK cell activities, with anti-dickkopf-related protein 3 (DKK3), anti-protein S (PROS1), and anti-pigment epithelium-derived factor (PEDF) demonstrating remarkable recovery (Fig. 11A-C). This suggests that the inhibitory effect of the ADSC secretome on NK cell activity may be partially dependent on these novel candidates and previously known major regulatory proteins.

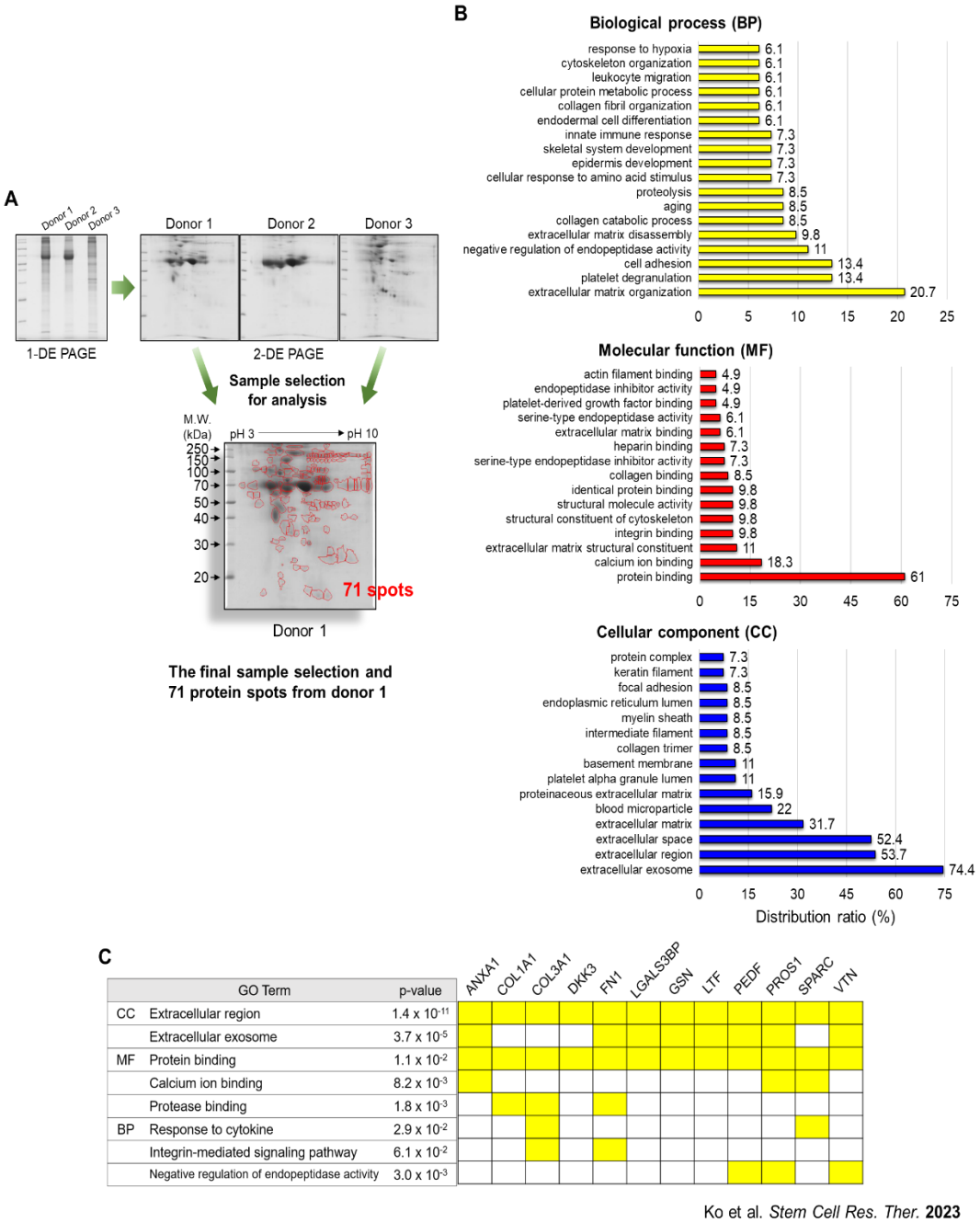

C

	GO Term	p-value
CC	Extracellular region	1.4×10^{-11}
	Extracellular exosome	3.7×10^{-5}
MF	Protein binding	1.1×10^{-2}
	Calcium ion binding	8.2×10^{-3}
	Protease binding	1.8×10^{-3}
BP	Response to cytokine	2.9×10^{-2}
	Integrin-mediated signaling pathway	6.1×10^{-2}
	Negative regulation of endopeptidase activity	3.0×10^{-3}

ANXA1, COL1A1, COL3A1, DKK3, FN1, LGALS3BP, GSN, LTF, PEDF, PROS1, SPARC, VTN

Ko et al. *Stem Cell Res. Ther.* **2023**

Figure 10. Proteomic and gene ontology (GO) analysis of the adipose tissue-derived stem cell (ADSC) secretome: Identification of immunomodulatory candidates. (A) Secretome profiling

workflow. The illustration outlines the steps involved in secretome profiling prior to LC-MS/MS analysis. Protein patterns in ADSC secretome sets from three different donors were identified and fractionated through 1-DE and 2-DE gel electrophoresis. Before LC-MS/MS analysis for protein composition identification, 71 protein spots were extracted from donor 1 during 2-DE electrophoresis and subsequently developed using Image MasterTM 2D Platinum (GE Healthcare, Chicago, IL). (B) GO enrichment analysis. To understand the functional significance of the 83 identified proteins within the ADSC secretome, a GO enrichment analysis was conducted. The analysis, performed using the DAVID tools algorithm, revealed categories with a P value < 0.05 for each type, shedding light on biological processes (BP), molecular functions (MF), and cellular compartments (CC). (C) A compiled list of immunomodulatory proteins, likely pertinent to NK cell biology, is presented. Each protein is categorized based on representative GO terms (left), including CC, MF, and BP. The arrangement follows the order of highest protein content (right), as determined by the DAVID tools algorithm. Notable proteins such as annexin A1 (ANXA1), collagen alpha-1(I) chain (COL1A1), collagen alpha-1(III) chain (COL3A1), dickkopf-related protein 3 (DKK3), fibronectin (FN1), galectin-3-binding protein (LGALS3BP), gelsolin (GSN), lactotransferrin (LTF), pigment epithelium-derived factor (PEDF), vitamin K-dependent protein S (PROS1), secreted protein acidic and rich in cysteine (SPARC), and vitronectin (VTN) are included.

Table 1. 83 proteins within the ADSC secretome

Uniprot_ID	Accession	Gene	Protein
MMP2_HUMAN	P08253	*MMP2*	72 kDa type IV collagenase
ACTB_HUMAN	P60709	*ACTB*	Actin, cytoplasmic 1
ACTN1_HUMAN	P12814	*ACTN1*	Actinin alpha 1
ACTN4_HUMAN	O43707	*ACTN4*	Actinin alpha 4
Q562M3_HUMAN	Q562M3	*ACT*	Actin-like protein
FETUA_HUMAN	P02765	*AHSG*	Alpha-2-HS-glycoprotein
A2MG_HUMAN	P01023	*A2M*	alpha-2-macroglobulin
L8E9Z3_HUMAN	L8E9Z3	*HRC*	Alternative protein HRC
ANXA1_HUMAN	P04083	*ANXA1*	Annexin A1
B4GA1_HUMAN	O43505	*B4GAT1*	Beta-1,4-glucuronyltransferase 1
BTD_HUMAN	P43251	*BTD*	Biotinidase
CO1A1_HUMAN	P02452	*COL1A1*	Collagen alpha-1(I) chain
CO3A1_HUMAN	P02461	*COL3A1*	Collagen alpha-1(III) chain
CO6A1_HUMAN	P12109	*COL6A1*	Collagen alpha-1(VI) chain
CO1A2_HUMAN	P08123	*COL1A2*	Collagen alpha-2(I) chain
CO5A2_HUMAN	P05997	*COL5A2*	Collagen alpha-2(V) chain
CO6A3_HUMAN	P12111	*COL6A3*	Collagen alpha-3(VI) chain
CFAH_HUMAN	P08603	*CFH*	Complement factor H
C1R_HUMAN	P00736	*C1r*	Complement C1r subcomponent
C1S_HUMAN	P09871	*C1s*	Complement C1s subcomponent
CFAB_HUMAN	P00751	*CFB*	Complement factor B
F5BAB3_HUMAN	F5BAB3	*CYTB*	Cytochrome b
PGS2_HUMAN	P07585	*DCN*	Decorin
DCD_HUMAN	P81605	*DCD*	Dermcidin
DSG1_HUMAN	Q02413	*DSG1*	Desmoglein-1
DKK3_HUMAN	Q9UBP4	*DKK3*	dickkopf WNT signaling pathway inhibitor 3
EF2_HUMAN	P13639	*EEF2*	Elongation factor 2
EMIL2_HUMAN	Q9BXX0	*EMILIN2*	EMILIN-2
CD248_HUMAN	Q9HCU0	*CD248*	Endosialin

(Continued on next page)

Table 1. 83 proteins within the ADSC secretome (Continued)

Uniprot_ID	Accession	Gene	Protein
FBN1_HUMAN	P35555	*FBN1*	Fibrillin-1
FINC_HUMAN	P02751	*FN1*	Fibronectin
FBLN1_HUMAN	P23142	*FBLN1*	Fibulin-1
LG3BP_HUMAN	Q08380	*LGALS3BP*	Galectin-3-binding protein
GELS_HUMAN	P06396	*GSN*	Gelsolin
HSP13_HUMAN	P48723	*HSPA13*	Heat shock 70 kDa protein 13
ISLR_HUMAN	O14498	*ISLR*	Immunoglobulin superfamily containing leucine-rich repeat protein
IBP6_HUMAN	P24592	*IGFBP6*	Insulin-like growth factor-binding protein 6
ITIH2_HUMAN	P19823	*ITIH2*	Inter-alpha-trypsin inhibitor heavy chain H2
K1C10_HUMAN	P13645	*KRT10*	Keratin, type I cytoskeletal 10
K1C14_HUMAN	P02533	*KRT14*	Keratin, type I cytoskeletal 14
K1C16_HUMAN	P08779	*KRT16*	Keratin, type I cytoskeletal 16
K1C9_HUMAN	P35527	*KRT9*	Keratin, type I cytoskeletal 9
K2C1_HUMAN	P04264	*KRT1*	Keratin, type II cytoskeletal 1
K22E_HUMAN	P35908	*KRT2*	Keratin, type II cytoskeletal 2 epidermal
K2C5_HUMAN	P13647	*KRT5*	Keratin, type II cytoskeletal 5
K2C6B_HUMAN	P04259	*KRT6B*	Keratin, type II cytoskeletal 6B
K2C6C_HUMAN	P02538	*KRT6C*	Keratin, type II cytoskeletal 6C
TRFL_HUMAN	P02788	*LTF*	Lactotransferrin
LAMB1_HUMAN	P07942	*LAMB1*	Laminin subunit beta-1
LAMC1_HUMAN	P11047	*LAMC1*	Laminin subunit gamma-1
LUM_HUMAN	P51884	*LUM*	Lumican
MOES_HUMAN	P26038	*MSN*	Moesin
NID1_HUMAN	P14543	*NID1*	Nidogen-1
NUCB1_HUMAN	Q02818	*NUCB1*	Nucleobindin-1
OLFL3_HUMAN	Q9NRN5	*OLFML3*	Olfactomedin-like protein 3
PTX3_HUMAN	P26022	*PTX3*	Pentraxin-related protein PTX3
PEDF_HUMAN	P36955	*SERPINF1*	Pigment epithelium-derived factor

(Continued on next page)

Table 1. 83 proteins within the ADSC secretome (Continued)

Uniprot_ID	Accession	Gene	Protein
IC1_HUMAN	P05155	*SERPING1*	Plasma protease C1 inhibitor
PLOD1_HUMAN	Q02809	*PLOD1*	Procollagen-lysine,2-oxoglutarate 5-dioxygenase 1
PE2R4_HUMAN	P35408	*PTGER4*	Prostaglandin E2 receptor EP4 subtype
PDIA3_HUMAN	P30101	*PDIA3*	Protein disulfide-isomerase A3
PTMA_HUMAN	P06454	*PTMA*	Prothymosin alpha
KPYM_HUMAN	P14618	*PKM*	Pyruvate kinase PKM
GDIA_HUMAN	P31150	*GDI1*	Rab GDP dissociation inhibitor alpha
RLGPB_HUMAN	Q86X10	*RALGAPB*	Ral GTPase-activating protein subunit beta
ARH37_HUMAN	A1IGU5	*ARHGEF37*	Rho quanine nucleotide exchange factor 37
PRPC_HUMAN	P02810	*PRH1*	Salivary acidic proline-rich phosphoprotein 1/2
ANT3_HUMAN	P01008	*SERPINC1*	Serpin family C member 1
S12A7_HUMAN	Q9Y666	*SLC12A7*	Solute carrier family 12 member 7
SPRC_HUMAN	P09486	*SPARC*	SPARC
TRAC_HUMAN	P01848	*TRAC*	T cell receptor alpha chain constant
TIAM2_HUMAN	Q8IVF5	*TIAM2*	T-lymphoma invasion and metastasis-inducing protein 2
BGH3_HUMAN	Q15582	*TGFBI*	Transforming growth factor beta induced
TKT_HUMAN	P29401	*TKT*	Transketolase
Q3T7B8_HUMAN	Q3T7B8	*TRIT1*	tRNA isopentenylpyrophosphate transferase isoform 5
ADAT1_HUMAN	Q9BUB4	*ADAT1*	tRNA-specific adenosine deaminase 1
SYWC_HUMAN	P23381	*WARS1*	Tryptophan--tRNA ligase, cytoplasmic
VASN_HUMAN	Q6EMK4	*VASN*	Vasorin
VIME_HUMAN	P08670	*VIM*	Vimentin
VTDB_HUMAN	P02774	*GC*	Vitamin D-binding protein
PROS_HUMAN	P07225	*PROS1*	Vitamin K-dependent protein S
VTNC_HUMAN	P04004	*VTN*	Vitronectin
WDR1_HUMAN	O75083	*WDR1*	WD repeat-containing protein 1

Ko et al. *Stem Cell Res. Ther.* **2023**

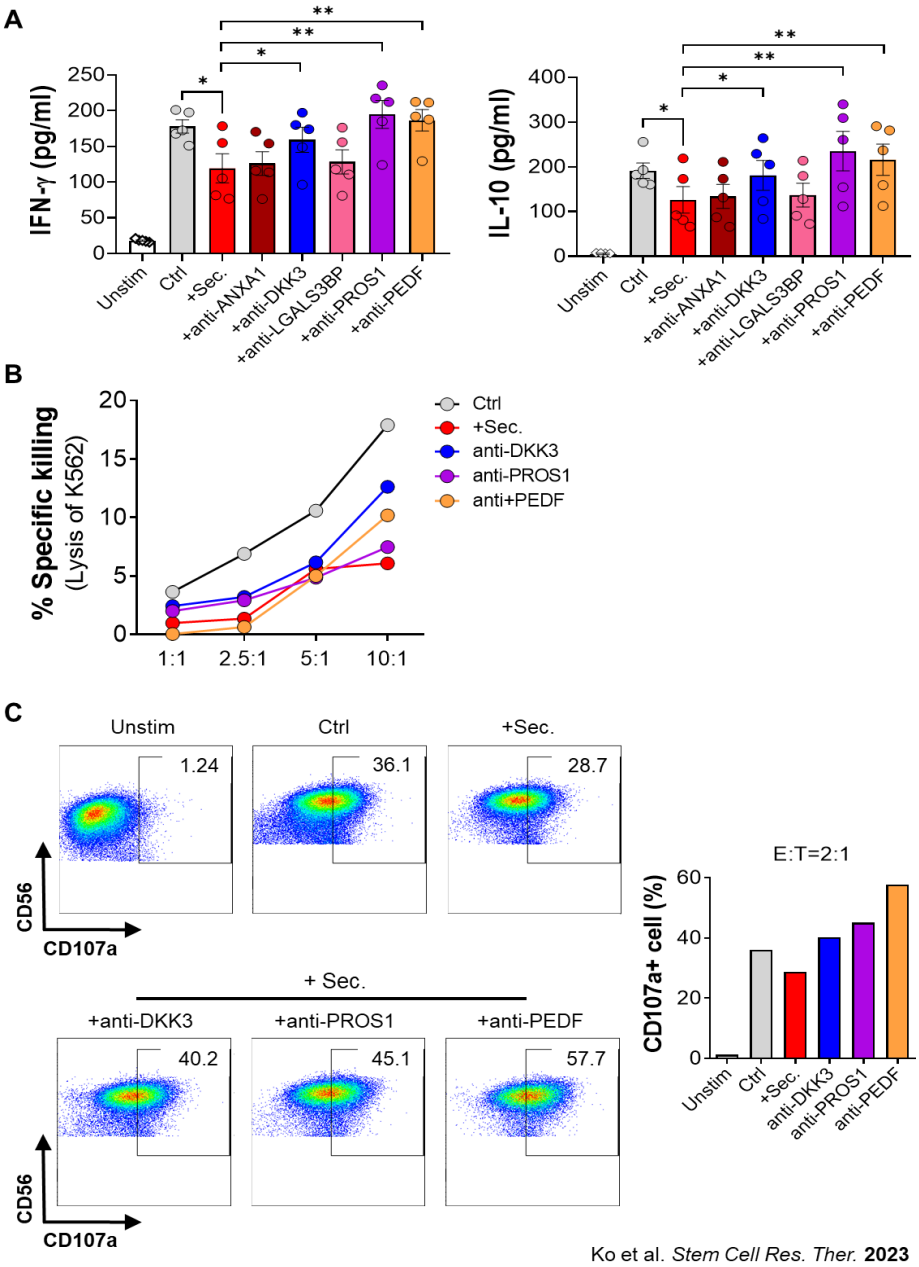

Ko et al. *Stem Cell Res. Ther.* **2023**

Figure 11. Impact of neutralizing antibodies on adipose tissue-derived stem cell (ADSC) secretome's modulation of NK-92 cell effector function. NK-92 cells, activated with IL-2 (5 ng/ml), were treated for 48 hours with the ADSC secretome (150 μg/ml) alongside neutralizing

antibodies (1 μg/ml) against specific candidates to explore the recovery of cellular activity. Unstimulated NK cells served as the negative control (*Unstim*). (A) The concentrations of IFN-γ and IL-10 in culture supernatants, measured by ELISA, with error bars representing mean ± SEM of five independent experiments. Statistical significance was determined by Student's paired two-tailed *t*-test; $*P < 0.05$. (B) Post-incubation, NK-92 cells were co-cultured with K562 target cells for 4 hours at indicated E:T ratios to evaluate cytotoxicity. (C) Degranulation capacity. NK-92 cells were stained with PE-conjugated CD107a antibodies and co-cultured with K562 cells for 4 hours at specified E:T ratios to assess the level of exocytosis. Flow cytometry measured the degranulation marker CD107a, as shown in the dot blot (left side), and the frequency of $CD107a^+$ NK cells (right side). Representative data are presented.

3.1.6. Unraveling molecular changes in activated NK cells induced by the ADSC secretome

To decipher the underlying molecular mechanisms responsible for the suppression of IL-2–mediated NK cell activity by the ADSC secretome, we conducted mRNA sequencing (mRNA-seq) for transcriptional expression profiling using NK cells isolated from the blood of six healthy donors. Intriguingly, significant differences in gene expression emerged following a 48-hour treatment with the ADSC secretome compared to the IL-2 alone control group. Out of the 352 differentially expressed genes (DEGs) exhibiting more than a two-fold change, 253 displayed upregulation, while 99 were downregulated (Fig. 12A). Employing hierarchical clustering analysis, we organized samples and genes based on similar expression patterns (Fig. 12B). Further examination of the GO classifications for all 352 genes revealed relatively heightened expression of specific genes associated with phosphatase and ubiquitin ligase subunits, including *PTPRF*, *PTPN14*, *DUSP4*, and *DTX1*, in IL-2-activated NK cells treated with the ADSC secretome (Fig. 12C). These genes may contribute to the observed reduction in phosphorylated JAK1 and JAK3 levels. Subsequent real-time PCR confirmed the significant upregulation of the *DUSP4* gene in human blood NK cells treated with the ADSC secretome, distinguishing it from the IL-2 alone control group (Fig. 12D). Moreover, an elevated expression level of DUSP4 protein, in contrast to DTX1 protein, was noted in the ADSC secretome-treated group (Fig. 12E). Thus, these findings suggest that the ADSC secretome induces increased expression of *DUSP4* mRNA and DUSP4 protein in IL-2–activated NK cells.

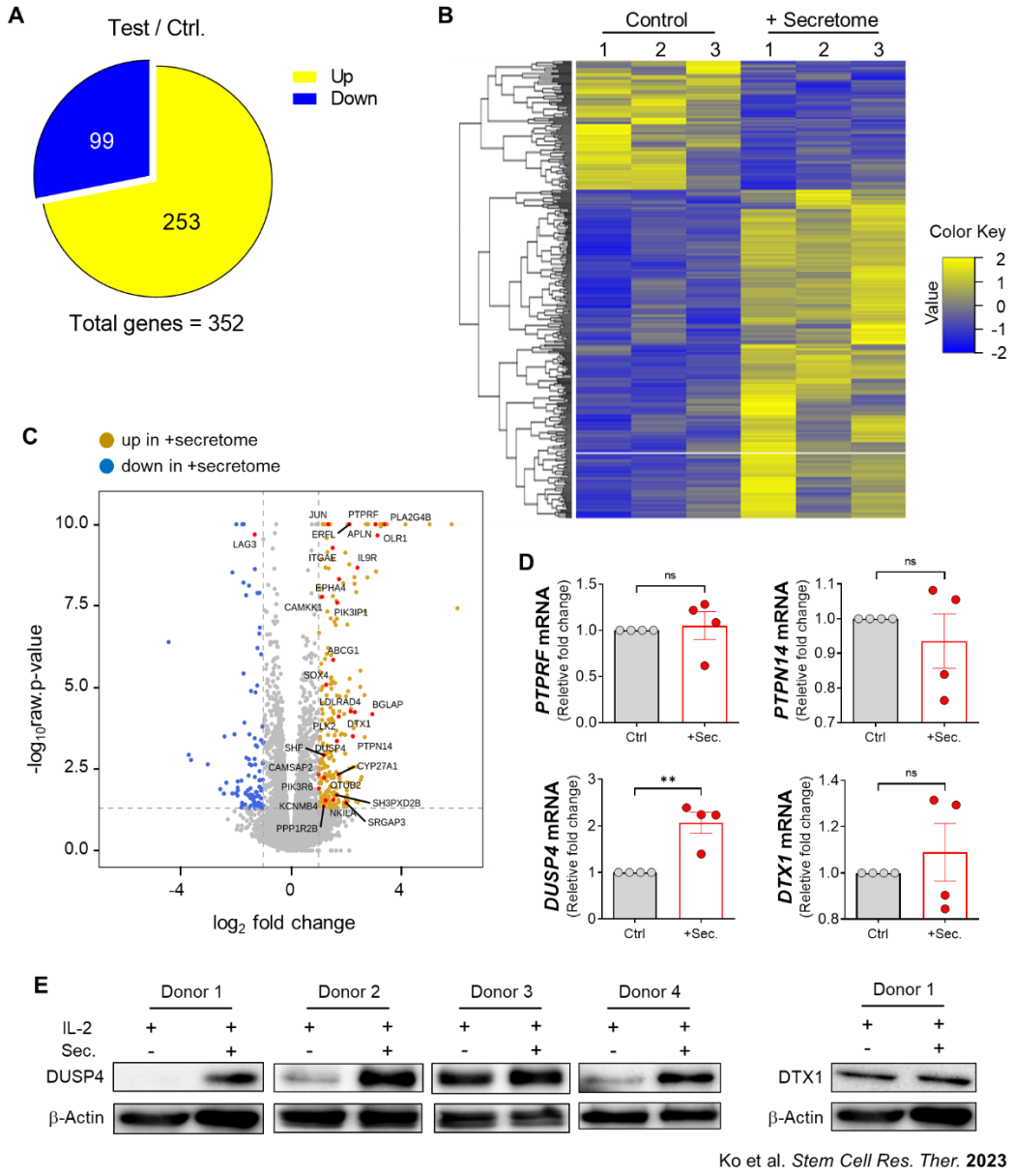

Ko et al. *Stem Cell Res. Ther.* **2023**

Figure 12. The ADSC secretome modulates the transcricptome of human primary NK cells, influencing the expression of genes associated with cell activity regulation, including the upregulation of DUSP4. Human primary NK cells, obtained from PBMCs of a healthy donor, were cultured for 48 hours with the ADSC secretome at a concentration of 150 μg/ml, or without it, in the

presence of 10 ng/ml of rhIL-2 (n = 6). (A) A total of 352 differentially expressed genes (DEGs) were identified, including 99 down-regulated genes (depicted in blue) and 253 up-regulated genes (depicted in yellow) in the secretome-treatment group compared to the IL-2 alone control group, based on fold change and *P* value criteria ($P < 0.05$, and $|fc| \geq 2$). (B) Hierarchical clustering grouped the 352 DEGs based on the similarity of expression levels and presented them in a heat map using Z-score for normalized values (log_2 based), ranging from low expression (depicted in blue) to high expression (depicted in yellow). (C) A volcano plot of gene expression in human primary NK cells, obtained through mRNA-seq (n = 6), indicated selected genes (depicted in red) associated with the regulation of cell activity. Down-regulated (depicted in blue) and up-regulated (depicted in mustard) differentially expressed genes in the secretome-treatment group were highlighted. (D) Focused on mRNA levels of up-regulated differentially expressed genes associated with phosphatase or ubiquitin ligase among the genes displayed in C. (E) Immunoblot analysis of protein levels for DUSP4 (left) and DTX1 (right) in NK cells from human blood. The presented RNA-seq data meet the conditions of adjusted $P < 0.05$, and $|fc| \geq 2$. Error bars represent mean ± SEM of four healthy donors. Statistical tests were conducted using Student's paired two-tailed *t*-test; not significant (ns), $^{**}P < 0.01$.

Chapter 2

3.2. Immunomodulatory effects of the ADSC secretome on mouse NK cells and lupus murine model

3.2.1. Modulation of IL-2–induced activation in mouse primary NK cells by the ADSC secretome

To explore the impact of the ADSC secretome on the effector function and immune phenotype of mouse primary NK cells, mirroring observations in human NK cells from Chapter 1, NK cells were isolated from the mouse spleen, stimulated with rmIL-2, and cultured for 48 hours with the ADSC secretome. Subsequent flow cytometry analysis revealed that the ADSC secretome led to a reduction in both the expression level and frequency of receptor-positive cells, including NKp46, DNAM1 (CD226), and 2B4 (CD244)—all activating receptors on mouse NK cells (Fig. 13A). Additionally, the expression levels of inhibitory receptors on mouse NK cells, such as Ly49A, Ly49C/I, and CD94, either decreased or remained stable in the presence of the ADSC secretome. Notably, CD96 was the only inhibitory receptor that exhibited an increased expression level in the presence of the ADSC secretome compared to the IL-2 alone control group (Fig. 13B). In summary, these findings demonstrate that the ADSC secretome, in the context of mouse NK cells, results in decreased mean expression levels and proportions of activating receptor-positive NK cells (NKp46, DNAM1, and 2B4), while, among all inhibitory receptors, only CD96 shows increased expression, consistent with the results observed in human NK cells from Chapter 1.

To assess the effector function of mouse NK cells, the levels of effector cytokines and cytolytic granules were measured by flow cytometry after intracellular staining. Functional activity, including the ability to lyse Calcein-AM-labeled YAC-1 target cells isolated from the lymphoblast of a mouse with lymphoma, was also measured using a fluorometer. We observed a significant decrease in the levels of all effector molecules, such as IFN-γ, IL-10, perforin, and granzyme B (Fig. 13C). Moreover, a significant decrease in cytotoxic activity was observed in mouse primary NK cells at all E:T ratios (Fig. 13D). Taken together, these data demonstrate that the ADSC secretome also has a regulatory effect on the activity of mouse primary NK cells, consistent with the findings in human NK cells.

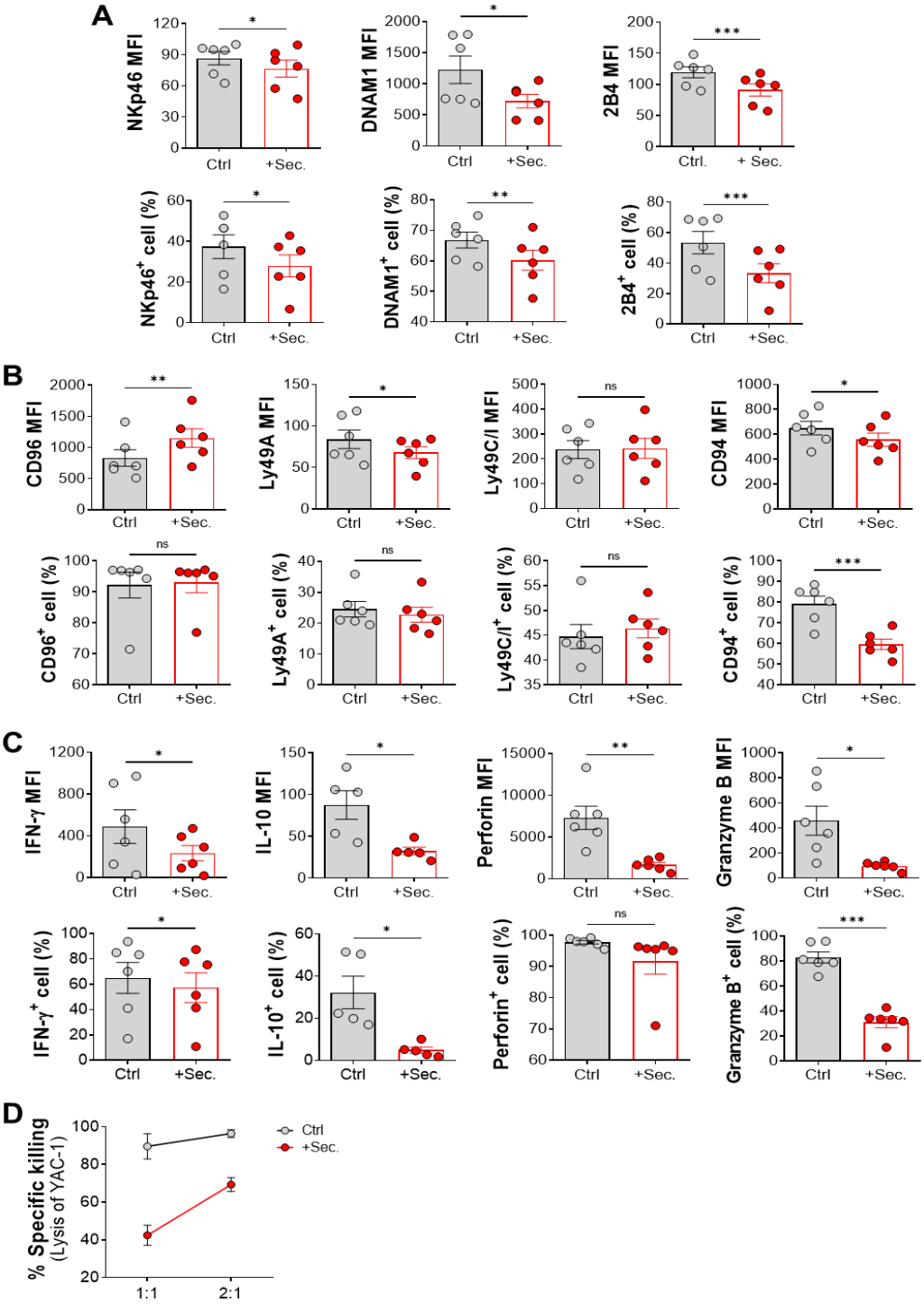

Figure 13. Alteration in receptor expression and effector function of mouse natural killer (NK) cells induced by the adipose tissue-derived stem cell (ADSC) secretome. Mouse primary NK cells, stimulated with IL-2 (100 ng/ml) were cultured for 48 hours with 100 μg/ml of the ADSC secretome (red circles; *+Sec.*), or without it as a control (gray circles; *Ctrl*). (A to C) Flow cytometry analysis of activating receptors, including NKp46, DNAM1, and 2B4 (A; MFI and frequencies), inhibitory receptors, such as CD96, Ly49A, Ly49I/C, and CD94 (B; MFI and frequencies), and effector molecules, such as IFN-γ, IL-10, perforin, and granzyme B (C; MFI and frequencies). Error bars represent mean ± SEM of five to six independent experiments. Statistical tests were determined by Student's paired two-tailed *t*-test; not significant (ns), $*P < 0.05$, $**P < 0.01$, $***P < 0.001$. (D) Cytotoxicity of mouse NK cells against YAC-1 target cells at the indicated NK:YAC-1 (E:T, effector:target) ratios of 1:1 and 2:1.

3.2.2. *In vivo* changes induced by administration of the ADSC secretome in the context of lupus nephritis animal model

So far, we have revealed how the ADSC secretome regulates NK cell activity in detail, both *in vitro* and *ex vivo*, with human and murine subjects. To further extend these studies to an *in vivo* setting, especially in the context of lupus nephritis, a major cause of morbidity and mortality in SLE patients leading to end-stage kidney disease,[78,79] we tested the immunomodulatory effects of the ADSC secretome in a lupus nephritis mouse model. NZB/W F1 mice were treated with the ADSC secretome or PBS, starting at 22 weeks of age, and disease progression was monitored (Fig. 14A). The PBS-treated mice, serving as the vehicle group, developed severe symptoms characterized by high-scoring proteinuria (Fig. 14B), slow weight gain (Fig. 14D), and poor survival rates (Fig. 14F), as expected in this model. Compared to the PBS mice, ADSC secretome-treated mice maintained negligible proteinuria (around score 1 on average) from weeks 22 to 34 and exhibited lower proteinuria levels than the PBS group until week 42 (Fig. 14, B and C). Additionally, they gained body weight and showed a marginally preferable survival rate compared to the PBS group, although it was not statistically significant (Fig. 14, D and E).

Higher serum levels of blood urea nitrogen (BUN) and creatinine are associated with impaired renal function, reduced glomerular filtration rate, and low serum albumin in lupus nephritis. We collected serum data demonstrating significantly high BUN and creatinine levels and low albumin in PBS-treated mice (Fig. 15A-C), as expected. On the other hand, ADSC secretome-treated mice showed significantly restored levels of BUN and albumin, resembling values observed in healthy mice (Fig 15A, C). ADSC secretome-treated mice also had reduced serum creatinine close to healthy group but not statistically significant (Fig. 15B). Since the detection of anti-double-stranded DNA (anti-dsDNA) antibodies is critical for SLE diagnosis and their levels are positively correlated with SLE disease activity, we also analyzed the serum levels of anti-dsDNA IgG. While

PBS-treated mice showed significantly higher levels of anti-dsDNA IgG than healthy mice, ADSC secretome-treated mice exhibited lower levels compared to the PBS group (Fig. 15D).

Serum cytokine and immunoglobulin levels are associated with the disease activity in SLE patients.[80-83] Therefore, we measured cytokine and immunoglobulin levels in serum from NZB/W F1 mice undergoing lupus nephritis and treatments. In PBS-treated mice, most cytokines gradually increased until 39 weeks of age and then showed a pattern that was somewhat alleviated at 41 weeks of age, whereas in ADSC secretome-treated mice, with the exception of serum monocyte chemoattractant protein-1 (MCP-1), most cytokines were constantly maintained at lower levels until 41 weeks of age, although not statistically significant compared to PBS-treated mice (Fig. 15E). In healthy mice, all serum cytokine concentrations were almost undetectable at 41 weeks of age (data not shown). Notably, we observed a significantly higher serum level of total IgG1 in ADSC secretome-treated mice compared to PBS-treated mice from weeks 27 to 39, while levels of other total immunoglobulins, including IgM, IgG2a, IgG2b, and IgG3, were either nearly identical or displayed slight differences between the two groups (Fig. 15F). Taken together, these results suggest that the ADSC secretome enhances renal function, improves survival, and maintains low serum levels of inflammatory cytokines and anti-dsDNA IgG, while concurrently elevating serum levels of total IgG1 in NZB/W F1 mice.

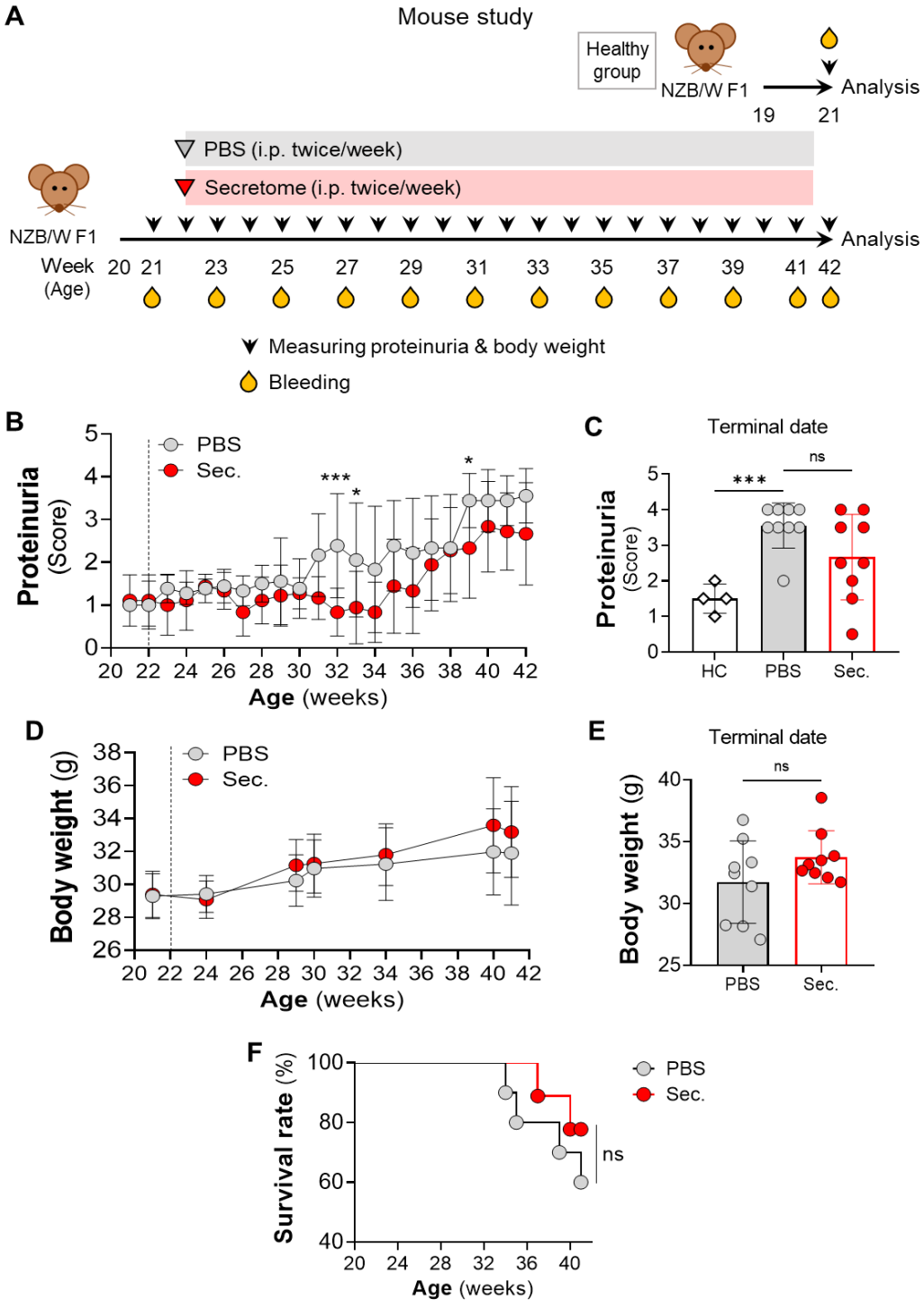

Figure 14. Changes in clinical manifestations in F1 hybrids of New Zealand black and white (NZB/W F1) mice following administration of the adipose tissue-derived stem cell (ADSC) secretome. (A) Schematic diagram of mouse study, including sample collection. NZB/W F1 mice received the ADSC secretome (red) or PBS (gray) starting at 22 weeks of age, as described in methods (n = 10 for PBS group, n = 9 for ADSC secretome group, and n = 4 for the healthy group). (B) Proteinuria progression over time. For mice succumbing to severe lupus nephritis during the treatment, a proteinuria score of 4 was assigned. Data were analyzed using a two-way ANOVA with Sidak's multiple comparison test. (C) Proteinuria levels for the different treatment groups, including the healthy control (*HC*; white diamonds), at the terminal date. Data were analyzed using Student's unpaired two-tailed *t*-test. (D) Body weights over time. (E) Body weights for the two groups at the terminal date. (F) Survival rates with Kaplan-Meier curve for each group. Data were analyzed using a Log-rank (Mantel-Cox) test. Values represent the mean ± SEM of one experiment. Asterisks indicate statistical significance; not significant (ns), $*P < 0.05$, $***P < 0.001$.

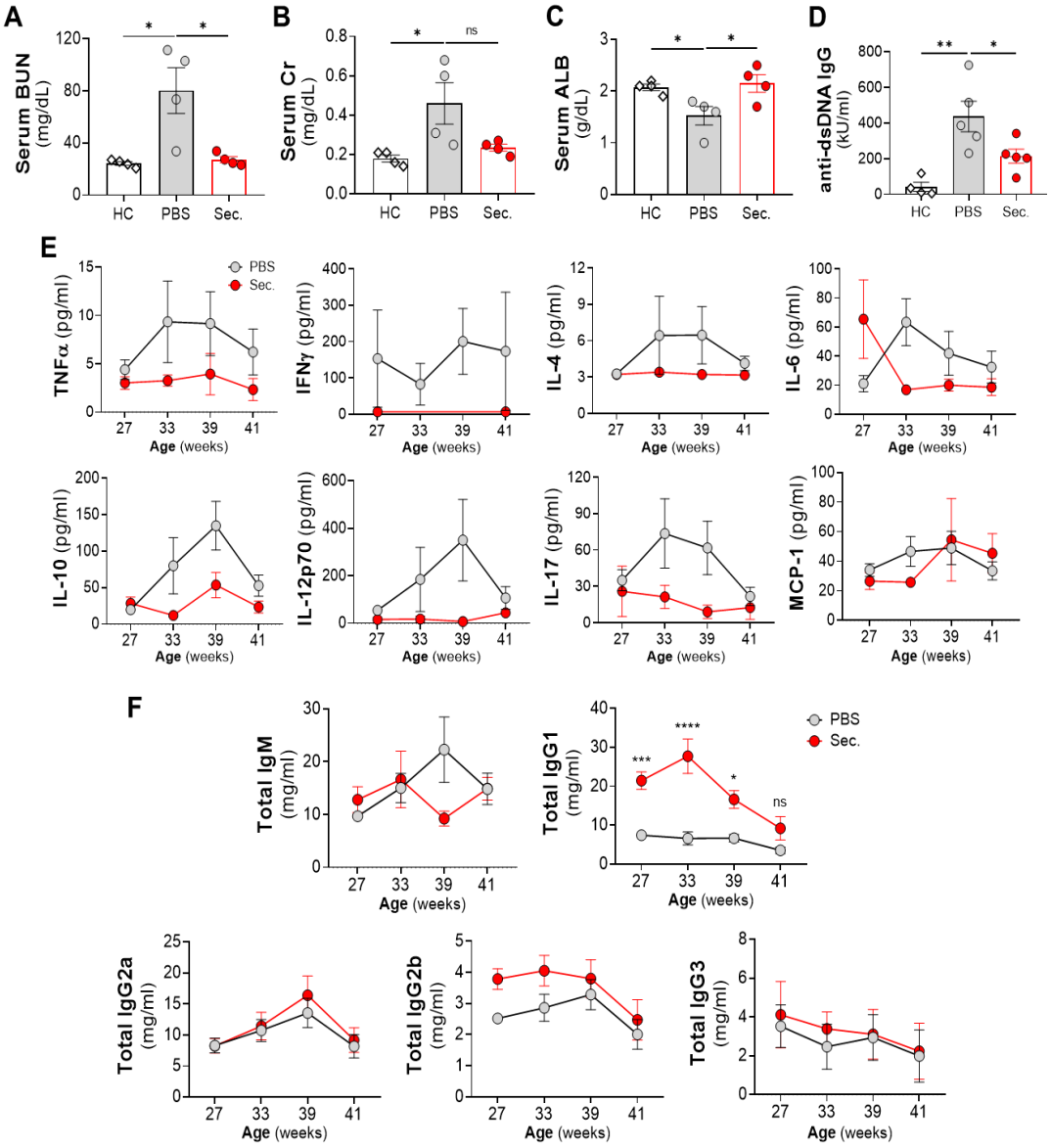

Figure 15. Evaluation of renal function and temporal changes in serum cytokines and immunoglobulins in F1 hybrids of New Zealand black and white (NZB/W F1) mice after administration of the adipose tissue-derived stem cell (ADSC) secretome. (A to D) Blood urea nitrogen (BUN), creatinine (Cr), albumin (ALB), and anti-double-stranded DNA immunoglobulin

G (anti-dsDNA IgG) levels measured from terminal serum samples from healthy control (*HC*; white diamonds), PBS-treated (*PBS*; gray circles), and ADSC secretome-treated (*Sec.*; red circles) mice. Data were analyzed using Student's unpaired two-tailed *t*-test. (E) Levels of serum cytokines (TNF-α, IFN-γ, IL-4, IL-6, IL-10, IL-12p70, IL-17, MCP-1) and (F) serum total immunoglobulins (IgM, IgG1, IgG2a, IgG2b, IgG3) measured between weeks 27 to 41. Data were analyzed using a two-way ANOVA with Sidak's multiple comparison test. Values represent the mean ± SEM of one experiment. Axsterisks indicate statistical significance; not significant (ns), $*P < 0.05$, $***P < 0.001$, $****P < 0.0001$.

3.2.3. Reduction in infiltrating immune cells in the kidney and improvement of renal pathology by ADSC secretome treatment in NZB/W F1 mice

Subsequently, we investigated the impact of ADSC secretome treatment on secondary lymphoid organs, especially the spleen, which is highly active in the immune response during lupus nephritis, as well as on the target organ, the kidneys. We noted a moderate increase in the absolute number of spleen cells in PBS-treated mice compared to healthy mice, with a lower cell count in ADSC secretome-treated mice than in PBS-treated mice, though not statistically significant (Fig. 16A). While the absolute number of kidney cells was slightly reduced in lupus nephritis mice compared to healthy mice, there was no significant difference among all groups (Fig. 16A). However, the frequency of $CD45^+$ leukocytes in the kidneys of PBS-treated mice showed a significant increase compared to healthy mice, whereas a marked reduction was observed in ADSC secretome-treated mice compared to PBS-treated mice (Fig. 16B).

Lupus nephritis is characterized by the accumulation of immune complexes, including IgG and C3, leading to progressive damage to the glomerular, tubular, and vascular structures.[84] In the histological examination of PAS-stained kidney tissue, PBS-treated mice exhibited significantly extensive glomerular injury characterized by mesangial cellular proliferation and extracapillary proliferation, along with crescent lesions associated with necrosis of the tuft and rupture of the capillary walls, including enlarged glomeruli, as expected (Fig. 16C-E). In contrast, ADSC secretome-treated mice showed remarkably intact glomerular structures, similar to the healthy group (Fig. 16C-E). Immunofluorescence staining for IgG and C3 on frozen renal tissue revealed that PBS-treated mice had higher IgG and C3 deposition in the glomeruli compared to the healthy group, whereas ADSC secretome-treated mice exhibited a notable reduction, resembling levels observed in healthy mice (Fig. 16C, F, and G). Overall, these findings suggest that the ADSC

secretome limits the infiltration of leukocytes into the kidneys and reduces immune complex deposition in the glomeruli, thereby protecting against renal damage.

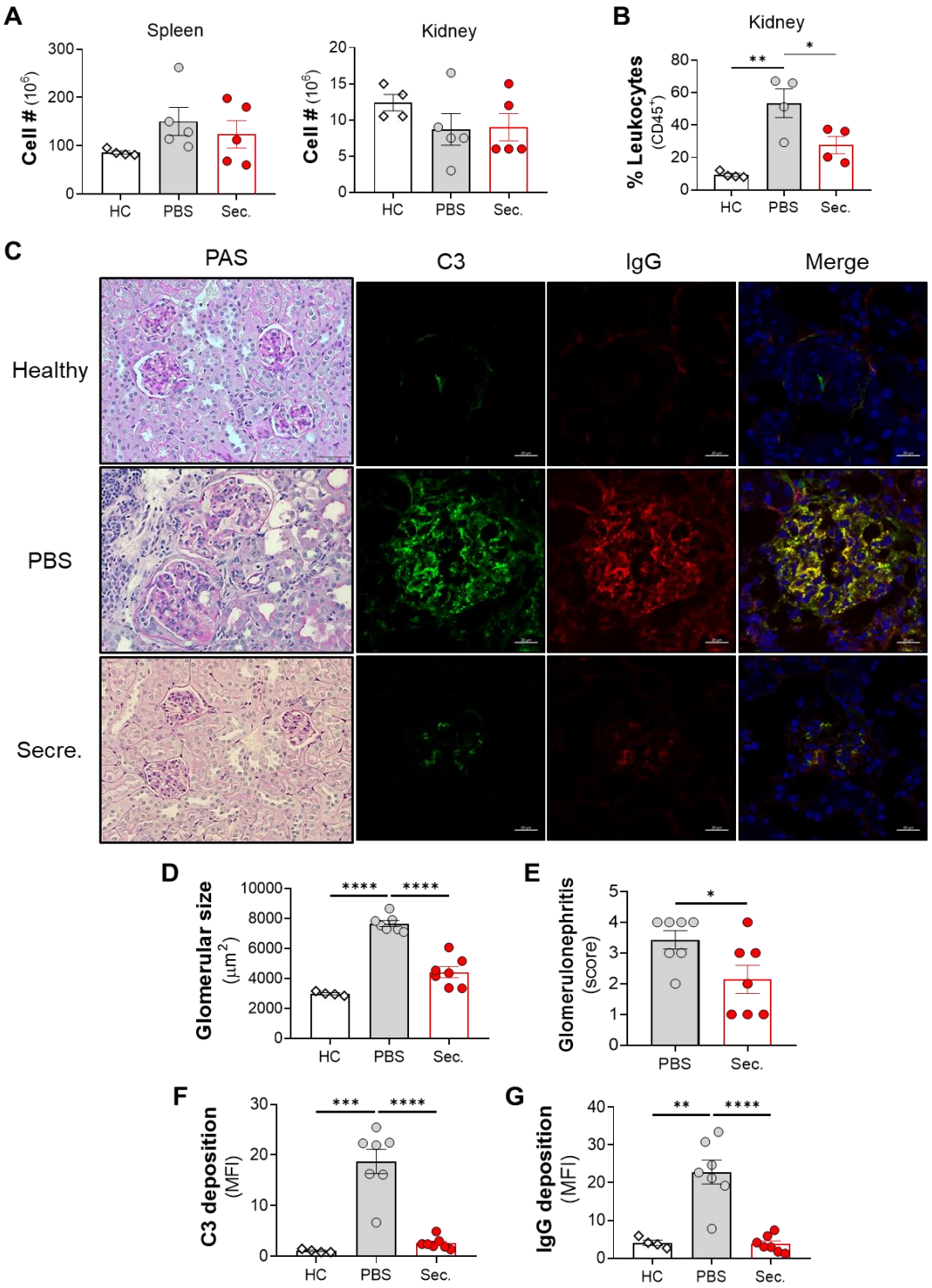

Figure 16. Attenuation of leukocyte infiltration into the kidneys and amelioration of glomerular injury in F1 hybrids of New Zealand black and white (NZB/W F1) mice following adipose tissue-derived stem cell (ADSC) secretome administration. The spleens and kidneys from healthy control (*HC*; white diamonds), PBS-treated (*PBS*; gray circles), and ADSC secretome-treated (*Sec.*; red circles) mice were analyzed for (A) total cell counts in spleens and kidneys and (B) frequency of kidney-infiltrating leukocytes ($CD45^+$) measured by flow cytometry. (C) Representative images of glomeruli in kidney sections stained with periodic acid-Schiff (PAS; scale bars: 50 μm) and fluorescent antibodies against complement 3 (C3; FITC; green) and immunoglobulin G (IgG; Alexa-594; red) (scale bars: 20 μm). (D) Measurement of average glomerulus size, and (E) assessment of glomerulonephritis score based on histological glomerular injury (PAS staining). (F) Mean fluorescence intensity (MFI) of C3 (green), and (G) IgG (red) deposition quantitated by ImageJ software based on immunofluorescence staining. Error bars represent mean ± SEM. Statistical tests were determined by Student's unpaired two-tailed *t*-test; $*P < 0.05$, $**P < 0.01$, $***P < 0.001$, $****P < 0.0001$.

3.2.4. The immune cell profiling in the spleen and kidneys of NZB/W F1 mice: impact of ADSC secretome treatment on immune cell populations

We observed a moderate increase in the absolute number of spleen cells and a significant increase of kidney-infiltrated immune cells in the context of lupus nephritis using NZB/W F1 mice, verifying the attenuation of kidney-infiltrated immune cells and protection against glomerular injury by ADSC secretome treatment. To assess the immune cell profile in the spleen and kidneys of NZB/W F1 mice with lupus nephritis and the effect of the ADSC secretome on of them, we conducted a comprehensive flow cytometric analysis of cell populations. The proportion of monocytes ($F4/80^{-}CD11b^{+}$), which can differentiate into macrophages and contribute to SLE, significantly increased in both the spleen and kidneys of PBS-treated mice compared to healthy mice (Fig. 17A). However, the ADSC secretome had no impact on the proportion of monocytes. In the spleen, the proportion of macrophages ($F4/80^{+}CD11b^{+}$) also remarkably increased, like monocytes in PBS-treated mice compared to healthy mice, whereas in the kidney, it was significantly reduced, and there was no change with ADSC secretome treatment in both organs (Fig. 17B). The proportion of neutrophils ($CD11b^{+}Ly6G^{+}$), which can promote autoantibody production and tissue injury, was affected only in the kidneys. It exhibited a slight increase upon administration of PBS compared to healthy conditions but then decreased significantly to healthy levels upon administration of the ADSC secretome (Fig. 17C). The proportion of B cells ($TCR\beta^{-}B220^{+}$), which play a crucial role in SLE pathogenesis, was affected only in the spleen. It exhibited a notable increase upon administration of PBS compared to healthy conditions but then decreased significantly upon administration of the ADSC secretome (Fig. 17D). The proportion of total T cells ($TCR\beta^{+}$), which are crucial contributors to SLE, significantly decreased in the spleen but

conversely increased in the kidneys of PBS-treated mice compared to healthy mice. However, no significant changes were observed due to the ADSC secretome (Fig. 17E). In PBS-treated mice, analyzing the frequency of $CD4^+$ and $CD8^+$ T cells within the total T cell population, $CD4^+$ T cells ($TCR\beta^+CD4^+$) significantly increased in both the spleen and kidneys, while $CD8^+$ T cells ($TCR\beta^+CD8^+$) decreased substantially. However, both cell subsets exhibited changes in their frequencies only in the spleen, influenced by the ADSC secretome (Fig. 17F-G). Taken together, these data suggest that in the context of lupus nephritis, the proportion of most immune cells increases, with the exception of $CD8^+$ T cells in the spleen. Specifically, there is an increased proportion of monocytes, neutrophils, total T cells, and $CD4^+$ T cells in the kidneys, along with a reduced proportion of macrophages and $CD8^+$ T cells. Furthermore, the ADSC secretome modulates the proportion of neutrophils in the kidneys and B cells in the spleen, as well as splenic $CD4^+$ and $CD8^+$ T cells.

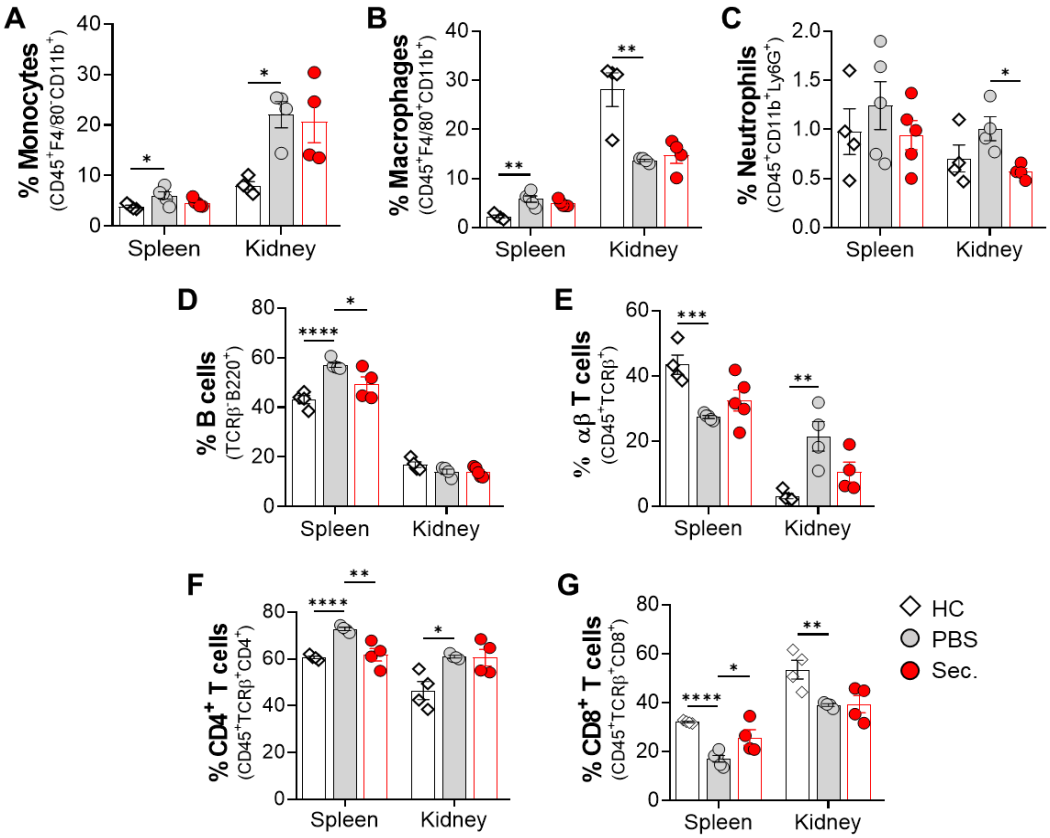

Figure 17. Changes in immune cell populations in the spleen and kidneys of F1 hybrids of New Zealand black and white (NZB/W F1) mice with lupus nephritis (LN) following adipose tissue-derived stem cell (ADSC) secretome treatment. (A to G) The spleens and kidneys from healthy control (*HC*; white diamonds), PBS-treated (*PBS*; gray circles), and ADSC secretome-treated (*Sec.*; red circles) mice were analyzed for immune cell populations. Percentages of (A) monocytes ($F4/80^-$ $CD11b^+$), (B) macrophages ($F4/80^+CD11b^+$), (C) neutrophils ($CD11b^+Ly6G^+$), (D) B cells ($TCR\beta^-$ $B220^+$), (E) total T cells ($TCR\beta^+$), (F) $CD4^+$ T cells ($TCR\beta^+CD4^+$), and (G) $CD8^+$ T cells ($TCR\beta^+CD8^+$) in the spleen and kidneys characterized by flow cytometry. Error bars represent mean ± SEM. Statistical tests were determined by Student's unpaired two-tailed *t*-test; not significant (not shown), $*P < 0.05$, $**P < 0.01$, $***P < 0.001$, $****P < 0.0001$.

3.2.5. NK cell characterization in NZB/W F1 mouse strain and alterations of NK cell phenotype after administration of the ADSC secretome

Given the limited understanding of NK cell involvement in SLE, we aimed to profile NK cell populations and their phenotypes in peripheral tissues such as blood and spleen, as well as in kidneys, the target organs affected by the disease, using the NZB/W F1 murine model. Simultaneously, we investigated the impact of the ADSC secretome on NK cell alterations. The percentage of NK cells ($NK1.1^+$) decreased in both the blood and spleen; however, a distinct increase was observed in the kidneys of PBS-treated mice compared to healthy mice (Fig. 18A). These results align with previous findings, indicating a significantly lower proportion of NK cells in the peripheral blood of SLE patients and in the blood and spleen of lupus-prone MRL/*lpr* mice, compared to controls.[50,51,57,58,85] Additionally, there was an observed increase in the proportion of NK cells in the target organ, the kidneys.[51,58,85] Interestingly, mice administered with the ADSC secretome exhibited a remarkably lower proportion of NK cells in the kidneys compared to PBS-treated mice, similar to the proportion of healthy mice (Fig. 18A). These data indicate that in the NZB/W F1 model of lupus nephritis, peripheral NK cells, including those in the blood and spleen, may migrate to and accumulate in the kidneys. Furthermore, administration of the ADSC secretome hinders the infiltration of NK cells into the kidneys.

Next, we investigated the expression patterns of surface receptors and intracellular cytokines on NK cells in the blood, spleen, and kidneys. In the blood, the frequency of activating receptors such as NKG2D and DNAM1, along with CD122 (IL-2Rβ) and the inhibitory receptor CD96, significantly decreased in PBS-treated mice compared to healthy controls. However, ADSC secretome-treated mice exhibited a substantial recovery, bringing the frequency levels close to those observed in healthy mice, with the exception of CD96 (Fig. 18B). The frequencies of

activating receptor-positive NK cells, including NKp46 and 2B4, as well as CD25 (IL-2Rα) and the inhibitory receptor Ly49I, showed no significant differences between the healthy and PBS groups. However, in the ADSC secretome-treated group, a significant increase was observed for all of these receptors (Fig. 18B).

In the spleen, the frequencies of most receptors, except 2B4, CD25, and Ly49I, significantly decreased in PBS-treated mice compared to healthy mice (Fig. 18C). The frequencies of $NKG2D^+$ and $DNAM1^+$ NK cells were significantly restored to near-healthy levels by the ADSC secretome (Fig. 18C). On the other hand, the frequencies of cytokine-releasing NK cells, including IFN-γ and IL-10, showed no differences among all groups (Fig. 18D). However, in the case of the frequencies of cytolytic granule-releasing NK cells, such as perforin and granzyme B, PBS-treated mice exhibited a remarkably lower proportion of $perforin^+$ and a higher proportion of granzyme B^+ NK cells compare to healthy mice (Fig. 18D). Interestingly, ADSC secretome-treated mice showed a remarkable recovery in the proportion of $perforin^+$ NK cells and identical levels in the proportion of granzyme B^+ NK cells compared to the PBS group (Fig. 18D). Since perforin facilitates granzymes to be delivered to target cells, NK cells with a failure to secrete functional perforin cannot fully exert granzyme-mediated cytotoxicity.[86,87] Thus, these results suggest that in PBS-treated mice, splenic NK cells have a defect in cytotoxicity, secreting lower perforin, but ADSC secretome treatment raises perforin secretion to enable normal function in splenic NK cells.

In the kidney, the frequencies of most receptors, except 2B4, CD96, and Ly49I, significantly decreased in PBS-treated mice compared to healthy mice (Fig. 18E). Interestingly, ADSC secretome-treated mice exhibited a remarkable recovery in the proportion of $NKG2D^+$ NK cells compared to the PBS group (Fig. 18E). Although not statistically significant, the frequencies of NKp46, CD25, and CD122-positive NK cells showed a moderate recovery to near-healthy levels

in ADSC secretome-treated mice (Fig. 18E). Moreover, slight changes in the frequency of 2B4, CD96, and Ly49I between the healthy and PBS groups were regulated by ADSC secretome treatment to near-normal levels, although they were not statistically significant (Fig. 18E). On the other hand, the frequency of IFN-γ-producing NK cells in PBS-treated mice were significantly decreased compared to healthy mice, but it was recovered by ADSC secretome treatment, nearly reaching healthy levels (Fig. 18F). Althogh not statistically significant, the frequency of IL-10-producing NK cells in PBS-treated mice were slightly decreased compared to that in healthy mice, while in some individuals treated with the ADSC secretome, it was increased above normal levels (Fig. 18F). Moreover, the frequencies of perforin- and granzyme B-producing NK cells exhibited some degree of disfunction phenotype, indicating an imbalance in the secretion of both cytolytic granules in PBS-treated mice. However, these levels showed some recovery toward normal levels upon ADSC secrertome treatment, ableit not statistically significant (Fig. 18F).

A marked downregulation of multiple activating receptors, sustained high expression of inhibitory receptors, decreased secretion of effector cytokines, and weakened cytotoxicity or degranulation of NK cells represent characteristic features of dysfunction.[88,89] These observations indicate that peripheral NK cells in lupus nephritis NZB/W mice exhibit a consistent exhaustion phenotype, indicative of dysfunction, across the blood, spleen, and kidneys. Furthermore, ADSC secretome treatment appears to mitigate this dysfunctional state of NK cells by modulating the expression of activating and inhibitory receptors, thereby promoting the recovery of cytokine and cytolytic granule secretion to normal levels, particularly evident in the kidneys.

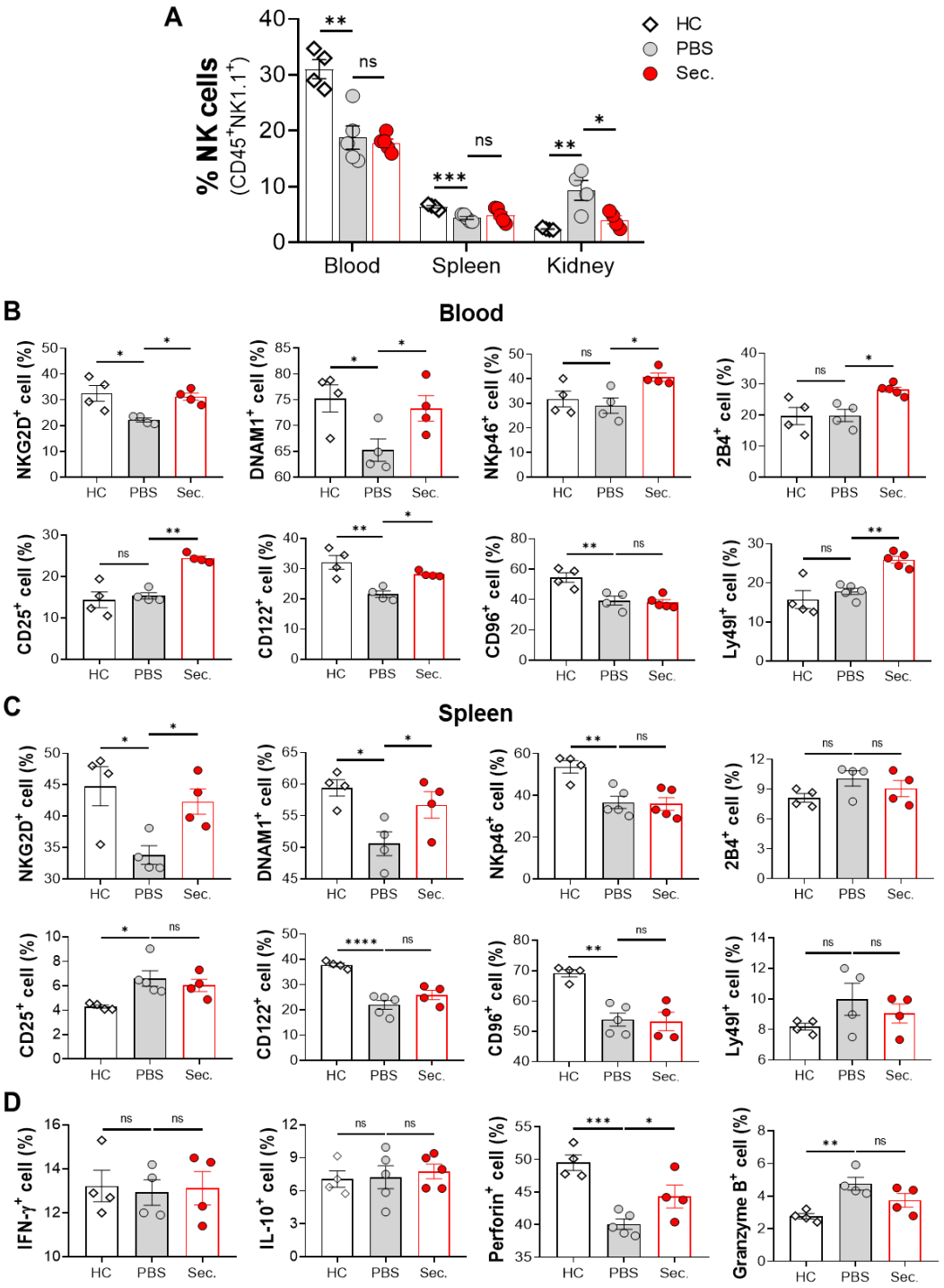

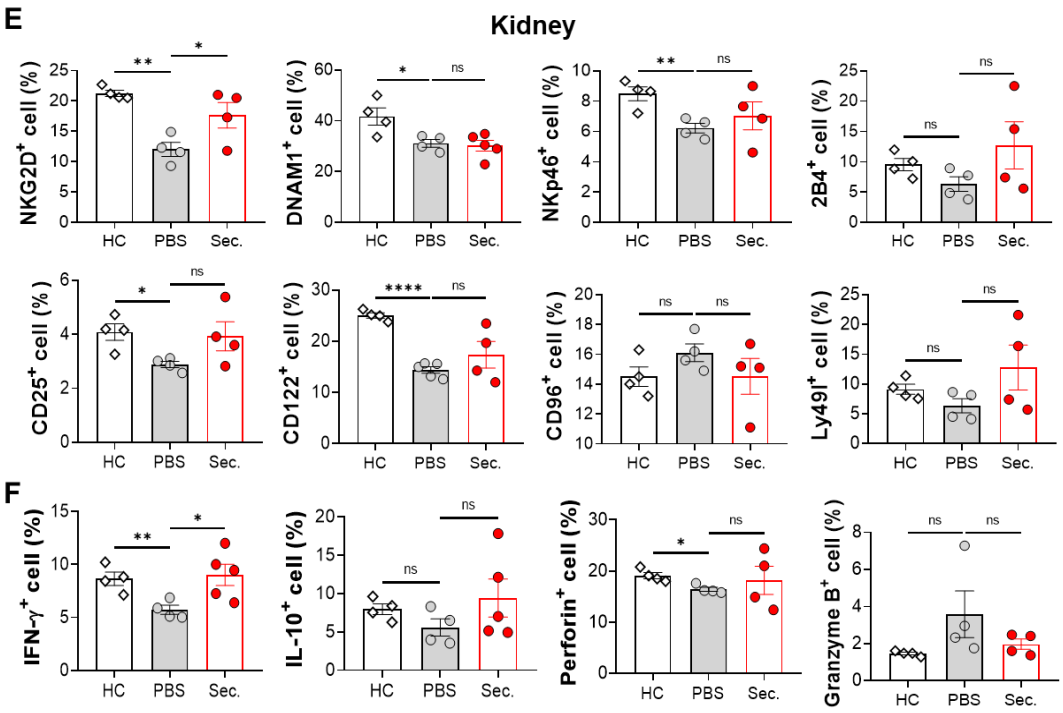

Figure 18. Distribution and phenotype characterization of natural killer (NK) cells in blood, spleen, and kidneys of F1 hybrids of New Zealand black and white (NZB/W F1) mice using flow cytometry analysis. (A) Percentages of $CD45^+NK1.1^+$ NK cells in the indicated organs of healthy (*HC*; white diamons), PBS-treated (*PBS*; gray circles), and ADSC secretome-treated (*Sec.*; red circels) NZB/W F1 mice. Data were analyzed using a Student's unpaired two-tailed *t*-test. (B) Percentages of cells expressing activating receptors, including $NKG2D^+$, $DNAM1^+$, $NKp46^+$, and $2B4^+$, as well as IL-2R subunits $CD25^+$ and $CD122^+$, and inhibitory receptors $CD96^+$ and $Ly49I^+$, were analyzed in the NK ($CD45^+NK1.1^+$) cell population in the blood. (C) Percentages of cells expressing surface receptors as displayed in B and (D) intracellular effector molecules, including IFN-γ^+, IL-10^+, $perforin^+$, and granzyme B^+, were analyzed in the NK ($NK1.1^+$) cell population in the spleen. (E) Percentages of cells expressing surface receptors and (F) intracellular effector molecules as displayed in D were analyzed in the NK ($CD45^+NK1.1^+$) cell population in the kidneys.

Data were analyzed using a Student's unpaired two-tailed *t*-test. Error bars represent mean ± SEM. Statistical tests were determined by 1-way ANOVA followed by Holm-Sidak's multiple-comparison test. Asterisks indicate statistical significance; not significant (ns), $*P < 0.05$, $**P < 0.01$, $***P < 0.001$, $****P < 0.0001$.

3.2.6. Impact of ADSC secretome treatment on T and B cell compartments in NZB/W F1 lupus nephritis mice

T and B cells are implicated as pivotal contributors to the pathogenesis of lupus. Elevated counts of $CD4^+$ T follicular helper (Tfh) and T peripheral helper (Tph) cells foster B cell activation, promoting the production of autoantibodies.[90,91] Anomalies in the activation and proliferation of various B cell subsets serve as a central element in the initiation and advancement of SLE pathology.[92] To assess the effect of the ADSC secretome on T and B cell populations in the spleen and kidneys, we performed a comprehensive flow cytometric analysis of T and B cells in both organs of NZB/W F1 mice. We found that the frequencies of $CD8^+$ T ($TCR\beta^+CD8^+$) cell subpopulations, categorized based on the surface expression of CD44 and CD62L (referred to as naïve and activated/memory types), were altered in the spleen and kidneys due to the lupus environment. Interestingly, ADSC secretome treatment regulated these frequencies to levels near those observed in healthy conditions (Fig. 19A). Meanwhile, the frequencies of cytokine-producing $CD8^+$ T cells including IFN-γ, IL-4, and IL-17, were not affected by the ADSC secretome in both the spleen and kidneys (Fig. 19B upper). However, the frequencies of cytotoxic $CD8^+$ T cells (CTLs) secreting perforin and granzyme B, especially in the kidneys, significantly decreased after ADSC secretome administration (Fig. 19B bottom).

In the case of $CD4^+$ T ($TCR\beta^+CD4^+$) cell subpopulations, their frequencies of Th1 cells (IFN-γ^+), Th2 cells (IL-4^+), and Th17 cells (IL-17^+) in ADSC secretome-treated mice were significantly reduced only in the spleen compared to PBS-treated mice (Fig. 19C). Moreover, the frequencies of Tfh cells ($CXCR5^+PD1^+$) and regulatory T cells (Treg; $CD25^+FOXP3^+$) in the spleen were remarkably increased in PBS-treated mice; however, they showed a significant decrease after ADSC secretome treatment (Fig. 19D, E).

Upon scrutinizing B cell subpopulations, we noted changes in the frequencies of transitional type 1 B cells (T1 B; $B220^{+}CD19^{+}IgM^{+}IgD^{lo}$), transitional type 2 B cells (T2 B; $B220^{+}CD19^{+}IgM^{+}IgD^{+}$), and mature B cells ($B220^{+}CD19^{+}$ $IgM^{lo}IgD^{+}$) in both the spleen and kidneys due to the lupus environment. Although not all changes reached statistical significance, there was a discernible trend in the frequencies of T1 B cells, T2 B cells, and mature B cells in both organs that seemed to be restored to normal levels following the administration of the ADSC secretome (Fig. 19F upper). The frequencies of germinal center B cells ($B220^{+}CD19^{+}GL7^{+}$), plasma cells ($B220^{lo}CD19^{-}CD138^{+}$), and regulatory B cells (Breg; $B220^{+}CD19^{+}CD1d^{+}$ $IL\text{-}10^{+}$) did not experience any modulatory effect by the ADSC secretome (Fig. 19F middle, bottom), but only those of memory B cells ($B220^{+}CD19^{+}$ $CD138^{-}IgG1^{+}$) in the spleen dramatically increased after ADSC secretome treatment (Fig. 19F bottom). Taken together, these data demonstrate the potential therapeutic efficacy of the ADSC secretome in experimental lupus nephritis, particularly affecting $CD8^{+}$ T cells present in the kidneys, $CD4^{+}$ T cells in the spleen, and B cells in the spleen and kidneys undergoing the transitional stage, as well as splenic memory B cells.

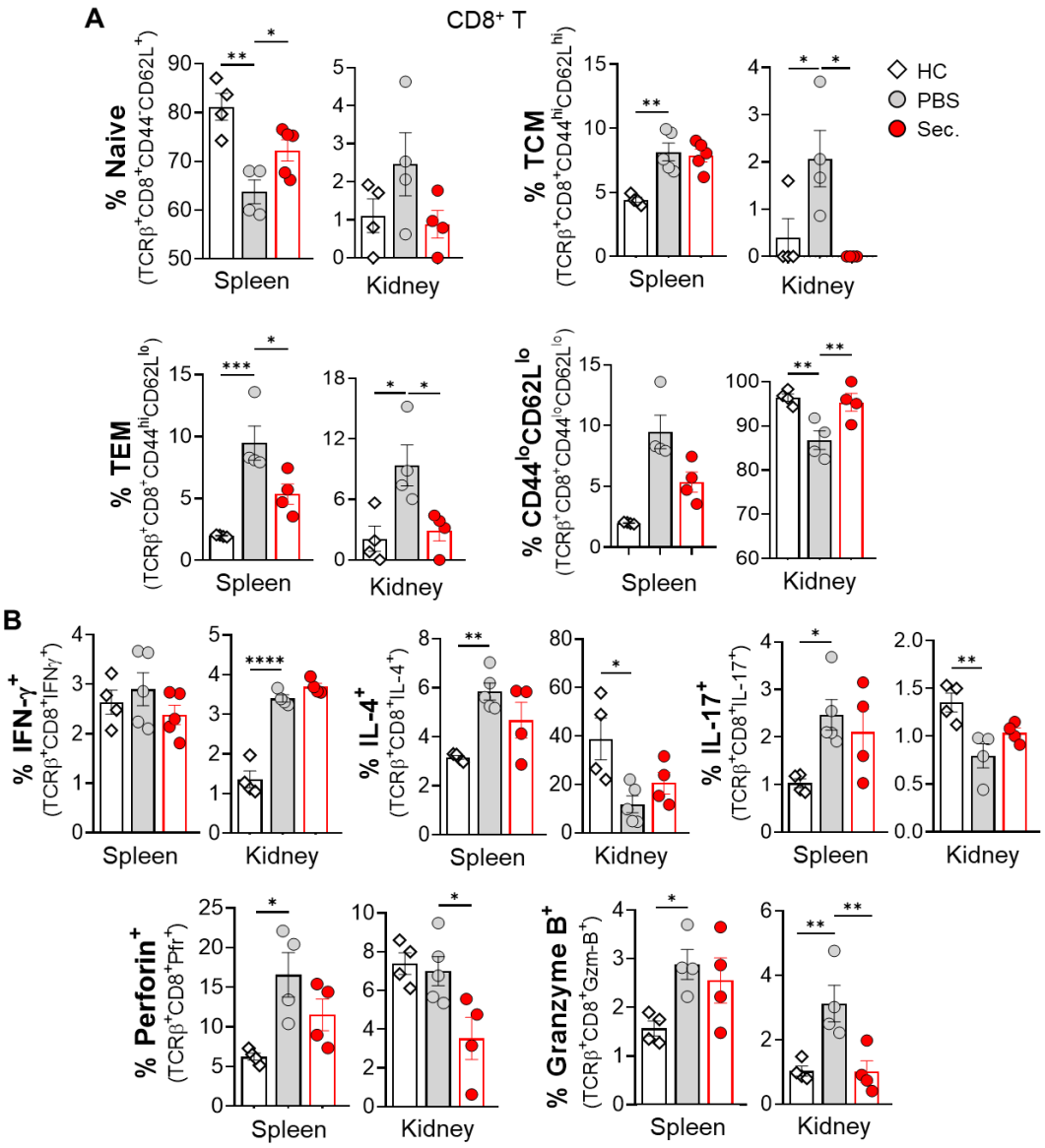

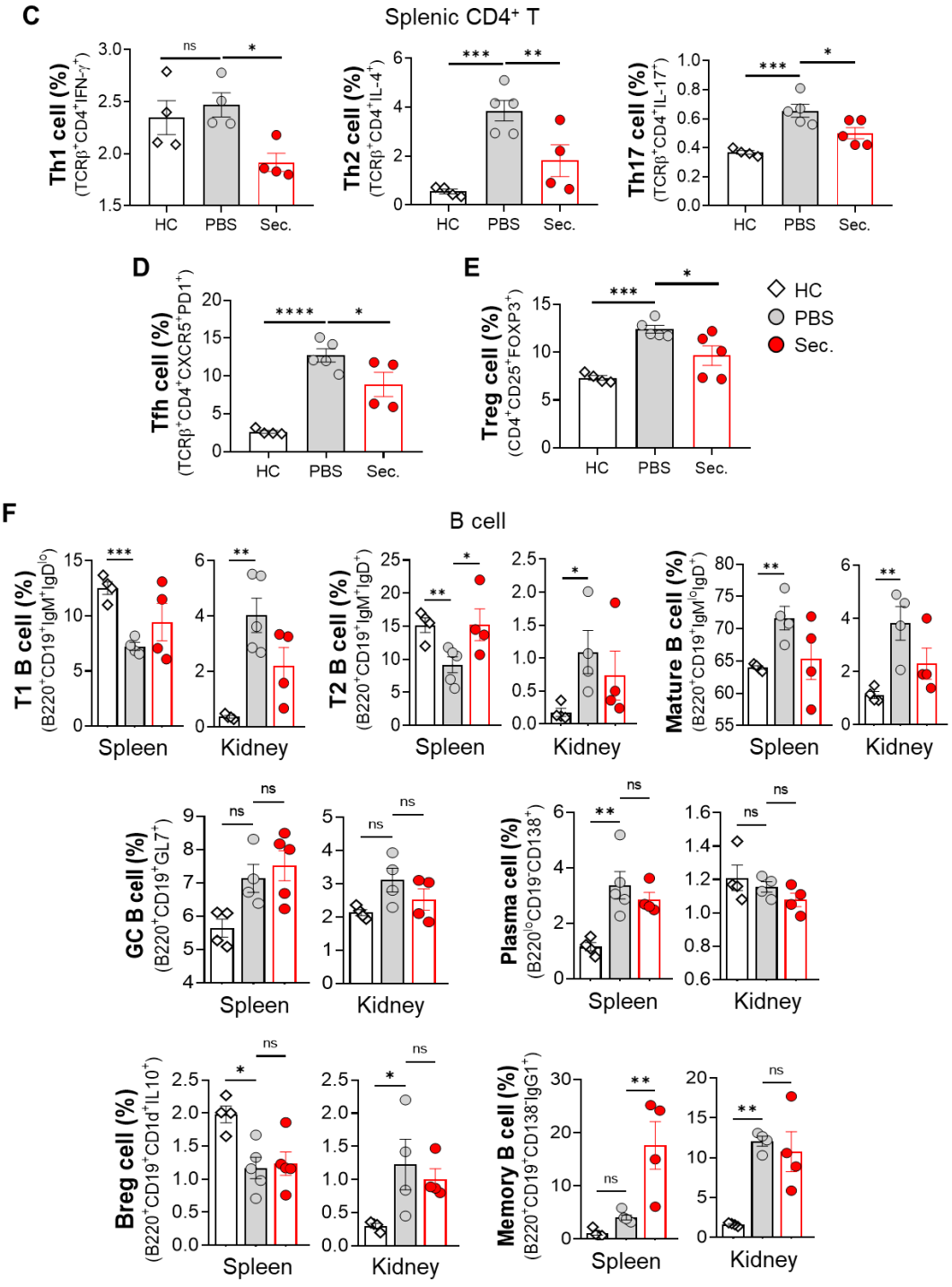

Figure 19. Analysis of multiple T and B cell subpopulations in the spleen and kidneys of F1 hybrids of New Zealand black and white (NZB/W F1) mice. (A) Percentages of naïve T cells ($CD44^{-}CD62L^{+}$), central memory T cells (TCM; $CD44^{hi}CD62L^{hi}$), effector memory T cells (TEM; $CD44^{hi}CD62L^{lo}$), and $CD44^{lo}CD62L^{lo}$ cells, on the $CD8^{+}$ T cell ($TCR\beta^{+}CD8^{+}$) gating in the indicated organs of healthy (*HC*; white diamonds), PBS-treated (*PBS*; gray circles), and ADSC secretome-treated (*Sec.*; red circels) NZB/W F1 mice. (B) Percentages of cells expressing intracellular effector molecules, including IFN-γ^{+}, IL-4^{+}, IL-17^{+}, perforin^{+}, and granzyme B^{+}, on the $CD8^{+}$ T cell ($TCR\beta^{+}CD8^{+}$) gating in the indicated organs. (C) Percentages of T helper 1 cells (Th1; IFN-γ^{+}), T helper 2 cells (Th2; IL-4^{+}), T helper 17 cells (Th17; IL-17^{+}), (D) follicular helper T cells (Tfh; $CXCR5^{+}PD1^{+}$), and (E) regulatory T cells (Treg; $CD25^{+}FOXP3^{+}$), on the $CD4^{+}$ T cell ($TCR\beta^{+}CD4^{+}$) gating in the spleen. (F) Percentages of transitional type 1 B cells (T1 B; $B220^{+}CD19^{+}IgM^{+}IgD^{lo}$), transitional type 2 B cells (T2 B; $B220^{+}CD19^{+}IgM^{+}IgD^{+}$), mature B cells ($B220^{+}CD19^{+}IgM^{lo}IgD^{+}$), germinal center B cells (GC B; $B220^{+}CD19^{+}GL7^{+}$), plasma cells ($B220^{lo}CD19^{-}CD138^{+}$), regulatory B cells (Breg; $B220^{+}CD19^{+}CD1d^{+}IL\text{-}10^{+}$), and memory B cells (MBC; $B220^{+}CD19^{+}CD138^{-}IgG1^{+}$) in the indicated organs. Error bars represent mean ± SEM. Statistical tests were determined by 1-way ANOVA followed by Holm-Sidak's multiple-comparison test; not significant (ns), $*P < 0.05$, $**P < 0.01$, $***P < 0.001$, $****P < 0.0001$.

4. Discussion

This work offers valuable insights into the fundamental biology of regulating NK cell activity through the MSC secretome in the context of both transient stimulation by IL-2 and sustained stimulation by chronic inflammation. In Chapter 1, we discovered that the ADSC secretome restricts IL-2–induced effector functions of NK cells while preserving their proliferative capacity and revealed its mechanism of action.[63] Extant studies on MSC secretome-mediated regulation of NK cell activity[24,25,27,28] have concentrated on specific aspects, resulting in fragmented information. In contrast, this study has considerable meaning in that it provides a comprehensive understanding of the interaction between NK cells and the MSC secretome.

We observed that the ADSC secretome specifically influenced the functional aspects of NK cells, such as cytokine secretion (IFN-γ, IL-10, granzyme B, GM-CSF, and perforin), cytotoxicity, and degranulation, without impacting their proliferation. This effect was associated with the upregulation of the inhibitory receptor CD96 and the downregulation of activating receptors (NKG2D, NKp30, and NKp46). Despite the well-known inhibitory role of CD96, its precise function in NK cells remains unclear.[93-96] This study suggests that CD96 may be implicated in constraining NK cell activation rather than facilitating it.

Furthermore, diminished IL-2Rα and IL-2Rγ expression levels were noted in NK cells treated with the ADSC secretome. This observation implies that the ADSC secretome might play a role in diminishing the responsiveness of NK cells to IL-2 by hindering the interaction of IL-2 with the IL-2Rαβγ trimeric complex, which exhibits the highest binding affinity for its ligand IL-2.[75] However, the mechanisms governing the modulation of IL-2R subunit expression by the MSC secretome necessitate additional exploration.

This study also illuminated the impact of the ADSC secretome on signaling pathways within NK cells. We observed a reduction in the intensity of IL-2–induced JAK1 and JAK3 phosphorylation, resulting in diminished phosphorylation of STAT5 and AKT. These results suggest that the ADSC secretome attenuates IL-2 signaling in NK cells without impeding cell proliferation. It is plausible that the ADSC secretome diminished the PI3K/AKT pathway, crucial for NK cell effector function,[97-99] while preserving a minimum essential isoform of pSTAT5 to sustain STAT5-driven survival signals.[100]

Here, we demonstrated that the ADSC secretome-induced inhibition of NK cell function involves the upregulation of CIS, rather than SHPs or SHIPs, in the cytoplasm. This upregulation contributes to the degradation or dephosphorylation of pJAK1, pJAK3, and pSTAT5.[39,40,101,102] This observation aligns with a study on NK cell negative regulation, emphasizing CIS as a crucial suppressor of IL-15 signaling in NK cells through interaction with the activation loop peptides of JAK1 and JAK3.[35] Additionally, our investigation revealed the upregulation of DUSP4 by the ADSC secretome in human primary NK cells isolated from peripheral blood, as confirmed by mRNA sequencing, qRT-PCR, and western blotting. DUSP4, a key phosphatase expressed in various immune cells, including NK cells, modulates MAP kinase activity to influence the inflammatory response induced by LPS[103] and regulates STAT5 activity in T cell differentiation.[104] Although the direct relationship between the regulators (CIS, DUSP4) and the negative regulation of IL-2 signaling in NK cells may not be fully elucidated in our findings, their upregulation stands as a significant observation in an effort to control inappropriate or excessive activation of NK cells. Taken together, the ADSC secretome modulates NK cell activity by attenuating IL-2 signaling, achieved through the inhibition of JAK1 and JAK3 phosphorylation, facilitated by the enhanced expression of CIS and DUSP4 (Fig. 20).

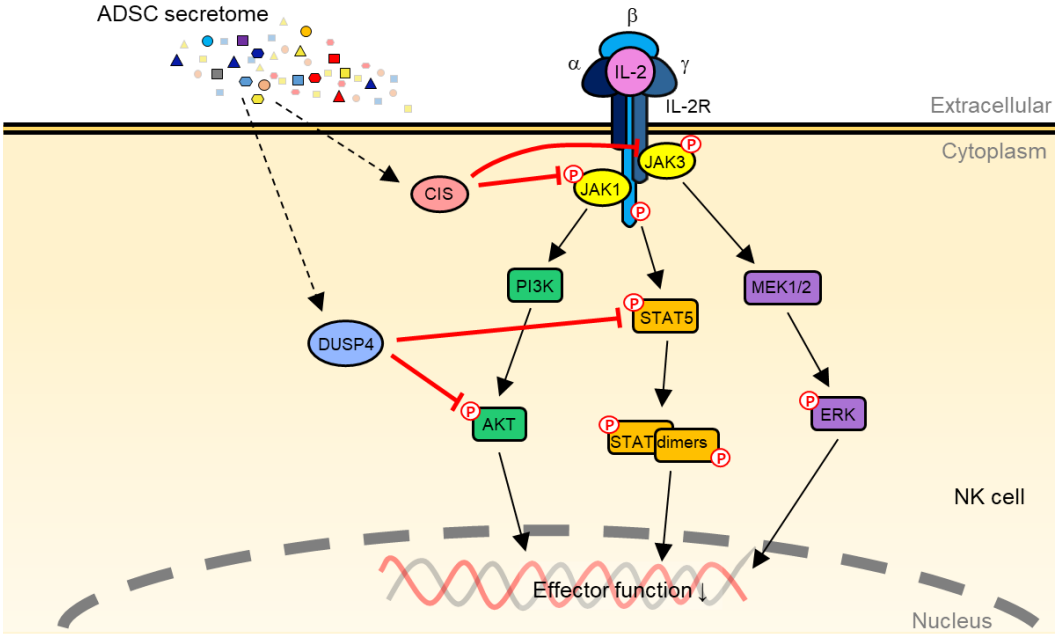

Ko et al. *Stem Cell Res. Ther.* **2023**

Figure 20. Potential mechanism of the regulation of IL-2 signaling pathway by the adipose tissue-derived stem cell (ADSC) secretome. The ADSC secretome triggers an increase in CIS and DUSP4 expression in NK cells, resulting in a dampened effector function of NK cells while sustaining cell proliferation. CIS binds to pJAK1 and pJAK3, directing them towards proteasomal degradation, thereby inhibiting their enzymatic activity. Simultaneously, DUSP4 dephosphorylates pSTAT5 and pAKT, attenuating the amplitude of the IL-2 signaling cascade.

To date, it has been reported that several molecules within the MSC secretome, such as transforming growth factor β (TGF-β),[24,28] indoleamine-pyrrole 2,3-dioxygenase (IDO),[27] prostaglandin E2 (PGE2),[24] thrombospondin 1,[28] and activin A,[25] regulate the proliferation and activity of NK cells. Interestingly, in this study, we identified 12 new candidates associated with the immunomodulatory capacity of the ADSC secretome by characterizing its contents through

proteomic analysis. We further validated the immunomodulatory potential of these candidates using neutralizing antibody against each one. Future investigations are required to elucidate the precise roles of these 12 putative factors in immunomodulation and to understand how they specifically control NK cell activity.

In Chapter 2, we observed that the ADSC secretome also inhibits IL-2–induced effector functions and modulates surface receptors of mouse NK cells isolated from the spleen, similar to observations in human NK cells. These findings suggest a consistent effect of the ADSC secretome on NK cells across both human and mouse species, highlighting the potential benefits of utilizing cells from both species for further detailed studies on these mechanisms of action.

Furthermore, we revealed the distribution and detailed phenotype of NK cells in the blood, spleen, and kidneys during disease progression in a spontaneous murine model of lupus, NZB/W F1 mice, and their alteration by treatment with the ADSC secretome. We also examined the complexity of immune cell populations in the spleen and kidneys of these mice. We found: (1) the therapeutic effect of the ADSC secretome on lupus nephritis mice, which results in improved renal function, lower serum levels of inflammatory cytokines and anti-dsDNA IgG, reduced kidney infiltration of leukocytes, preserved renal pathology, and decreased accumulation of immune complexes in the kideys; (2) an abundance of NK cells in the kidneys compared to a decrease in the blood and spleen in the context of lupus nephritis, indicating the accumulation of NK cells in target tissue of lupus nephritis, consistent with previous studies, and a reduction in kidney-infiltrating NK cells due to the ADSC secretome; (3) consistency in the phenotypic profile of peripheral NK cells, including blood, splenic, and renal NK cells, showing signs of exhaustion such as decreased activating receptors, upregulation of the inhibitory receptor Ly49I, decresed IFN-γ production, and a defect in cytotoxicity due to an imbalance in perforin and granzyme secretion,

and the restoration of these exhausted states by the ADSC secretome; (4) the regulation of T and B cell cell subsets in spleen and kidneys, along with renal neutrophils, through treatment with the ADSC secretome in the LN environment.

Current knowledge of the role of NK cells in SLE primarily comes from studies on human peripheral blood due to the rarity of patient kidney biopsies.[45,105] However, it is unclear whether blood accurately reflects the functions of tissue-localized NK cells in the development of SLE.[48,106] Furthermore, the phenotypic and functional features of NK cells in SLE target tissue have not been sufficiently revealed. Previous human studies using blood[49,50,57,107-110] have demonstrated that: (1) increased disease activity is associated with a decrease in the frequency and number of NK cells; (2) lupus NK cells exhibit functional abnormalities, characterized by either lower cytokine secretion and killing ability, or increased IFN-γ secretion but reduced killing capacity, indicating the cause of a genetic defect in cell function or lupus serum autoantibodies targeting NK cells receptors; (3) phenotypically, these NK cells are not exhausted but demonstrate an activated state with a proinflammatory phenotype. Recent studies utilizing single-cell RNA-Seq (scRNA-Seq) on kidney biopsies from LN patients have revealed an abundance of NK cells within patient kidneys. These NK cells exhibit strongly active phenotype and may be major sources of IFN-γ and cytolytic granules in the kidneys alongside cytotoxic $CD8^+$ T cells, suggesting a role in tissue damage in LN.[48,111] However, the role of NK cells in SLE remains a topic of debate. They may either promote inflammation and tissue damage by secreting cytokines that activate other immune cells[50] or alleviate inflammation and tissue damage by eliminating activated T cells and macrophages and secreting cytokines that suppress T cell differentiation.[112] So far, only four studies using MRL/*lpr* mice, another mouse model of SLE, have been published. Two of these studies demonstrated a more cytotoxic phenotype in liver and lung NK cells than in pre-diseased mice.[113,114] The other two

studies showed a relationship between the number of kindey-infiltrating NK cells and the active phase of the disease, suggesting the contribution of NK cells to lupus pathogenesis.[51,58]

In this study, we observed a lower frequency of NK cells in the blood and spleen, but a higher frequency in the inflamed kidneys of NZB/W F1 lupus mice, indicating their migration to inflamed tissue. Additionally, we found surprisingly little phenotypic and functional evidence of increased activation or effector function of NK cells; instead, we observed evidence of exhaustion and dysfunction in the NK cells of NZB/W F1 mice. We demonstrated that peripheral NK cells from diseased NZB/W F1 mice showed a significantly decreased frequency of activating receptor-positive cells, such as $NKG2D^+$, $DNAM1^+$, and $NKp46^+$, as well as the IL-2 receptor subunit $CD122^+$ ($IL\text{-}2R\beta^+$), but a maintained frequency of the inhibitory receptor $Ly49I^+$, though not $CD96^+$, compared to those of healthy mice. Moreover, they also exhibited dysfunction in cytotoxicity due to an imbalance in the expression of perforin and granzyme B in the spleen and kidneys, and, in particular, a significantly low frequency of IFN-γ^+ cells in the kidneys. Considering our observations, lupus nephritis NK cells exhibiting a dysfunctional phenotype may not be major sources of IFN-γ and cytolytic granules in the periphery, which are causing tissue damage; rather, they may play a differnet role in lupus nephritis.

Due to the many advangates of MSC secretome, inducing immune balance in inflammatory or autoimmune diseases using MSC secretome is a promising treatment option, and many related studies are currently in progress. In Chapter 2, we confirmed the efficacy of the ADSC secretome in lupus nephritis mice through long-term treatment follow up. ADSC secretome treatment induced decreased frequencies of splenic $CD4^+$ T cell subpopulations, including Th1, Th2, Th17, and Tfh cells, which exacerbate SLE, compared to the diseased condition. On the other hand, no distinct changes were observed in the kidney-infiltrating $CD4^+$ T cell subpopulations among the groups

(data not shown). These clusters were not also clearly distinguishable from each subtype's signatures, similar to a previous study with scRNA-seq on kidney samples from LN patients.[48] These results suggest that $CD4^+$ T cell polarization in the spleen, rather than the kidney, may be a major pathogenic factor in the NZB/W mouse model of LN, and that ADSC secretome administration modulates this splenic $CD4^+$ T cell polarization.

Furthermore, we found that $CD8^+$ T cell subpopulations were more prominent in the kidneys than in the spleen, unlike of $CD4^+$ T cells in the diseased condition. In the diseased mice, effector and central memory $CD8^+$ T cells in the spleen were expanded, accompanied by a contration of naïve $CD8^+$ T cells. However, in ADSC secretome-treated mice, these populations were regulated to normal levels. Additionally, although IFN-γ-producing and perforin- and granzyme B-producing cytotoxic $CD8^+$ T cells (CTLs), which play roles similar to NK cells, were expanded in the inflamed kidney, similar to a previous study on patients' kidneys,[48] only the frequency of CTLs was reduced by ADSC secretome treatment. These results suggest that although there is an abundance of CTLs and NK cells in the inflamed kidneys of NZB/W mice, the major source of IFN-γ and cytolytic granules in this tissue may come from CTLs, not NK cells, indicating a role for cytotoxic activity in LN. It also suggests that the ADSC secretome affects splenic memory types of $CD8^+$ T cells as well as kidney-infiltrating CTLs to modulate their activities.

Considering the effect of the ADSC secretome to lupus NK cells during the alleviation of LN, the ADSC secretome induced the restoration of their exhuanstion phenotype to normal levels. This suggests a regulatory function of NK cells in LN to eliminate the self-reactive immune responses and that the ADSC secretome supports their regulatory role through phenotypic changes in them. It has been proposed that NK cells play a protective role in autoimmune diseases such as rheumatoid arthritis (RA) and multiple sclerosis (MS) in both humans and mice through NK cell-

mediated lysis, which depends on the expression of multiple surface receptors.[115-118] NK cells can directly kill autoreactive T cells, but not resting T cells. They can also indirectly inhibit autoreactive T cells by eliminating antigen-presenting cells (APCs), especially dendritic cells (DCs), thereby preventing an autoimmune response.[118] However, it is possible that chronic exposure to cytokines and autoantibodies in the lupus environment may excessively stimulate NK cells, inducing an exhaustion phenotype[88,89,119] that prevents them from performing their regulatory function.

We previously observed in Chapter 1 that the ADSC secretome suppresses the activity of NK cells transiently stimulated by IL-2 through tuning the expression of activating and inhibitory receptors and upregulating negative regulators within NK cells. Based on these findings and several previous studies, we hypothesized that the hyperactivity of NK cells caused by autoimmune responses would exacerbate lupus nephritis and that the ADSC secretome could modulate these inflammatory responses. Unexpectedly, as shown in Chapter 2, we noted that the ADSC secretome reverted the dysfunction of NK cells with exhaustion phenotype to normal when exposed to the chronic inflammatory environment in the NZB/W lupus mice. These findings raise the possibility that the bioactive molecules in the ADSC secretome have the advantage of playing beneficial roles depending on the surrounding environment to maintain homeostasis in the body. This highlights the need to investigate the key factors and mechanisms behind this multifunctional effect.

The characteristics of lupus-like disease in NZB/W F1 mice include overactive B cells, irregular germinal center formation, and an accumulation of plasma cells and memory B cells.[120] We demonstrated that the frequency of total B cells significantly increased in the spleen, not in the kidneys, of NZB/W mice with active lupus nephritis. This suggests that the pathogenic activity of B cells mainly occurs in the spleen rather than in the inflammatory kidneys. Additionally, the increased frequency of transitional B (TrB) cells is associated with active SLE. These cells are immature B cells originating from bone marrow and are considered precursors to mature B cells.

Although, like Bregs, TrB cells play a protective role both in healthy conditions and immune diseases, their regulatory functions are impaired in SLE, thereby failing to remove autoreactive B cell responses.[121] We showed that the frequency of T1 B and T2 B cells was significantly increased in the inflammatory kidneys, while it was conversely reduced in the spleen, with a maintained higher frequency of mature B cells in both organs. Upon treatment with the ADSC secretome, the frequency of these three subtypes of B cells showed a trend towards recovery to levels observed in healthy condition. It is believed that most of the TrB cells differentiate into mature B cells, and this mature state and plasma cells, which present autoantibodies, are dominant in the spleen. In contrast, immature B cells continuously flow into the kidneys, leading to the active development of TrB cells and mature B cells, which contributes to the kidney inflammation. Additionally, the ADSC secretome may exert an influence on B cell differentiation stages, from T1 B to mature B cells, to modulate B cell responses in both organs.

Treg cells, a subset of $CD4^+$ T cells, are vital in preserving self-tolerance by suppressing self-reactive immune cells. Dysfunctions in Treg cells or their deficiency are believed to contribute to the development of SLE.[122] Despite extensive research on Treg cells, studies report conflicting findings on their frequency in SLE, with some indicating increases and others decreases based on disease activity.[111] In this study, we found a significantly higher frequency of splenic Tregs in the diseased NZB/W mice compared to controls. However, in ADSC secretome-treated mice, we observed a decrease in Treg frequency. This may be due to Tregs expanding or differentiating more in response to autoimmune disease to suppress excessive immune responses, but not enough to offset conventional T cell proliferation.[122] Moreover, the administration of the ADSC secretome significantly reduces overall inflammation, which appears to correspond with a decrease in splenic Treg frequency. However, the specific molecules within the ADSC secretome that potentially decrease cellularity and the mechanisms by which these molecules affect the cells, ultimately

ameliorating nephritis, remain outstanding questions. Although it is only assumed, among the 83 proteins identified by proteomics, as shown in Chapter 1, some may partially exert effects on immune cells, including NK cells in lupus mice. In the future studies, it will be interesting to address these issues.

This study provided an in-depth examination of peripheral and kidney-localized NK cells by characterizing lupus NK cells in NZB/W F1 mice. It confirmed the importance of the ADSC secretome in regulating the phenotype and distribution of NK cells, as well as the cellularity of various immune cells, resulting in the protection of target tissue and alleviation of inflammation (Fig. 21).

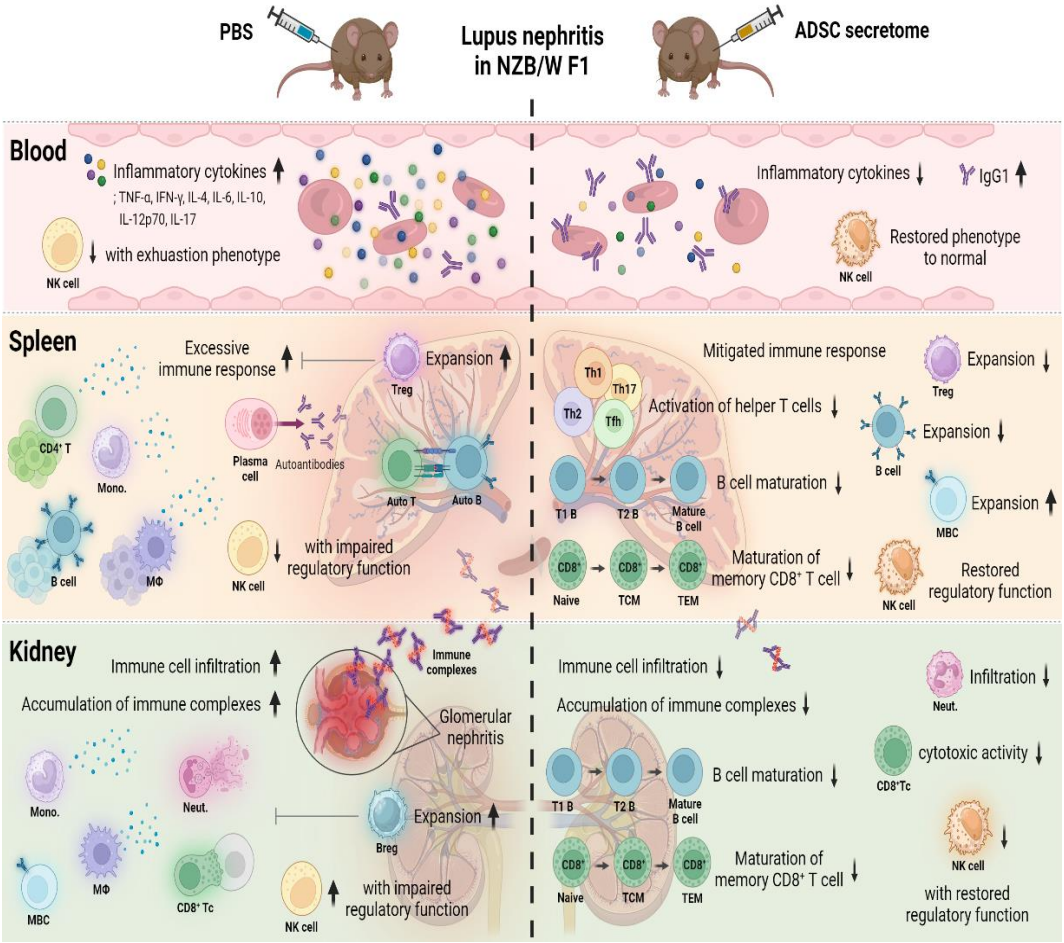

Figure 21. Mitigating effects of the adipose tissue-derived stem cell (ADSC) secretome on lupus nephritis (LN) in F1 hybrids of New Zealand black and white (NZB/W F1) mice with a focus on natural killer (NK) cell biology. NK cells may have a role in autoimmune surveillance by eliminating self-reactive immune cells. In the autoimmune environment of LN, peripheral NK cells are likely recruited to the inflamed kidneys to repress autoreactive cells, leading to a reduction in NK cell frequency in peripheral blood and spleen. At this stage, NK cells do not exhibit an activated effector profile but rather display an exhaustion phenotype with suppressed regulatory function due to chronic inflammation. Following the administration of the ADSC secretome in NZB/W mice,

overall inflammation is greatly reduced and renal structure and function are preserved. the ADSC secretome may partially contribute to restored NK cell activity by regulating the expression of activating and inhibitory receptors on NK cells, thereby aiding in inflammation control. As a result of reduced inflammation, NK cells no longer seem to be recruited to the kidneys. Notable immune cells included are NK cells, $CD4^+$ T cells ($CD4^+$ T), monocytes (Mono.), B cells, macrophages (MΦ), plasma cells, regulatory T cells (Treg), autoreactive T or B cells (Auto T or Auto B), neutrophils (Neut.), memory B cells (MBC), cytotoxic $CD8^+$ T cells ($CD8^+$ Tc), regulatory B cells (Breg), T helper 1 cells (Th1), T helper 2 cells (Th2), T helper 17 cells (Th17), follicular helper T cells (Tfh), transitional type 1 B cells (T1 B), transitional type 2 B cells (T2 B), mature B cells, naïve $CD8^+$ T cells (Naïve), central memory $CD8^+$ T cells (TCM), and effector memory $CD8^+$ T cells (TEM). This illustration was generated using the BioRender.com website.

It is hoped that this study will enable researchers to specifically target these soluble factors within the MSC secretome, thereby paving the way for new therapeutic avenues in inflammatory diseases.

5. Conclusion

This study aimed to shed light on the underlying mechanisms governing NK cell activity modulation by the ADSC secretome and to delineate the characteristic alterations in NK cells within the context of lupus nephritis, along with investigating the regulatory effects of ADSC secretome treatment. In Chapter 1, based on observations from our previously published paper,[63] we meticulously analyzed the surface receptor expression profile of human NK cells transiently stimulated by IL-2, identified negative regulatory pathways, and elucidated the signaling molecules modulating NK cell function. Furthermore, we introduced novel candidates for immune regulation originating from MSCs. At the beginning of Chapter 2, we confirmed the reproducibility of the downregulation effect of the ADSC secretome on mouse NK cells transiently stimulated by IL-2. Subsequently, we found that NK cells in the lupus NZB/W mice may exhibit an exhaustion phenotype due to continuous exposure to chronic inflammation. The ADSC secretome upregulated the suppressed regulatory functions of NK cells, unlike in the case of transient stimulation, and suppressed the frequency of other inflammatory cells, thereby ameliorating lupus nephritis. Our findings contribute to a deeper understanding of the mechanisms underlying the effects of the secretome on NK cells and pave the way for evaluating the therapeutic potential of NK cell function modulation through the ADSC secretome in inflammatory and autoimmune diseases characterized by aberrant NK cell activation, including lupus nephritis. Moreover, these results provide crucial insights for the development of biological therapies utilizing stem cell-derived products in future clinical trials aimed at addressing the limitations of current SLE treatments.

REFERENCES

1. Shi Y, Wang Y, Li Q, Liu K, Hou J, Shao C, et al. Immunoregulatory mechanisms of mesenchymal stem and stromal cells in inflammatory diseases. Nat. Rev. Nephrol. 2018;14:493-507.
2. Baraniak PR, McDevitt TC. Stem cell paracrine actions and tissue regeneration. Regen. Med. 2010;5:121-43.
3. Murphy MB, Moncivais K, Caplan AI. Mesenchymal stem cells: environmentally responsive therapeutics for regenerative medicine. Exp. Mol. Med. 2013;45:e54.
4. Harman RM, Marx C, Van de Walle GR. Translational Animal Models Provide Insight Into Mesenchymal Stromal Cell (MSC) Secretome Therapy. Front. Cell. Dev. Biol. 2021;9:654885.
5. L PK, Kandoi S, Misra R, S V, K R, Verma RS. The mesenchymal stem cell secretome: A new paradigm towards cell-free therapeutic mode in regenerative medicine. Cytokine Growth Factor Rev. 2019;46:1-9.
6. Daneshmandi L, Shah S, Jafari T, Bhattacharjee M, Momah D, Saveh-Shemshaki N, et al. Emergence of the Stem Cell Secretome in Regenerative Engineering. Trends Biotechnol. 2020;38:1373-84.
7. Munoz-Perez E, Gonzalez-Pujana A, Igartua M, Santos-Vizcaino E, Hernandez RM. Mesenchymal Stromal Cell Secretome for the Treatment of Immune-Mediated Inflammatory Diseases: Latest Trends in Isolation, Content Optimization and Delivery Avenues. Pharmaceutics 2021;13:1802.
8. Tran C, Damaser MS. Stem cells as drug delivery methods: application of stem cell secretome for regeneration. Adv. Drug Deliv. Rev. 2015;82-83:1-11.
9. Kusuma GD, Carthew J, Lim R, Frith JE. Effect of the Microenvironment on Mesenchymal Stem Cell Paracrine Signaling: Opportunities to Engineer the Therapeutic Effect. Stem Cells Dev. 2017;26:617-31.
10. Ferreira JR, Teixeira GQ, Santos SG, Barbosa MA, Almeida-Porada G, Goncalves RM. Mesenchymal Stromal Cell Secretome: Influencing Therapeutic Potential by Cellular Pre-conditioning. Front. Immunol. 2018;9:2837.
11. Harrell CR, Fellabaum C, Jovicic N, Djonov V, Arsenijevic N, Volarevic V. Molecular Mechanisms Responsible for Therapeutic Potential of Mesenchymal Stem Cell-Derived Secretome. Cells 2019;8:467.

12. Lee MJ, Kim J, Kim MY, Bae Y-S, Ryu SH, Lee TG, et al. Proteomic Analysis of Tumor Necrosis Factor-α-Induced Secretome of Human Adipose Tissue-Derived Mesenchymal Stem Cells. J. Proteome Res. 2010;9:1754-62.
13. Kim HS, Choi DY, Yun SJ, Choi SM, Kang JW, Jung JW, et al. Proteomic Analysis of Microvesicles Derived from Human Mesenchymal Stem Cells. J. Proteome Res. 2012;11:839-49.
14. Pires AO, Mendes-Pinheiro B, Teixeira FG, Anjo SI, Ribeiro-Samy S, Gomes ED, et al. Unveiling the Differences of Secretome of Human Bone Marrow Mesenchymal Stem Cells, Adipose Tissue-Derived Stem Cells, and Human Umbilical Cord Perivascular Cells: A Proteomic Analysis. Stem Cells Dev. 2016;25:1073-83.
15. Maffioli E, Nonnis S, Angioni R, Santagata F, Cali B, Zanotti L, et al. Proteomic analysis of the secretome of human bone marrow-derived mesenchymal stem cells primed by pro-inflammatory cytokines. J. Proteomics 2017;166:115-26.
16. Infante A, Rodriguez CI. Secretome analysis of in vitro aged human mesenchymal stem cells reveals IGFBP7 as a putative factor for promoting osteogenesis. Sci. Rep. 2018;8:4632.
17. Kim HK, Lee SG, Lee SW, Oh BJ, Kim JH, Kim JA, et al. A Subset of Paracrine Factors as Efficient Biomarkers for Predicting Vascular Regenerative Efficacy of Mesenchymal Stromal/Stem Cells. Stem Cells 2019;37:77-88.
18. Mitchell R, Mellows B, Sheard J, Antonioli M, Kretz O, Chambers D, et al. Secretome of adipose-derived mesenchymal stem cells promotes skeletal muscle regeneration through synergistic action of extracellular vesicle cargo and soluble proteins. Stem Cell Res. Ther. 2019;10:116.
19. Kehl D, Generali M, Mallone A, Heller M, Uldry AC, Cheng P, et al. Proteomic analysis of human mesenchymal stromal cell secretomes: a systematic comparison of the angiogenic potential. NPJ Regen. Med. 2019;4:8.
20. Doron G, Klontzas ME, Mantalaris A, Guldberg RE, Temenoff JS. Multiomics characterization of mesenchymal stromal cells cultured in monolayer and as aggregates. Biotechnol. Bioeng. 2020;117:1761-78.
21. Shin S, Lee J, Kwon Y, Park KS, Jeong JH, Choi SJ, et al. Comparative Proteomic Analysis of the Mesenchymal Stem Cells Secretome from Adipose, Bone Marrow, Placenta and Wharton's Jelly. Int. J. Mol. Sci. 2021;22:845.

22. Ranganath SH, Levy O, Inamdar MS, Karp JM. Harnessing the mesenchymal stem cell secretome for the treatment of cardiovascular disease. Cell Stem Cell 2012;10:244-58.
23. Xie M, Xiong W, She Z, Wen Z, Abdirahman AS, Wan W, et al. Immunoregulatory Effects of Stem Cell-Derived Extracellular Vesicles on Immune Cells. Front. Immunol. 2020;11:13.
24. Sotiropoulou PA, Perez SA, Gritzapis AD, Baxevanis CN, Papamichail M. Interactions between human mesenchymal stem cells and natural killer cells. Stem Cells 2006;24:74-85.
25. Chatterjee D, Marquardt N, Tufa DM, Hatlapatka T, Hass R, Kasper C, et al. Human Umbilical Cord-Derived Mesenchymal Stem Cells Utilize Activin-A to Suppress Interferon-gamma Production by Natural Killer Cells. Front. Immunol. 2014;5:662.
26. Cui R, Rekasi H, Hepner-Schefczyk M, Fessmann K, Petri RM, Bruderek K, et al. Human mesenchymal stromal/stem cells acquire immunostimulatory capacity upon cross-talk with natural killer cells and might improve the NK cell function of immunocompromised patients. Stem Cell Res. Ther. 2016;7:88.
27. Di Trapani M, Bassi G, Midolo M, Gatti A, Kamga PT, Cassaro A, et al. Differential and transferable modulatory effects of mesenchymal stromal cell-derived extracellular vesicles on T, B and NK cell functions. Sci. Rep. 2016;6:24120.
28. Fan Y, Herr F, Vernochet A, Mennesson B, Oberlin E, Durrbach A. Human Fetal Liver Mesenchymal Stem Cell-Derived Exosomes Impair Natural Killer Cell Function. Stem Cells Dev. 2019;28:44-55.
29. Smyth MJ, Cretney E, Kelly JM, Westwood JA, Street SE, Yagita H, et al. Activation of NK cell cytotoxicity. Mol. Immunol. 2005;42:501-10.
30. Cooper MA, Fehniger TA, Caligiuri MA. The biology of human natural killer-cell subsets. Trends Immunol. 2001;22:633-40.
31. Robertson MJ. Role of chemokines in the biology of natural killer cells. J. Leukocyte Biol. 2002;71:173-83.
32. Vivier E, Nunès JA, Vély F. Natural Killer Cell Signaling Pathways. Science 2004;306:1517-9.
33. Long EO. Negative signaling by inhibitory receptors: the NK cell paradigm. Immunol. Rev. 2008;224:70-84.
34. Lauwerys BR, Garot N, Renauld JC, Houssiau FA. Cytokine production and killer activity of NK/T-NK cells derived with IL-2, IL-15, or the combination of IL-12 and IL-18. J. Immunol. 2000;165:1847-53.

35. Delconte RB, Kolesnik TB, Dagley LF, Rautela J, Shi W, Putz EM, et al. CIS is a potent checkpoint in NK cell-mediated tumor immunity. Nat. Immunol. 2016;17:816-24.
36. Raulet DH, Vance RE. Self-tolerance of natural killer cells. Nat. Rev. Immunol. 2006;6:520-31.
37. Vivier E, Ugolini S, Blaise D, Chabannon C, Brossay L. Targeting natural killer cells and natural killer T cells in cancer. Nat. Rev. Immunol. 2012;12:239-52.
38. Lanier LL. Up on the tightrope: natural killer cell activation and inhibition. Nat. Immunol. 2008;9:495-502.
39. Shuai K, Liu B. Regulation of JAK-STAT signalling in the immune system. Nat. Rev. Immunol. 2003;3:900-11.
40. Morris R, Kershaw NJ, Babon JJ. The molecular details of cytokine signaling via the JAK/STAT pathway. Protein Sci. 2018;27:1984-2009.
41. Yoshimura A, Naka T, Kubo M. SOCS proteins, cytokine signalling and immune regulation. Nat. Rev. Immunol. 2007;7:454-65.
42. Sun JC, Lanier LL. NK cell development, homeostasis and function: parallels with CD8+ T cells. Nat. Rev. Immunol. 2011;11:645-57.
43. Mandal A, Viswanathan C. Natural killer cells: In health and disease. Hematol. Oncol. Stem Cell Ther. 2015;8:47-55.
44. Tsokos GC, Lo MS, Costa Reis P, Sullivan KE. New insights into the immunopathogenesis of systemic lupus erythematosus. Nat. Rev. Rheumatol. 2016;12:716-30.
45. Scheffschick A, Fuchs S, Malmström V, Gunnarsson I, Brauner H. Kidney infiltrating NK cells and NK-like T-cells in lupus nephritis: presence, localization, and the effect of immunosuppressive treatment. Clin. Exp. Immunol. 2022;207:199-204.
46. Lech M, Anders HJ. The pathogenesis of lupus nephritis. J. Am. Soc. Nephrol. 2013;24:1357-66.
47. Chalmers SA, Glynn E, Garcia SJ, Panzenbeck M, Pelletier J, Dimock J, et al. BTK inhibition ameliorates kidney disease in spontaneous lupus nephritis. Clin. Immunol. 2018;197:205-18.
48. Arazi A, Rao DA, Berthier CC, Davidson A, Liu Y, Hoover PJ, et al. The immune cell landscape in kidneys of patients with lupus nephritis. Nat. Immunol. 2019;20:902-14.
49. Park YW, Kee SJ, Cho YN, Lee EH, Lee HY, Kim EM, et al. Impaired differentiation and cytotoxicity of natural killer cells in systemic lupus erythematosus. Arthritis Rheum. 2009;60:1753-63.

50. Hervier B, Beziat V, Haroche J, Mathian A, Lebon P, Ghillani-Dalbin P, et al. Phenotype and function of natural killer cells in systemic lupus erythematosus: excess interferon-γ production in patients with active disease. Arthritis Rheum. 2011;63:1698-706.
51. Huang Z, Fu B, Zheng SG, Li X, Sun R, Tian Z, et al. Involvement of CD226+ NK cells in immunopathogenesis of systemic lupus erythematosus. J. Immunol. 2011;186:3421-31.
52. Henriques A, Teixeira L, Inês L, Carvalheiro T, Gonçalves A, Martinho A, et al. NK cells dysfunction in systemic lupus erythematosus: relation to disease activity. Clin. Rheumatol. 2013;32:805-13.
53. Ma H, Zhao L, Jiang Z, Jiang Y, Feng L, Ye Z. Dynamic changes in the numbers of different subsets of peripheral blood NK cells in patients with systemic lupus erythematosus following classic therapy. Clin. Rheumatol. 2014;33:1603-10.
54. Ye Z, Ma N, Zhao L, Jiang ZY, Jiang YF. Differential expression of natural killer activating and inhibitory receptors in patients with newly diagnosed systemic lupus erythematosus. Int. J. Rheum. Dis. 2016;19:613-21.
55. Lin SJ, Kuo ML, Hsiao HS, Lee PT, Chen JY, Huang JL. Activating and inhibitory receptors on natural killer cells in patients with systemic lupus erythematosis-regulation with interleukin-15. PLoS One 2017;12:e0186223.
56. Lin YL, Lin SC. Analysis of the CD161-expressing cell quantities and CD161 expression levels in peripheral blood natural killer and T cells of systemic lupus erythematosus patients. Clin. Exp. Med. 2017;17:101-9.
57. Liu M, Liu J, Zhang X, Xiao Y, Jiang G, Huang X. Activation status of CD56(dim) natural killer cells is associated with disease activity of patients with systemic lupus erythematosus. Clin. Rheumatol. 2021;40:1103-12.
58. Spada R, Rojas JM, Pérez-Yagüe S, Mulens V, Cannata-Ortiz P, Bragado R, et al. NKG2D ligand overexpression in lupus nephritis correlates with increased NK cell activity and differentiation in kidneys but not in the periphery. J. Leukoc. Biol. 2015;97:583-98.
59. Huang X, Li J, Dorta-Estremera S, Di Domizio J, Anthony SM, Watowich SS, et al. Neutrophils Regulate Humoral Autoimmunity by Restricting Interferon-γ Production via the Generation of Reactive Oxygen Species. Cell Rep. 2015;12:1120-32.
60. Yang C, Sun J, Tian Y, Li H, Zhang L, Yang J, et al. Immunomodulatory Effect of MSCs and MSCs-Derived Extracellular Vesicles in Systemic Lupus Erythematosus. Front. Immunol.

2021;12:714832.

61. Műzes G, Sipos F. Mesenchymal Stem Cell-Derived Secretome: A Potential Therapeutic Option for Autoimmune and Immune-Mediated Inflammatory Diseases. Cells 2022;11:2300.
62. Popis M, Konwerska A, Partyka M, Wieczorkiewicz M, Ciesiółka S, Stefańska K, et al. Mesenchymal stem cells and their secretome-candidates for safe and effective therapy for systemic lupus erythematosus. Med. J. Cell Biol. 2021;9:110-22.
63. Ko E, Yoon T, Lee Y, Kim J, Park YB. ADSC secretome constrains NK cell activity by attenuating IL-2-mediated JAK-STAT and AKT signaling pathway via upregulation of CIS and DUSP4. Stem Cell Res. Ther. 2023;14:329.
64. Perry D, Sang A, Yin Y, Zheng YY, Morel L. Murine models of systemic lupus erythematosus. J. Biomed. Biotechnol. 2011;2011:271694.
65. Li W, Titov AA, Morel L. An update on lupus animal models. Curr. Opin. Rheumatol. 2017;29:434-41.
66. Richard ML, Gilkeson G. Mouse models of lupus: what they tell us and what they don't. Lupus Sci. Med. 2018;5:e000199.
67. Bynoté KK, Hackenberg JM, Korach KS, Lubahn DB, Lane PH, Gould KA. Estrogen receptor-alpha deficiency attenuates autoimmune disease in (NZB x NZW)F1 mice. Genes Immun. 2008;9:137-52.
68. Koepsell SA, Miller JS, McKenna DH, Jr. Natural killer cells: a review of manufacturing and clinical utility. Transfusion 2013;53:404-10.
69. Martinet L, Smyth MJ. Balancing natural killer cell activation through paired receptors. Nat. Rev. Immunol. 2015;15:243-54.
70. Sivori S, Vacca P, Zotto GD, Munari E, Mingari MC, Moretta L. Human NK cells: surface receptors, inhibitory checkpoints, and translational applications. Cell Mol. Immunol. 2019;16:430-41.
71. Chester C, Fritsch K, Kohrt HE. Natural Killer Cell Immunomodulation: Targeting Activating, Inhibitory, and Co-stimulatory Receptor Signaling for Cancer Immunotherapy. Front. Immunol. 2015;6:601.
72. Xu H. Expressions of natural cytotoxicity receptor, NKG2D and NKG2D ligands in endometriosis. J. Reprod. Immunol. 2019;136:102615.
73. Huntington ND, Vosshenrich CA, Di Santo JP. Developmental pathways that generate natural-

killer-cell diversity in mice and humans. Nat. Rev. Immunol. 2007;7:703-14.

74. Spolski R, Li P, Leonard WJ. Biology and regulation of IL-2: from molecular mechanisms to human therapy. Nat. Rev. Immunol. 2018;18:648-59.
75. Hernandez R, Poder J, LaPorte KM, Malek TR. Engineering IL-2 for immunotherapy of autoimmunity and cancer. Nat. Rev. Immunol. 2022;22:614-28.
76. Waldmann TA. The biology of interleukin-2 and interleukin-15: implications for cancer therapy and vaccine design. Nat. Rev. Immunol. 2006;6:595-601.
77. Matalon O, Fried S, Ben-Shmuel A, Pauker MH, Joseph N, Keizer D, et al. Dephosphorylation of the adaptor LAT and phospholipase C–g by SHP-1 inhibits natural killer cell cytotoxicity. Sci. Signal. 2016;9:ra54.
78. Anders HJ, Saxena R, Zhao MH, Parodis I, Salmon JE, Mohan C. Lupus nephritis. Nat. Rev. Dis. Primers 2020;6:7.
79. Almaani S, Meara A, Rovin BH. Update on Lupus Nephritis. Clin. J. Am. Soc. Nephrol. 2017;12:825-35.
80. Koenig KF, Groeschl I, Pesickova SS, Tesar V, Eisenberger U, Trendelenburg M. Serum cytokine profile in patients with active lupus nephritis. Cytokine 2012;60:410-6.
81. Moreno-Torres V, Castejón R, Martínez-Urbistondo M, Gutiérrez-Rojas Á, Vázquez-Comendador J, Tutor P, et al. Serum cytokines to predict systemic lupus erythematosus clinical and serological activity. Clin. Transl. Sci. 2022;15:1676-86.
82. Yap DY, Yung S, Ma MK, Mok MM, Kwan LP, Chan GC, et al. Serum immunoglobulin G level in patients with lupus nephritis and the effect of treatment with corticosteroids and mycophenolate mofetil. Lupus 2014;23:678-83.
83. Almaghlouth I, Johnson SR, Pullenayegum E, Gladman D, Urowitz M. Immunoglobulin levels in systemic lupus erythematosus: A narrative review. Lupus 2021;30:867-75.
84. Anders HJ, Kitching AR, Leung N, Romagnani P. Glomerulonephritis: immunopathogenesis and immunotherapy. Nat. Rev. Immunol. 2023;23:453-71.
85. Fogel LA, Yokoyama WM, French AR. Natural killer cells in human autoimmune disorders. Arthritis Res. Ther. 2013;15:216.
86. Cullen SP, Brunet M, Martin SJ. Granzymes in cancer and immunity. Cell Death Differ. 2010;17:616-23.
87. Voskoboinik I, Whisstock JC, Trapani JA. Perforin and granzymes: function, dysfunction and

human pathology. Nat. Rev. Immunol. 2015;15:388-400.

88. Myers JA, Schirm D, Bendzick L, Hopps R, Selleck C, Hinderlie P, et al. Balanced engagement of activating and inhibitory receptors mitigates human NK cell exhaustion. JCI Insight 2022;7:e150079.
89. Alvarez M, Simonetta F, Baker J, Pierini A, Wenokur AS, Morrison AR, et al. Regulation of murine NK cell exhaustion through the activation of the DNA damage repair pathway. JCI Insight 2019;5:e127729.
90. Song W, Antao OQ, Condiff E, Sanchez GM, Chernova I, Zembrzuski K, et al. Development of Tbet- and CD11c-expressing B cells in a viral infection requires T follicular helper cells outside of germinal centers. Immunity 2022;55:290-307.e5.
91. Bocharnikov AV, Keegan J, Wacleche VS, Cao Y, Fonseka CY, Wang G, et al. PD-1hiCXCR5-T peripheral helper cells promote B cell responses in lupus via MAF and IL-21. JCI Insight 2019;4:e130062.
92. Panda SK, Facchinetti V, Voynova E, Hanabuchi S, Karnell JL, Hanna RN, et al. Galectin-9 inhibits TLR7-mediated autoimmunity in murine lupus models. J. Clin. Invest. 2018;128:1873-87.
93. Chan CJ, Martinet L, Gilfillan S, Souza-Fonseca-Guimaraes F, Chow MT, Town L, et al. The receptors CD96 and CD226 oppose each other in the regulation of natural killer cell functions. Nat. Immunol. 2014;15:431-8.
94. Georgiev H, Ravens I, Papadogianni G, Bernhardt G. Coming of Age: CD96 Emerges as Modulator of Immune Responses. Front. Immunol. 2018;9:1072.
95. Holmes VM, Maluquer de Motes C, Richards PT, Roldan J, Bhargava AK, Orange JS, et al. Interaction between nectin-1 and the human natural killer cell receptor CD96. PLoS One 2019;14:e0212443.
96. Fuchs A, Cella M, Giurisato E, Shaw AS, Colonna M. Cutting edge: CD96 (tactile) promotes NK cell-target cell adhesion by interacting with the poliovirus receptor (CD155). J. Immunol. 2004;172:3994-8.
97. Marcais A, Cherfils-Vicini J, Viant C, Degouve S, Viel S, Fenis A, et al. The metabolic checkpoint kinase mTOR is essential for IL-15 signaling during the development and activation of NK cells. Nat. Immunol. 2014;15:749-57.
98. Mao Y, van Hoef V, Zhang X, Wennerberg E, Lorent J, Witt K, et al. IL-15 activates mTOR and

primes stress-activated gene expression leading to prolonged antitumor capacity of NK cells. Blood 2016;128:1475-89.

99. Cifaldi L, Doria M, Cotugno N, Zicari S, Cancrini C, Palma P, et al. DNAM-1 Activating Receptor and Its Ligands: How Do Viruses Affect the NK Cell-Mediated Immune Surveillance during the Various Phases of Infection? Int. J. Mol. Sci. 2019;20:3715.
100. Rautela J, Souza-Fonseca-Guimaraes F, Hediyeh-Zadeh S, Delconte RB, Davis MJ, Huntington ND. Molecular insight into targeting the NK cell immune response to cancer. Immunol. Cell Biol. 2018;96:477-84.
101. Matsumoto A, Masuhara M, Mitsui K, Yokouchi M, Ohtsubo M, Misawa H, et al. CIS, a Cytokine Inducible SH2 Protein, Is a Target of the JAK-STAT5 Pathway and Modulates STAT5 Activation. Blood 1997;89:3148-54.
102. Aman MJ, Migone TS, Sasaki A, Ascherman DP, Zhu M, Soldaini E, et al. CIS associates with the interleukin-2 receptor beta chain and inhibits interleukin-2-dependent signaling. J. Biol. Chem. 1999;274:30266-72.
103. Jeffrey KL, Camps M, Rommel C, Mackay CR. Targeting dual-specificity phosphatases: manipulating MAP kinase signalling and immune responses. Nat. Rev. Drug Discov. 2007;6:391-403.
104. Hsiao WY, Lin YC, Liao FH, Chan YC, Huang CY. Dual-Specificity Phosphatase 4 Regulates STAT5 Protein Stability and Helper T Cell Polarization. PLoS One 2015;10:e0145880.
105. Spada R, Rojas JM, Barber DF. Recent findings on the role of natural killer cells in the pathogenesis of systemic lupus erythematosus. J. Leukoc. Biol. 2015;98:479-87.
106. Liu M, Liang S, Zhang C. NK Cells in Autoimmune Diseases: Protective or Pathogenic? Front. Immunol. 2021;12:624687.
107. Erkeller-Yuksel FM, Lydyard PM, Isenberg DA. Lack of NK cells in lupus patients with renal involvement. Lupus 1997;6:708-12.
108. Riccieri V, Spadaro A, Parisi G, Taccari E, Moretti T, Bernardini G, et al. Down-regulation of natural killer cells and of gamma/delta T cells in systemic lupus erythematosus. Does it correlate to autoimmunity and to laboratory indices of disease activity? Lupus 2000;9:333-7.
109. Green MR, Kennell AS, Larche MJ, Seifert MH, Isenberg DA, Salaman MR. Natural killer cell activity in families of patients with systemic lupus erythematosus: demonstration of a killing defect in patients. Clin. Exp. Immunol. 2005;141:165-73.

110. Suárez-Fueyo A, Bradley SJ, Katsuyama T, Solomon S, Katsuyama E, Kyttaris VC, et al. Downregulation of CD3ζ in NK Cells from Systemic Lupus Erythematosus Patients Confers a Proinflammatory Phenotype. J. Immunol. 2018;200:3077-86.
111. Dunlap GS, Billi AC, Xing X, Ma F, Maz MP, Tsoi LC, et al. Single-cell transcriptomics reveals distinct effector profiles of infiltrating T cells in lupus skin and kidney. JCI Insight 2022;7:e156341.
112. Popko K, Górska E. The role of natural killer cells in pathogenesis of autoimmune diseases. Cent. Eur. J. Immunol. 2015;40:470-6.
113. Magilavy DB, Steinberg AD, Latta SL. High hepatic natural killer cell activity in murine lupus. J. Exp. Med. 1987;166:271-6.
114. Nilsson N, Carlsten H. Enhanced natural but diminished antibody-mediated cytotoxicity in the lungs of MRLlpr/lpr mice. Clin. Exp. Immunol. 1996;105:480-5.
115. Gross CC, Schulte-Mecklenbeck A, Rünzi A, Kuhlmann T, Posevitz-Fejfár A, Schwab N, et al. Impaired NK-mediated regulation of T-cell activity in multiple sclerosis is reconstituted by IL-2 receptor modulation. Proc. Natl. Acad. Sci. U S A 2016;113:E2973-82.
116. Schuster IS, Coudert JD, Andoniou CE, Degli-Esposti MA. "Natural Regulators": NK Cells as Modulators of T Cell Immunity. Front. Immunol. 2016;7:235.
117. Lang PA, Crome SQ, Xu HC, Lang KS, Chapatte L, Deenick EK, et al. NK Cells Regulate CD8(+) T Cell Mediated Autoimmunity. Front. Cell. Infect. Microbiol. 2020;10:36.
118. Cruz-González DJ, Gómez-Martin D, Layseca-Espinosa E, Baranda L, Abud-Mendoza C, Alcocer-Varela J, et al. Analysis of the regulatory function of natural killer cells from patients with systemic lupus erythematosus. Clin. Exp. Immunol. 2018;191:288-300.
119. Segerberg F, Lundtoft C, Reid S, Hjorton K, Leonard D, Nordmark G, et al. Autoantibodies to Killer Cell Immunoglobulin-Like Receptors in Patients With Systemic Lupus Erythematosus Induce Natural Killer Cell Hyporesponsiveness. Front. Immunol. 2019;10:2164.
120. Davison LM, Alberto AA, Dand HA, Keller EJ, Patt M, Khan A, et al. S100a9 Protects Male Lupus-Prone NZBWF1 Mice From Disease Development. Front. Immunol. 2021;12:681503.
121. Zhou Y, Zhang Y, Han J, Yang M, Zhu J, Jin T. Transitional B cells involved in autoimmunity and their impact on neuroimmunological diseases. J. Transl. Med. 2020;18:131.
122. Ohl K, Tenbrock K. Regulatory T cells in systemic lupus erythematosus. Eur. J. Immunol. 2015;45:344-55.

ABSTRACT IN KOREAN

중간엽줄기세포 유래 분비단백체에 의한 자연살해세포 활성 및 염증 반응 조절

중간엽줄기세포(MSCs)는 면역조절 특성을 지니고 있으며, 분비단백체라고 불리는 이들의 수용성 물질들을 세포 밖으로 분비함으로써 자가면역질환에 치료 효과를 줄 수 있다. 그러나 분비단백체내 특정 주요 인자와 이들이 면역세포에 대해 작용하는 구체적인 메커니즘은 완전히 알려져 있지 않다. 이를 밝히기 위한 시험관 내 (*in vitro*) 실험에는 대부분 면역세포가 사용되어 왔으나, 자연살해세포(NK 세포)를 사용한 실험은 매우 드물며, NK 세포를 활용한 일부 연구에서 조차 일치하지 않는 결과를 보여왔다. NK 세포는 암이나 감염 환경에서 암세포, 바이러스에 감염된 세포 등 표적 세포를 직접 죽이거나 다른 면역 세포들의 활성을 돕는 기능을 갖는다. 하지만 자가면역 환경에서는 NK 세포 수 및 기능 이상이 관찰되며, 명확한 원인이나 이로 인한 질병 진행 관여 측면에서는 여전히 불분명하다.

본 연구의 목적은 첫째, 지방 조직에서 유래한 중간엽줄기세포 분비단백체 (ADSC secretome)가 NK 세포 활성에 미치는 영향과 그 작용 기전을 밝히는 것에 있다. 둘째, 자가면역질환 중 하나인 루푸스 신염에서 NK 세포의 특성을 분석하고, ADSC 분비단백체 투여로 인한 생체 내 (*in vivo*) NK 세포의 변화와 염증 조절 기전을 밝히는 것에 있다.

1장에서는, 인간 유래 NK 세포를 이용한 시험관 내 실험에서 ADSC 분비단백체

처치 효과와 그 작용 기전을 밝혔다. 이 내용은 2023년 11월에 'Stem Cell Research & Therapy' 학술지에 게재된 데이터를 기반하였다. ADSC 분비단백체는 IL-2에 의한 NK 세포의 정상적인 증식은 유지시키되 효과 기능만을 특이적으로 억제하였다. 이는 NK 세포 표면 활성 수용체 NKG2D, NKp30, NKp46 및 IL-2 수용체 CD25, CD132의 발현은 감소시키고, 억제 수용체 중 유일하게 CD96의 발현을 증가시킴으로써 NK 세포 활성 조절에 기여하는 것으로 여겨진다. NK 세포 내부에서는 ADSC 분비단백체가 음성 조절 단백질 CIS와 DUSP4의 발현을 증가시켜 IL-2의 신호 전달 경로 중 JAK1, JAK3의 인산화는 CIS가, STAT5, AKT의 인산화는 DUSP4가 저해함으로써 NK 세포의 활성을 특이적으로 억제할 것으로 여겨진다.

2장에서는, 먼저 실험용 생쥐 유래 NK 세포를 이용한 시험관 내 실험에서 ADSC 분비단백체 처치 효과를 확인하였다. 생쥐의 NK 세포 역시 ADSC 분비단백체에 의해 사람의 NK 세포와 동일한 변화를 나타냈다. 다음으로 자가면역질환인 루푸스 신염 동물모델 생쥐를 이용하여 루푸스 신염 환경의 NK 세포의 특성과 ADSC 분비단백체에 의한 생체 내 변화를 관찰하였다. 루푸스 신염의 NK 세포는 표적 장기인 신장으로 상당히 축적되었는데, 온전한 기능을 하지 못하는 탈진 표현형(exhaustion phenotype)을 나타냈다. 이는 NK 세포가 자가반응성 세포들을 제거함으로써 루푸스 환경에서 조직 보호 기능을 수행하나, 오랜 기간 지속적인 염증 자극으로 인해 기능 장애가 나타난 것으로 여겨진다. 게다가 ADSC 분비단백체를 투여하면 염증 반응이 완화되고 신장 구조와 기능이 온전하게 유지되었는데, 이는 ADSC 분비단백체가 비장과 신장 내 염증 세포들의 증식을 억제하면서, 동시에 NK

세포를 정상 표현형으로 회복시킴으로써 억제되었던 NK 세포의 조절 기능을 상향조절하는 것으로 여겨진다.

결론적으로, ADSC 분비단백체는 NK 세포의 활성이 일시적으로 증가할 때에는 효과 기능을 특이적으로 억제하고, 만성 염증으로 인해 제 기능을 하지 못할 때에는 효과 기능을 향상시킴으로써 주변의 환경에 따라 면역 반응을 조절하는 것으로 여겨진다. 따라서 MSC 분비단백체는 NK 세포 기능 조절을 통해 염증성 및 자가면역질환을 표적으로 하는 면역조절제로서의 잠재력을 기대할 수 있다.

핵심되는 말: 중간엽줄기세포, 분비단백체, 자연살해세포, 면역조절, 전신 홍반성 루푸스, 루푸스 신염, 염증반응